APPENDIX D

A Synoptic Climatology for Surface Winds Along the Southern Coast of Alaska

by

J. E. Overland and T. R. Hiester

September 1978

TABLE OF CONTENTS

Page

1. INTRODUCTION. 529

2. SUBJECTIVE WEATHER PATTERNS FOR COASTAL GULF OF ALASKA. 534

2.1 Technique. 534

2.2 The Six Surface Weather Type Patterns. 536

2.3 Pattern Climatology. 541

3. AUTOMATED WEATHER TYPING. . . . . , ... 545

3.1 Methodology and Results. 545

3.2 Comparison With the Subjective Types 546

4. LOCAL WIND FIELDS FOR NORTHEAST GULF OF ALASKA. 550

4.1 Procedure. 550

4.2 Description of Local Wind Fields 564

4.3 Evaluation. 568

REFERENCES. 574

APPENDIX A. Subjective Pattern Types 575

APPENDIX B. Automated Pattern Types. . . . . , ... 591

APPENDIX C. Local Wind Fields for Each Subjective Subtype. 601

1. Introduction

This report assembles a synoptic climatology to estimate surface winds over the water along the southern coast of Alaska from Yakutat to Kodiak Island. A synoptic climatology is a collection of generalized quasi-steady states of the atmosphere which are frequently observed or a continuum of states along particular storm tracks. The following classification is based upon sea level pressure analyses. Weather types aim to maintain the range of synoptic variability while grouping daily weather maps which have the same basic meteorological structure but slightly different locations or intensities. A synoptic climatology differs from calculation of means in that it specifies specific type patterns, such as a high or low pressure center, which could occur on any given day rather than forming an average over several possibly different sequential daily maps.

It should be recalled that atmospheric modes are continuous intime and that synoptic systems differ in size and intensity throughout their individual life cycle and from one storm to the-next. Given the assumption that classification is possible, our approach regards patterns of weather circulation as implicit functions of the static sea level pressure distribution (Barry and Perry, 1973). It differs from a kinematic approach in which synoptic weather maps are classified in terms of principal storm tracks. The former approach is most appropriate in regions where a proportion of features form and/or decay in situ or are persistant. Since the Gulf of Alaska is often the decay center for storms in the Pacific, the static approach is taken as a working hypothesis. Western Europe and the East Coast of the United States are examples where a kinematic approach would be more appropriate.

This study was initiated as part of the Outer Continental Shelf Environmental Assessment Project (OCSEAP) to provide local winds to an oil spill trajectory model, coupled with the ability to provide frequency of occurrence information from the meteorological record. The intent is to retain the influence of a daily wind variability on the dispersion of trajectories as part of a climatological assessment.

There are two approaches to map typing which can be referred to as objective (or at least automated) and subjective. Objective typing can be considered a pattern recognition problem involving digitized weather maps. Such techniques are generally based upon principal component analysis, factor analysis and their close relatives (Kendall and Stuart, 1975) or pattern correlation techniques (Lund, 1963). General objective techniques are being investigated as a companion study to the research reported here. The subjective approach involves assigning daily weather maps into different categories by a synoptic meteorologist. A rationale for subjective typing is that in order for patterns to be successful the underlying meteorological processes leading to these patterns should be recognizable.

This report establishes six subjectively derived weather types which are subdivided into twelve subtypes for the Northeast Gulf of Alaska (NEGOA) - Kodiak Island region. These six patterns were derived from combining and modifying patterns from two previous studies by Sorkina (1963) and Putnins (1966), subjective analysis of fall 1977- summer 1978 sea level pressure charts from the National Meteorological Center, and post modification of patterns based upon daily typing of candidate patterns. Post analysis indicated the necessity of including subtypes. Subtypes

within a type contain the same general distribution of features and meteorological basis but represent slight variations in locations of features which cause changes in the orientation of the geostrophic wind at the central location of the NEGOA coastline. These types are developed in chapter 2.

An additional resource for this study is the digitized sea level pressure grids for the northern hemisphere produced by the National Meteorological Center (Jenne, 1975). These fields are available for 1968-1975. Each subjective subtype was digitized on the same mesh as the Meteorological Center grid for twenty-four common points (figure 1). A daily map may then be quickly typed by computing its correlation with each of the subjective types. Such a procedure forms the basis for percent coverage and transition probability calculations for the various types.

The second approach to typing considered in this report consists of applying the pattern correlation technique (Lund, 1963) to the digitized daily weather maps. The pattern correlation technique consists of forming the correlation of each day with all other days during the year. The day with the highest number of correlations greater than a prescribed cut off value as type A. All days that correlate greater than the cut off value with type A are removed and the procedure is repeated to find type B; the analysis is continued until the data is exhausted. This procedure is applied to NEGOA as an independent check on the subjective typing and documented in chapter 3.

The relation of the surface wind fields over coastal waters of Alaska to geostrophic winds is complicated by coastal blocking, extensive air mass modification and mesoscale features induced by coastal topography. The available density of station data does not provide the resolution of the

spatial variation of the wind field over the water for input to trajectory calculations. As an alternative we have developed local wind fields on a 7½ minute latitude by 15 minute longitude grid which are the assumed local winds that occur with each synoptic scale subtype. These local patterns use a single point planetary boundary layer model proposed by Cardone (1969) to compute surface stress from the geostrophic wind, including corrections for thermal influence, and modify the near shore wind field based upon the field program of Reynolds, et al. (1978).

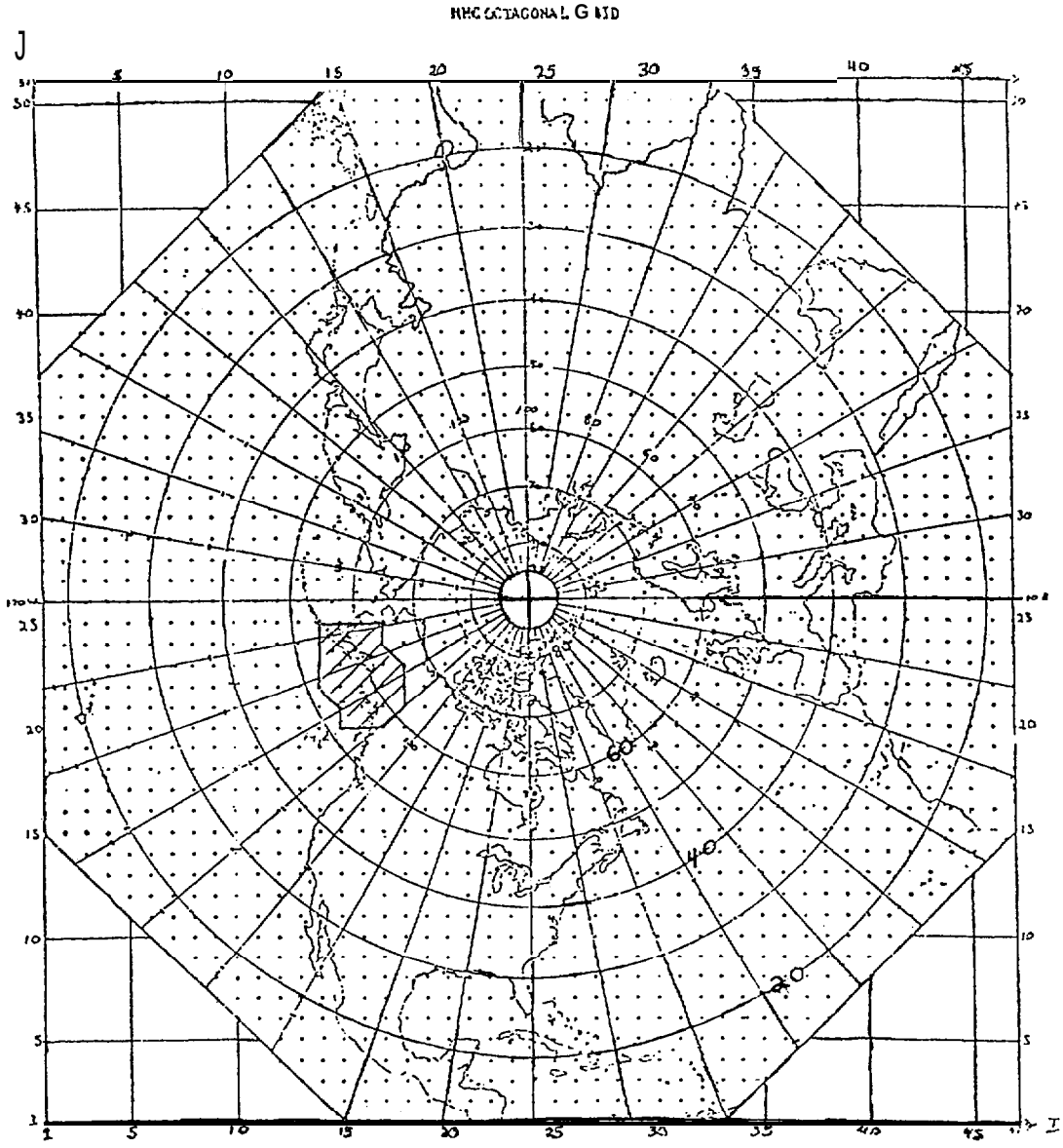

Figure #1 NMC 47 x 51 grid. There are 1,977 points in the entire grid. The subset of 24 points used in this study are shown by a lined region.

2. Subjective Weather Patterns for Coastal Gulf of Alaska

2.1 Technique

The two previous studies to find type patterns, duration, and transition probabilities which cover southern Alaska are Sorkina (1963) and Putnins (1966). Our six patterns result from modifying Putnins' patterns in the following ways:

a) combining like patterns

b) modifying them according to Sorkina's patterns

c) using fall, winter and spring of 77-78 sea level pressure analyses from the National Meteorological Center to test the patterns and to modify them accordingly.

Sorkina (1963) provides a description of the surface circulation patterns over the entire North Pacific Ocean. Fifteen patterns are obtained based on 16,000 daily synoptic maps spanning 47 years (1899-1939, 1954-1959). Each pattern is subjectively justified upon meteorological grounds. Seasonal duration and transitional probability statistics are established. Three underlying regional physical processes are evident which can be combined and rearranged to make each pattern. These are zones of cyclogenesis, high pressure regions, and regions for stagnation of lows. The horizontal temperature contrast between the northwest Pacific and the adjacent continent gives rise to the arctic front, a region of active cyclogenesis, which is oriented SW-NE near Japan in the mean. The newly formed cyclones travel rapidly toward the northeast. The curved coastline of Alaska is a region where low pressure centers stagnate. High pressure areas and zones of cyclogenesis tend to alternate at mid-latitudes, while regions of stagnation and zonal bands of rapid movement for lows alternate at higher latitudes. Sorkina

shows that each of her patterns is seasonally persistent and tends to lead to specific other patterns.

Sorkina's patterns were applied to a new data set, the daily Pacific surface analyses at 1800 GMT from September 1977 to December 1977, prepared by the Ocean Services Unit of the Weather Service Forecast Office in Seattle. An analysis of map sequences for the middle and eastern North Pacific showed that the daily maps would closely resemble one of Sorkina's patterns in general character for a day or two, followed by three or four days of less identifiable character as the cyclones moved rapidly from cyclongenesis regions to stagnation regions where the maps would again closely resemble a type pattern for another few days.

Sorkina (1963) provided a very useful reference; unfortunately, her type patterns cover the whole northern Pacific and do not adequately resolve the comparatively small and peripheral coastal Gulf of Alaska. Putnins' patterns are on a more applicable scale. However, Sorkina excels Putnins in establishing physical bases for her patterns and was used as a general guideline for deciding the final six type patterns.

Putnins' twenty-two patterns were also obtained from a large data set. Weather maps, both surface and 500 mb, for the period 1 January 1945 to 31 March 1963 were used to determine types "in such a way that for every date of this period a specific baric weather pattern could be assigned." Duration and transition frequencies were also found. The 500 mb patterns were used to assign either a 'cyclonic', 'anticyclonic' or 'mixed' designation to the flow pattern aloft. Most of Putnins' patterns can be related to one or another of Sorkina's patterns. Representative daily maps are shown by Putnins as examples of each type. However, little physical discussion is

given of each type and several of the infrequently occurring types seem arbitrary. Furthermore, his patterns apply to all of Alaska so that the difference between any two patterns is sometimes due to a difference occurring far from the coastal Gulf of Alaska. Thus many of this patterns have been grouped and redrawn to be more useful for Gulf of Alaska studies.

2.2 The Six Surface Weather Type Patterns

The six types (Table 1) represented by twelve subtype patterns are shown in Appendix A as figures Al - A12. All 22 of Putnins' patterns can be incorporated into these slightly more general patterns, and most of the 77-78 surface maps subjectively resemble one or another of the twelve. Subtypes consider the same meteorological conditions as the parent type, but represent slight variation in location of pressure centers which result in large wind direction changes over NEGOA. For example, the major subtypes for Type 1 are relocating the low center along the coast as seen in figure 2.

An example of how these patterns were obtained is given for the common case of a stagnating low pressure system tucked into the center of the coastal Gulf of Alaska. The underlying broad pattern, Sorkina's 4c, is shown in figure 3. Putnins' type patterns A_1 and A' shown in' figures 4 and 5 reveal more of the necessary details and the effect of the orientation of the land and ocean on the isobar pattern. Type pattern 1, figure 2, was thus determined concentrating on the orientation of the geostrophic wind along the coastal Gulf of Alaska.

Type pattern 1 (Figure Al - A4) is a manifestation of the natural stagnation region for cyclones provided in fall, winter and spring by the higher elevation, relatively cooled land to the north. Cold air in the interior

TABLE 1

Type	Description	Sorkina Type	Putnins Type	Dominant Season
I	Low in Gulf of Alaska	4C	A′, A_1, G, H	Winter
II	Aleutian Low	5b	A, C, E, A_c	Winter, Spring, Fall
III	High pressure in Alaskan Interior	6a	D, B, D	Winter
IV	Low pressure center over Central Alaska	la	A“, A_3, F	Summer
V	Pacific Anticyclone	lb, 5a	A''', A_2, E', E_1'	Summer
VI	Stagnating low off of Queen Charlotte Islands	7a	D', E“, E_1, F_1	Spring, Fall

of Alaska creates a very stable anticyclone over the Yukon, which can dominate the coast in the absence of cyclones, as typified by pattern 3 (Figure A7). In both cases the coastal mountains tend to contain the cold air while the relatively warmer water constitutes a good substrate for cyclonic conditions, making for closely packed isobars parallel to the coast.

Type pattern 2 (A5 and A6) represents the average position of cyclones as they are transported in the westerlies to eventually die cut in the northeastern Gulf. However, cyclones often linger over the central Aleutian Islands. This frequented position is associated with an Aleutian low at 500 mb as the disturbances align vertically in old age. Subtype 2.0 is more typical of winter and subtype 2.1 is more typical of summer and fall when the Aleutian low is adjacent to a strong east Pacific high pressure area.

In the summer the comparatively cool northeast Pacific Ocean surface provides for a well developed anticyclone. This often encroaches on the region and is the basis of type pattern 5 (A8 and A9). Subtypes 5.0 and 5.1 represent an east and west location for the main axis of the pressure ridge. In this milder part of the year, the equator to pole temperature gradient

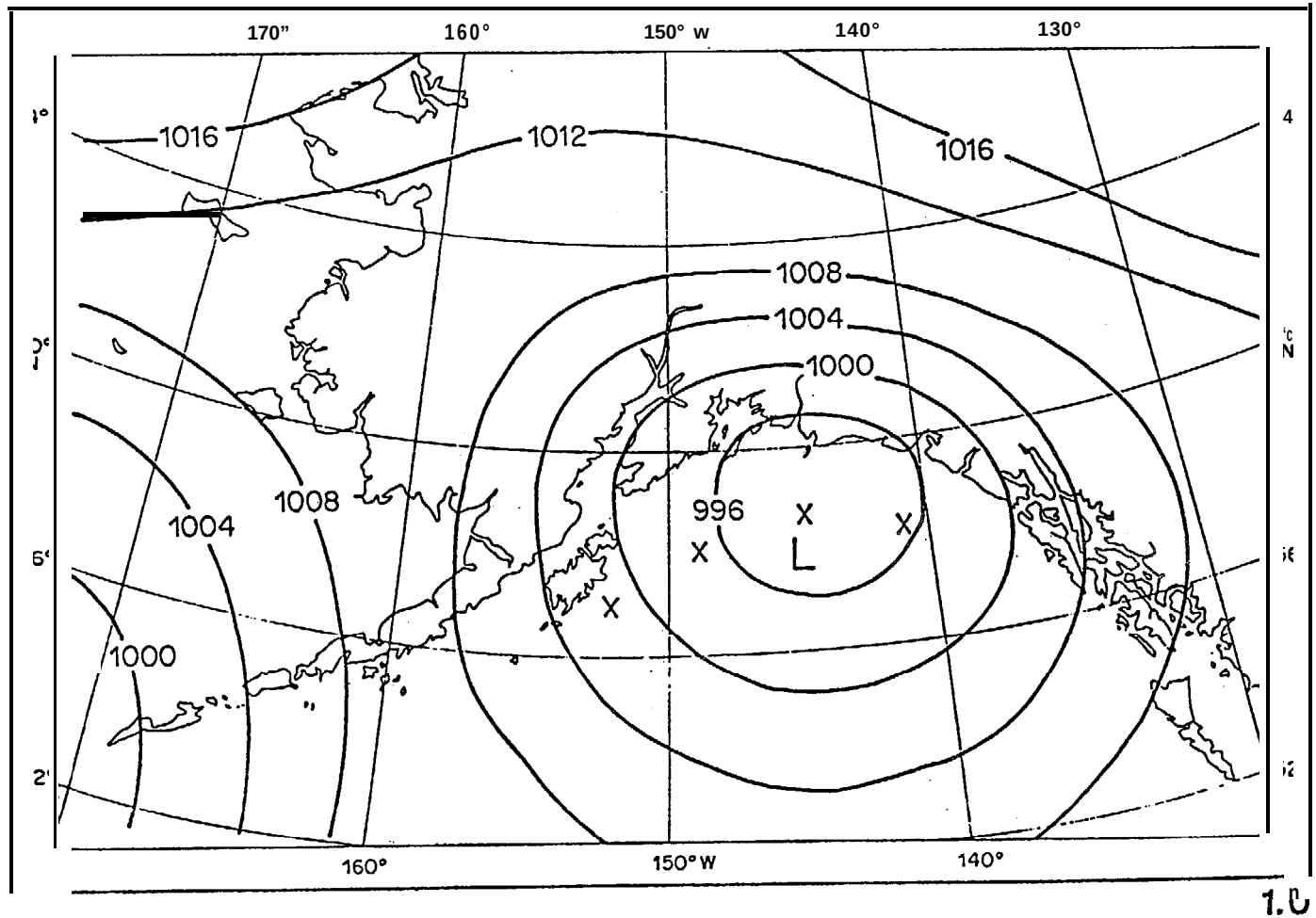

Figure 2. Subjective weather type 1.0. The "x" indicate locations of the low center for the four subtypes comprising type 1.0.

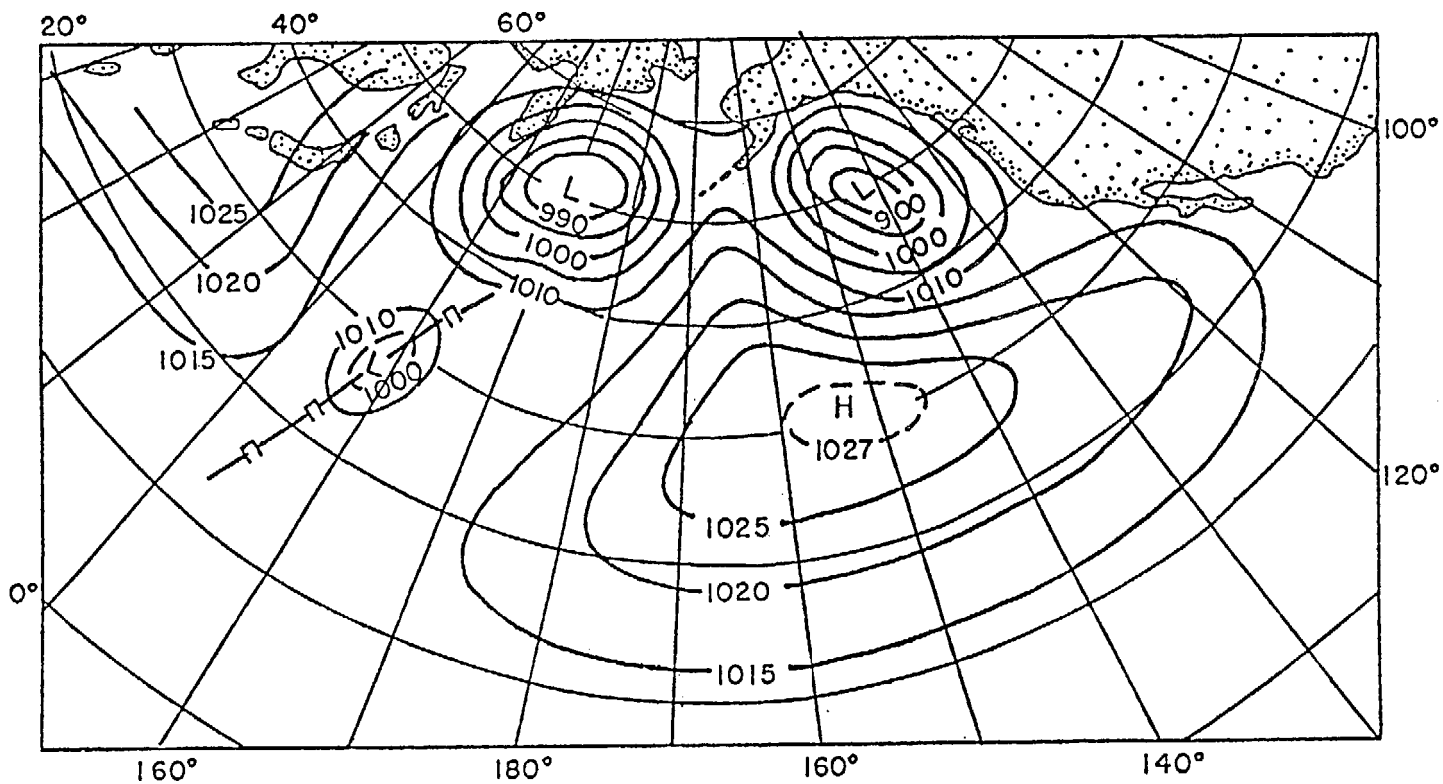

Figure 3. Sorkina s weather type 4c.

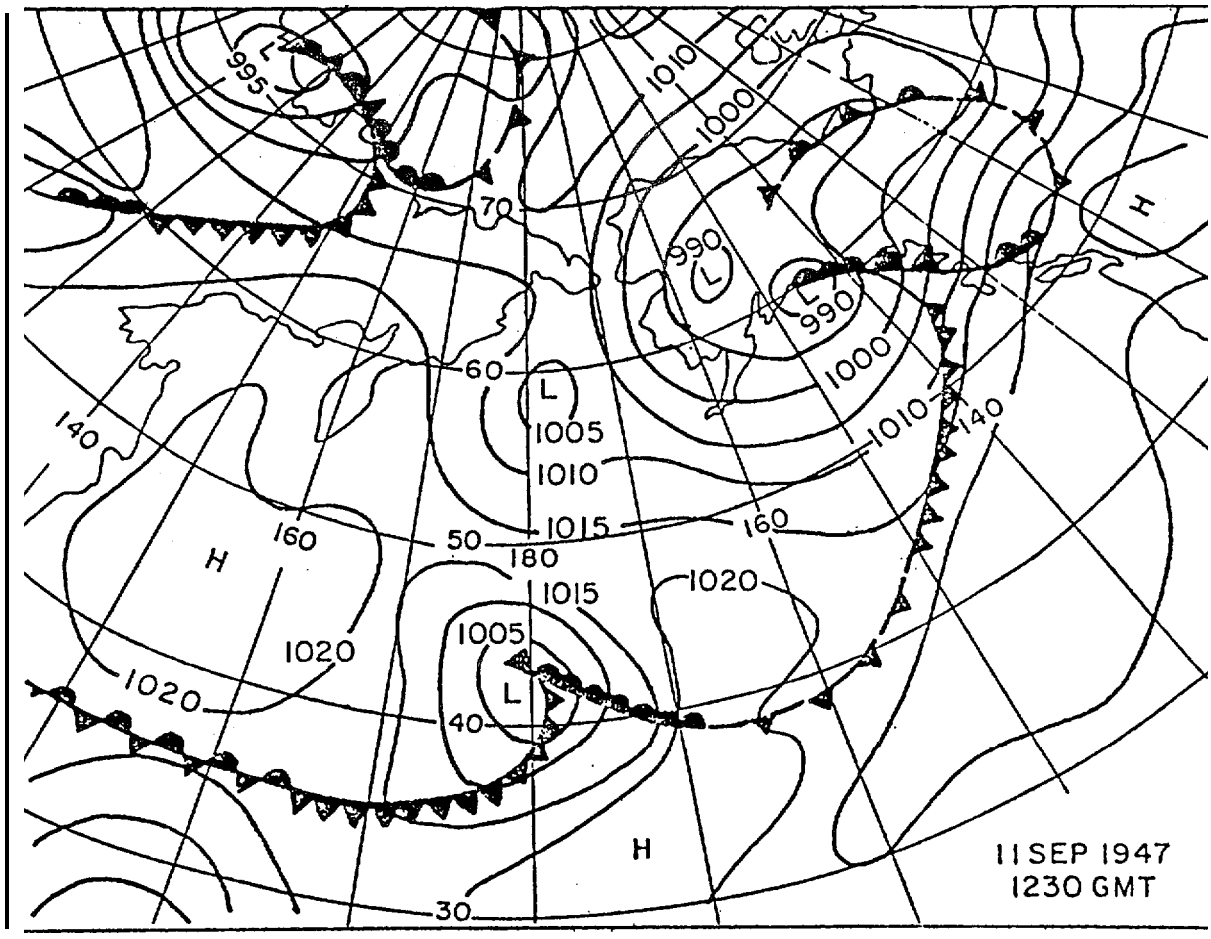

Figure 4. Putnins' weather type A_1.

lessens and cyclonic systems become weaker and are found farther to the north. Lows tend to move through the Alaska mainland, frequently being observed as shown in patterns 4.0 and 4.1 (A10 and A11).

Another commonly observed pattern, type 6 (A12), shows a cyclone positioned near the Queen Charlotte Islands, with a high over northeast Alaska and the Bering Sea. This occurs when cyclogenesis occurs farther to the east and south than for the lows observed in the other cases. The cyclone often retrogrades towards the central Gulf coast or may travel northeast

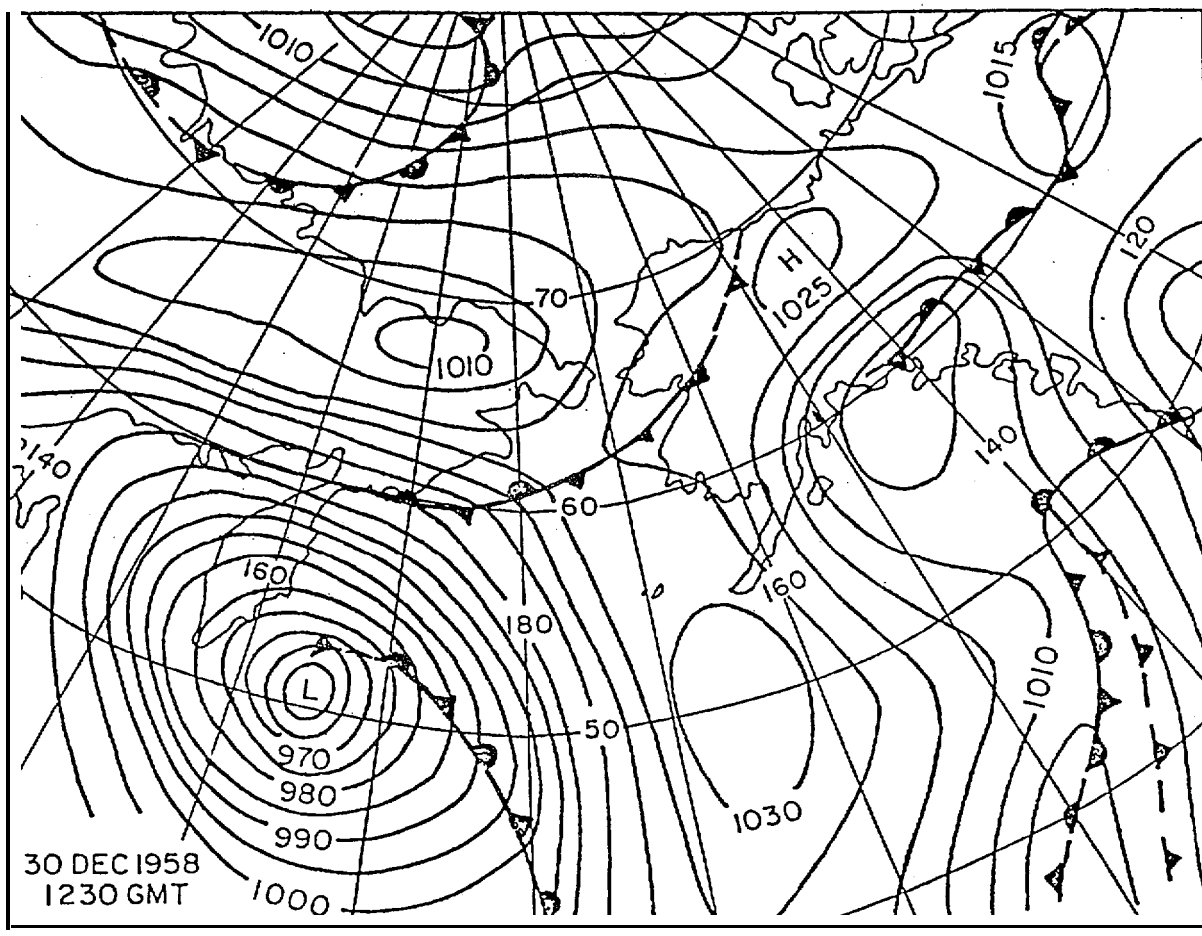

Figure 5. Putnins' weather type A′.

onto the continent, usually to die.

Each of the six patterns are listed in table 1 with the season it is commonly associated, the Putnins' patterns from which it is derived and the underlying Sorkina pattern.

2.3 Pattern Climatology

Automated sea level pressure analyses on a polar stereographic grid over the northern hemisphere produced at the National Meteorological Center (NMC) were obtained for 1968-1975. The mesh length is 381 km at 60° north

latitude. Since 1972 the analysis has consisted of fitting Hough functions to observed data (Flattery, 1970). Hough functions are solutions to Laplace's tidal equations, which imply a geostrophic relation between the wind and mass fields. The analysis is spectral in character fitting the entire atmosphere at once with 24 wave numbers in latitude and longitude and seven layers in the vertical. Prior to this time the analysis consisted of a local interpolation to grid points based upon Cressman (1959). Analyses are performed twice a day with a data receipt cutoff of ten hours after observation. It should be recalled that the analyses maps are dependent upon the availability of ship observations on a given day and are subject to interpolation and smoothing errors introduced by the analysis procedures. This was particularly noticeable as a lack of packing of the isobars along the coastlines in weather maps representing Type 1 synoptic conditions.

A subset of 24 grid points was extracted from each 12 hour map for the NEGOA region (figure 1). Each subjective subtype was also digitized to provide sea level pressure values at each of the 24 grid point locations. The correlation was then computed between each map and the twelve subtypes to determine the pattern for each 12 hour weatherman:

$$r_{it} = \sum_{m=1}^{24} P_{im} P_{tm} \left(\sum_{m-1}^{24} P_{im}^{2} \sum_{m=1}^{24} P_{tm}^{2} \right)^{-\frac{1}{2}}$$

where P_{im} and P_{tm} represent the deviation of pressures from the map average for data i and type t at grid point m. The weather type with the largest correlation is assigned to that map. The magnitude of the correlation is recorded along with the type.

The percent of occurrence of each type by year and season are listed in Table 2 and graphed in Figure 6. Percent of occurrence of each subtype

TABLE 2 TRANSITIONS FROM INITIAL TYPE TO FOLLOWING TYPE

Based on 12 Hourly Analyses 1968-1974

	Initial Type	% Occurrence of Initial Type	% of Initial Type Followed by Following Type					
			1	2	3	4	5	6
YEAR	1	16	47	17	6	13	2	15
	2	31	12	71	6	7	3	1
	3	9	14	15	56	1	1	13
	4	18	8	11	-0	60	16	5
	5	12	-0	24	1	15	59	1
	6	14	15	3	9	B	3	62
WINTER	1	23	57	15	6	6	1	15
	2	26	13	71	8	6	1	1
	3	19	10	10	70	-0	1	9
	4	7	19	14	1	42	13	11
	5	4	0	29	5	14	52	0
	6	21	14	2	9	4	1	70
SPRING	1	16	43	17	6	16	1	17
	2	37	11	73	6	7	2	1
	3	8	16	21	47	0	0	16
	4	16	8	14	1	54	16	7
	5	9	0	35	1	10	52	1
	6	14	16	4	8	10	4	58
SUMMER	1	8	34	20	4	27	5	10
	2	30	8	68	5	9	8	2
	3	3	27	20	29	2	7	15
	4	26	4	7	0	67	20	2
	5	27	-0	19	0	12	68	1
	6	6	14	7	4	15	7	52
FALL	1	18	45	18	6	14	1	16
	2	30	15	68	6	8	2	1
	3	8	16	18	43	3	1	19
	4	22	9	12	-o	60	13	6
	5	7	1	27	0	34	37	1
	6	15	15	2	10	9	3	61

is listed in Appendix A. The Aleutian low (pattern 2) is dominant in all seasons. Pattern 3 (high in interior of Alaska) is confirmed as a winter pattern and the east Pacific high pressure as a summer pattern. Lows to the north (pattern 4) peak in summer and lows to the southeast (pattern 6) peak in winter. The same tables also list transition probabilities. The large diagonal components, many over 50% are an indication of persistence of each pattern.

Figure 7 plots the percentage of days from the 1969-74 record which could be typed by at least one of the patterns at a given threshold value

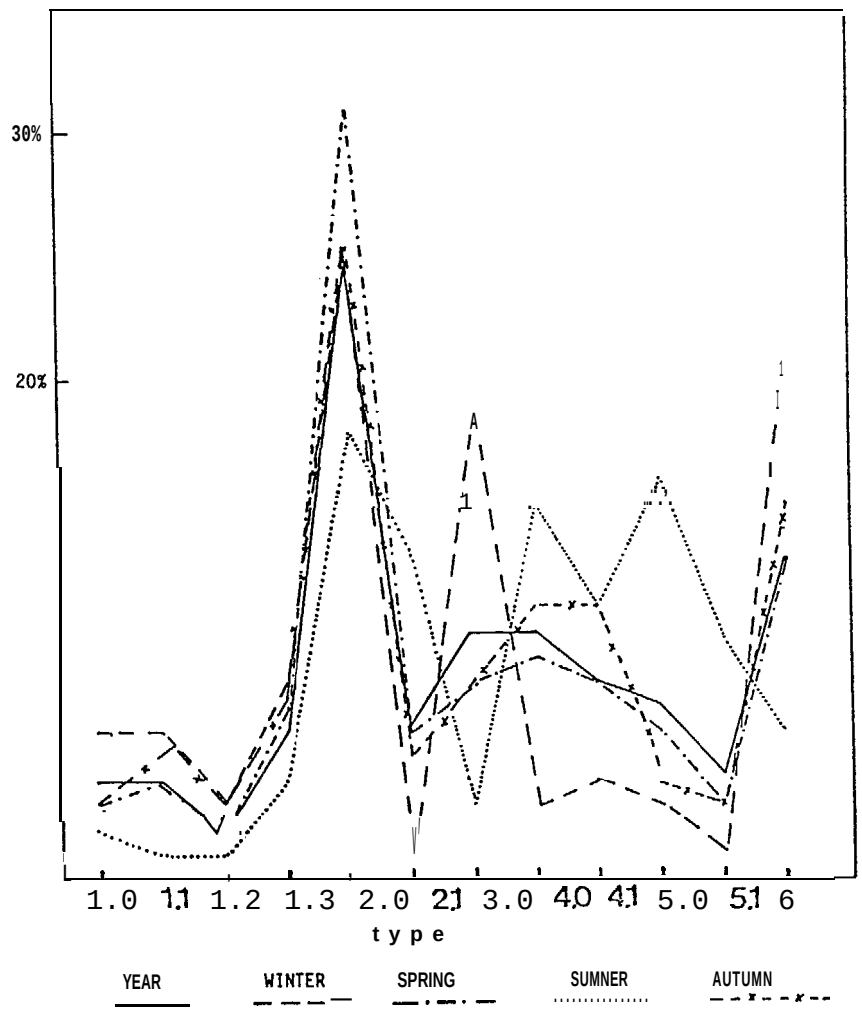

Figure 6. Percentage occurrence of synoptic weather type by season.

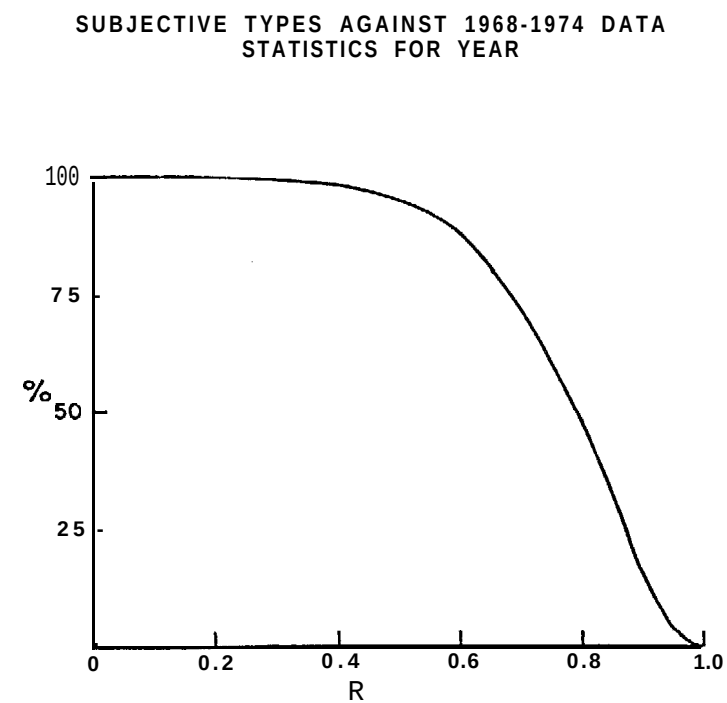

Figure 7. Percentage of 12-hour NMC pressure fields from 1968 to 1973 typed by at least one subtype at a given threshold.

of the correlation coefficient. Approximately 75% of the record can be typed with a correlation of 0.7 or better.

3. Automated Weather Typing

3.1 Methodology and Results

This section discusses an independent approach to map typing to compare with the subjective typing in the last chapter. The technique used is the pattern correlation technique (Lund, 1963, Basing, 1975, Singh et al, 1978). The procedure is as follows.

1) Correlation coefficients are computed for each existing 00 GMT map and all others for the year 1974. Accounting for missing data, this formed a correlation matrix of 354 x 354 elements.

2) "The correlation matrix is examined to determine which daily map is highly correlated with the greatest number of other maps. For this purpose highly correlated implies values greater than a cutoff value, r_c. The chart having the maximum number of correlations exceeding the threshold value is classified as type A.

3) All maps which correlated greater than r_c with type A are removed from the analysis.

4) The procedure is repeated to find type B, C, . . . until either all days are classified or they do not correlate with any remaining map. We designate that a type must have a minimum of ten members.

In following the above procedure certain arbitrary criteria are adopted in picking r_c. Too high a cutoff may produce a large number of types while too low a value may provide lumping of synoptically distinct patterns. Thus the procedure is automated, but not necessarily unique.

Table 3 shows the number of maps removed (out of 354) at each step of the procedure. The second column gives the percent of the 354 maps

TABLE 3
NUMBER OF DAYS FIT BY EACH PATTERN TYPE

	Cutoff= 0.8			cutoff = 0.7			Cutoff= 0.6	
Type	No. of Fits	% of Occurrence	Type	No. of Fits	Occurrence	Type	No. of Fits	% of Occurrence
A	77	24	AA	102	23	AAA	132	27
B	34	11	BB	49	15	BBB	63	18
C	29	10	CC	42	9	ccc	55	14
D	26	10	DD	44	15	DDD	31	11
E	24	13	EE	19	13	EEE	22	13
F	18	6	FF	17	12	FFF	14	17
G	14	10	GG	13	8	GGG	14	17
H	12	9	HH	10	5			
I	10	7						

which correlate the greatest with each of the patterns. It accounts for some days that were removed by an early step of the procedure but correlate highest with a latter pattern. Appendix B shows the days picked for cutoff of 0.8 and 0.7.

3.2 Comparison With the Subjective Types

Table 4 lists the date selected for each objective type A-I (0.8 cutoff) and it s correlation with each subjective subtype. Table 5 is a similar format for the 0.7 cutoff. Type A and AA are March and September dates which correlate strongly with type 2, This case is the Aleutian low pressure center which has the highest percent of occurrence (25%, Appendix A) in the 1968-74 record of any weather type. Subjective subtype 6.0, the second most frequent type, was closest to the second pick with the 0.7 cutoff and third with the 0.8 cutoff. Type B from early September is dissimilar to any of our patterns. It contains a migrating low in the central Gulf

TABLE 4

Type	Date	1.0	1.1	1.2	1.3	2.0	2.1	3.0	4.0	4.1	5.0	5.1	6,0	Closest Fit
A	3-23-74	.03	.35	-.05	.70	.96	.50	.63	.09	-.78	.07	-.72	-.35	2
B	9-08-74	.39	.73	.26	.90	.69	-.12	90	-.51	-.71	-.78	-.95	.51	1 or 3
C	1-16-74	.65	.67	.53	.40	-.12	-.53	.33	-.50	.09	-.89	-,33	.82	6
D	7-19-74	.06	-.24	-.00	-.64	-.87	-.11	-.85	.41	.86	.26	.83	-.05	4
E	8-08-74	-.24	-.25	-.30	-.09	.33	76	-.32	.76	-.07	.84	.19	-.94	5
F	7-04-74	-.39	-.61	0.38	-.74	-.51	,36	-.87	.76	.52	.88	.84	-.70	5
G	4-14-74	.43	.70	.07	.78	.69	.38	.43	.29	-.52	-.23	-.65	-.12	1
H	1-13-74	.32	.44	,47	.44	.19	-.67	.74	-.89	-.29	-.83	-.55	.87	6
I	10-03-74	.51	.14	.68	-.28	-.56	-.60	-.21	-.28	.73	-.28	.40	.51	4

TABLE 5

Type	Date	1.0	1.1	1.2	1.3	2.0	2.1	3.0	4.0	4.1	5.0	5.1	6.0	Closest Fit
AA	9-20-74	.13	.53	-.07	.86	.94	.48	.69	-.00	-.83	-.19	-.86	-.17	2
BB	9-09-74	.55	.69	.51	.57	.18	-.65	.70	-.63	-.29	-.94	-.60	.88	6
CC	6-23-74	.19	-.22	.17	-.65	-.77	-.06	-.85	,49	.92	.36	.85	-.19	4
DD	8-08-74	-.24	-.25	-.30	-.09	.33	.76	-.32	.76	.07	.84	.19	-.94	5
EE	1-02-74	-.08	.18	.06	.51	.80	.04	.78	-.34	-.78	-.07	-.66	.01	2
FF	2-21-74	.70	.41	.69	-.05	-.47	-.62	-.11	-.18	.60	-.52	.20	.65	1
GG	4-21-74	.57	.72	.18	.59	.25	.19	.14	.29	-.11	-.38	-.38	.08	1
HH	7-04-74	-.39	-.61	-.38	-.74	-.51	.36	-.87	.76	.52	.88	.84	-.70	5

south of our region. Types F and DD, and D and CC consists of summer cases similar to our couplets 4.0 and 5.0 versus 4.1 and 5.1. Subtypes 4.0 and 5.0 are high pressure to the southeast and 4.1 and 5.1 have high pressure to the southwest. Type 4 patterns have weak lows over interior Alaska. The automated typing sees the east or west orientation of the pressure gra-

client as more important than the inclusion of the weak low pressure centers.

After pattern DD, the number of fits for 0.7 drops by more than half. Pattern EE is halfway between type 2 and 3. Type FF and GG pick up pattern 1 while type HH is similar to an earlier type DD. Type G picks up pattern 1. Pattern H is much closer to our type 6 than pattern C. Pattern I is between our pattern 1 and 4 while pattern C lies between our 1 and 6.

All approaches, the two automated and subjective, point to four primary patterns, the Aleutian low, low over the southeast Gulf of Alaska, and east and west high pressure ridge orientation. The subjective approach and the 0.7 cutoff place low pressure centers in similar locations to produce the remaining types. After the first four primary patterns, the 0.8 cutoff also adds various low pressure centers to the basic group of four patterns, but has a different regional location from the other approaches, indicating a different grouping of migratory lows.

All digitized weather maps for 1968-73 were typed by comparison with the twelve subjective subtypes and the two automated sets of weather. In addition eight sets of ten maps were drawn at random from 1974, and used as weather types against the 1968-73 maps. Figure 8 shows that both automated types perform slightly better than the subjective classification scheme when compared to the NMC digitized sea level pressure grids.

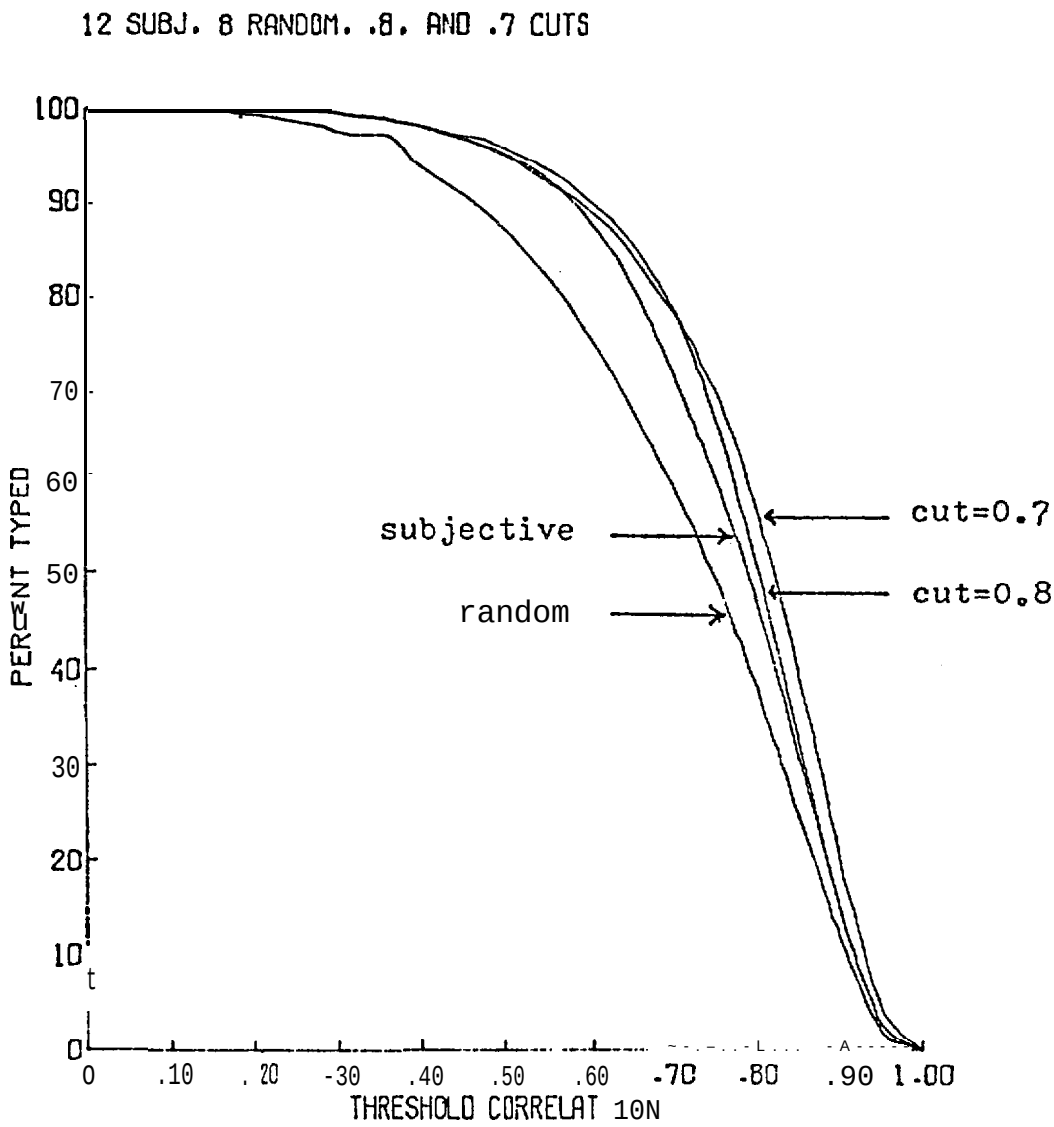

Figure 8. Percentage of 12 hour NMC pressure fields typed by the subjective approach, the two pattern correlation types and the average of eight sets of ten maps drawn at random from the NMC data set for 1974.

4. Local Wind Fields for NEGOA

4.1 Procedure

This section discusses the generation of local wind fields from surface pressure pattern types described in section 2. For use in the oil spill trajectory calculations all local wind speeds within a pattern will be scaled against an anemometer record. Therefore, the primary aim is to produce wind fields showing local direction and relative magnitude. Computation began by computing gradient wind speeds and directions from the patterns on a uniform set of grid points over the localized area shown in figure 9. The grid consisted of 800 boxes; each box was 7½ minutes in latitude by 15 minutes in longitude. At 60°N the boxes were 13.89 km on a side. Boundary layer thermal structure and air-sea temperature differences were estimated for each pattern. Cardone's (1969) planetary boundary layer model was used to estimate cross isobar flow angles (α) and surface friction velocities (u^*) over open ocean. Within 50 to 100 km of the coast data from coastal measurements and descriptions of coastal processes were used to modify Cardone's model output. The friction velocities were then converted to equivalent 10 m elevation neutral surface layer winds. The wind field away from the coast was smoothed and a final diagnostic check of the divergence field was made.

Since local winds will be scaled against an anemometer, the magnitude of the geostrophic wind within each pattern is of secondary importance. However, with higher wind speed cases the nonlinear effects of inertia on surface winds are important, causing larger relative variations in wind speed. Therefore, in computing local wind fields we biased the analysis toward the higher wind speed cases. Geostrophic wind speeds typically were taken between 10 and 20 m/see with some 25 m/see values where isobars are packed

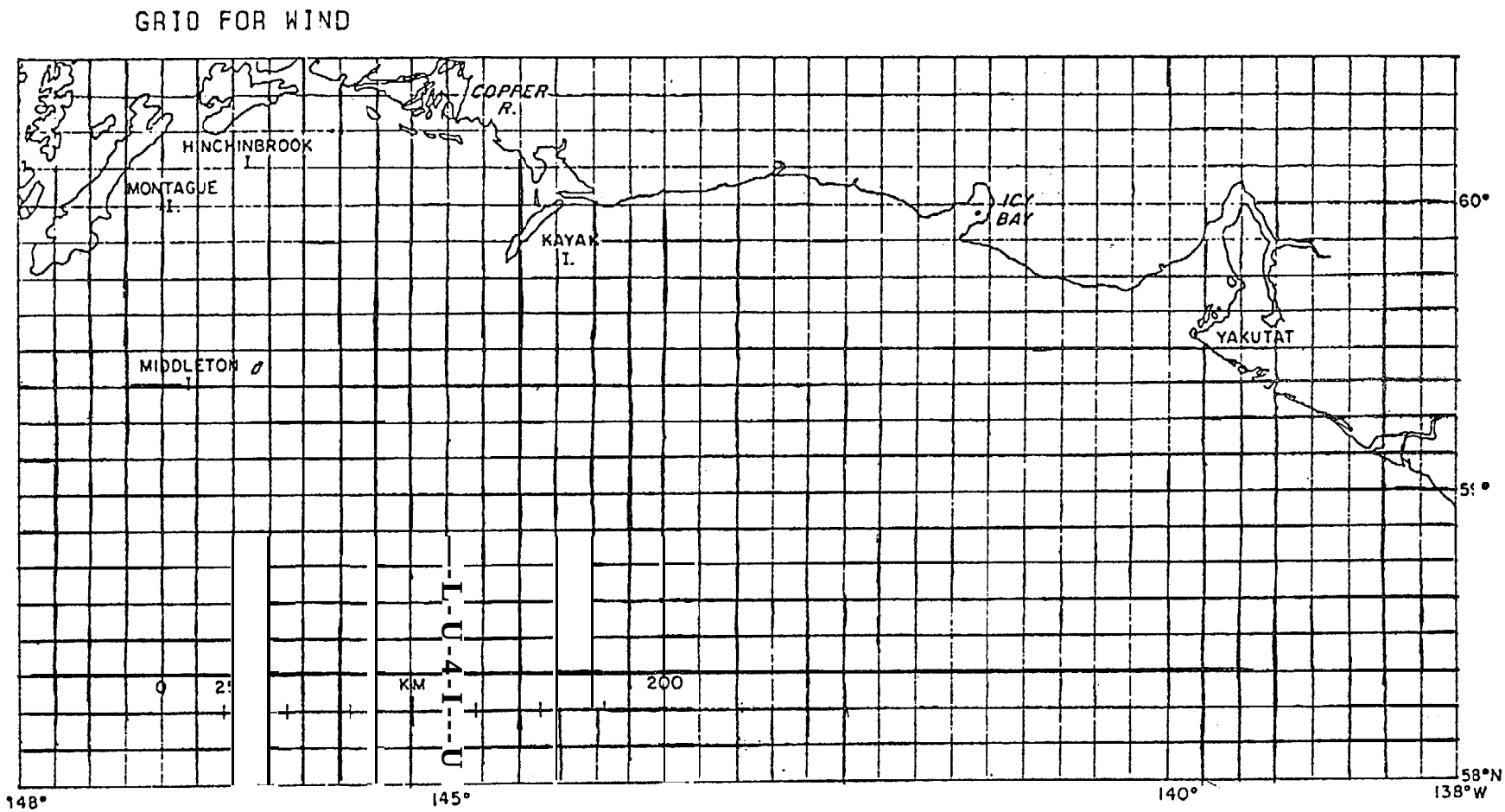

Figure 9. Grid network for estimating local winds.

along the coast. Gradient wind speed corrections were applied to regions of isobaric curvature.

We assumed a thermal structure for the marine planetary boundary layer (PBL) so that the baroclinicity of the PBL was consistent with an ideal storm structure and climatology. For example, pattern type 1 (figure 2) represents the stagnated low pressure center in the Gulf of Alaska. Our ideal storm consists of warm air advection behind a warm front and cold advection well behind the cold front. Nearshore, where offshore flow occurs we assume large horizontal air temperature gradients. The climatology for the winter months when storm type 1 prevails shows a mean surface air temperature distribution which reflects the large duration of pattern type 1. Isotherms were drawn to reproduce the climatological large scale temperature gradient and then distorted to be consistent with storm structure, packing the isotherms in frontal zones. Actual fronts were not created so as not to over-specify the generalized storm. Figure 10 shows the isotherms used for type 1 along with the isobars. From the isotherms, the magnitude and direction (relative to the surface geostrophic wind) of the baroclinic field (thermal wind) were determined. Baroclinicity for the other map types were similarly computed.

The distribution of air-sea temperature difference was also assumed for each pattern, also drawing on idealized storm structure and climatology. Figure 11 portrays the climatological air-sea temperature difference distributions from the OCSEAP Gulf of Alaska Climatic Atlas (Brewer, et. al, 1977). The climatic atlas covers several marine "areas" of which areas D and E are two. The western half of our grid is part of area D, and the eastern half is part of area E. During winter the mean air-sea temperature difference

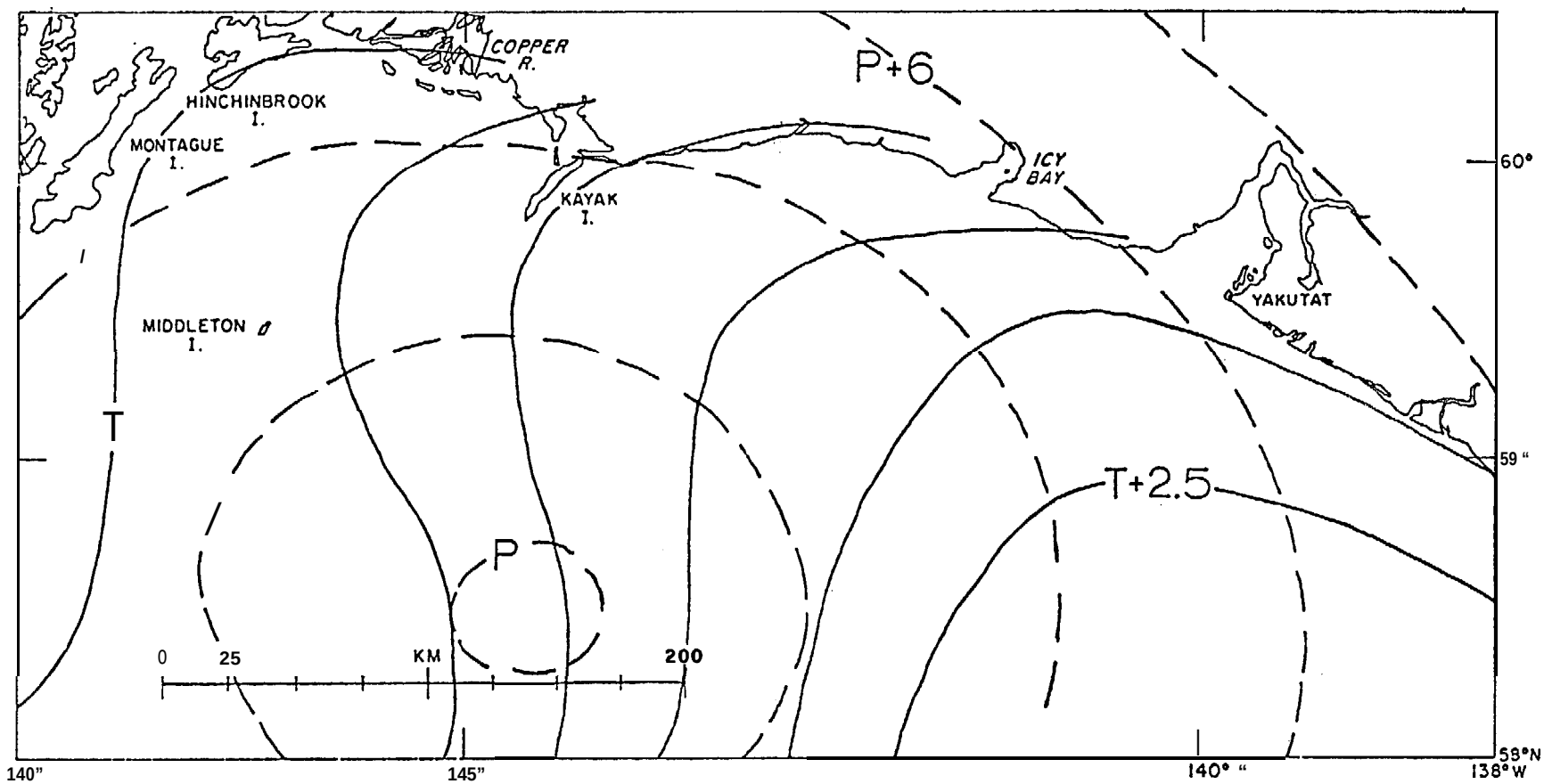

Figure 10. Isotherm pattern used to estimate local winds for pattern type 1.0.

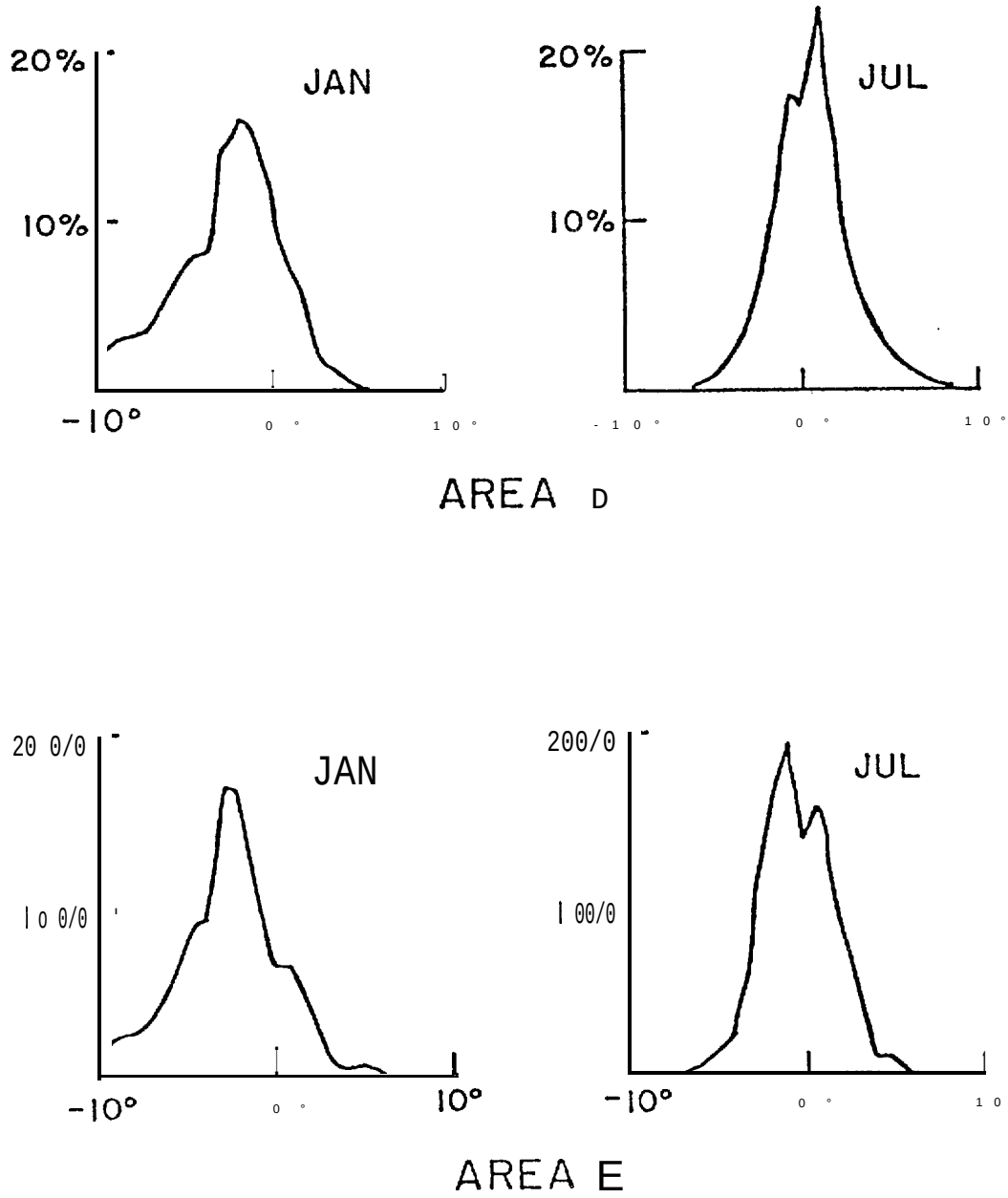

Figure 11. Climatological air-sea temperature distribution for the western Gulf of Alaska (D) and the eastern section (E). (After Brower et al. 1977).

is more negative and the distribution of air-sea temperature difference is broader, reflecting the vigorous temperature advection caused by the more severe winter storms. In area E, the air-sea temperature difference is more negative than in area D due to the advection of warm surface water into that region, and due to offshore flow of cool air. In the spatial distributions of air-sea temperature difference that we created, the means were commensurable with those in figure 11 and our most extreme deviations from the mean were generally within one standard deviation (based on figure 11) of the mean. Figure 12 shows the air-sea temperature differences used for type 1.

Cardone's (1969) Ekman layer model was used to provide the friction velocity u_* and cross isobar flow angle u. The inputs required are the gradient wind speed, G, the magnitude of the PBL horizontal temperature gradient, $\Delta\overline{T}$, the angle between the surface geostrophic wind and the thermal wind, η, and the air-sea temperature difference $\Delta\Theta$. Values of drag coefficient and inflow angle were interpolated from a set of curves produced by running Cardone's model. Figure 13 shows the behavior of u_*/G versus G, η, $\nabla\overline{T}$, and $\Delta\Theta$. Likewise, figure 14 shows the behavior of a.

Surface stress, u_*, was converted to a neutral stratification 10 m surface layer wind speed. That is, a logarithmic wind profile was assumed with the roughness length, Z_0, depending on u_* as (as in Cardone's model, CGS units)

$$z_0 = 0.684/u^* + 4.285 \times 10^{-5} u_*^2 - 4.43 \times 10^{-2}$$

Only constant drag coefficients or drift factors should be used with these winds as wind speed and stability corrections are already included.

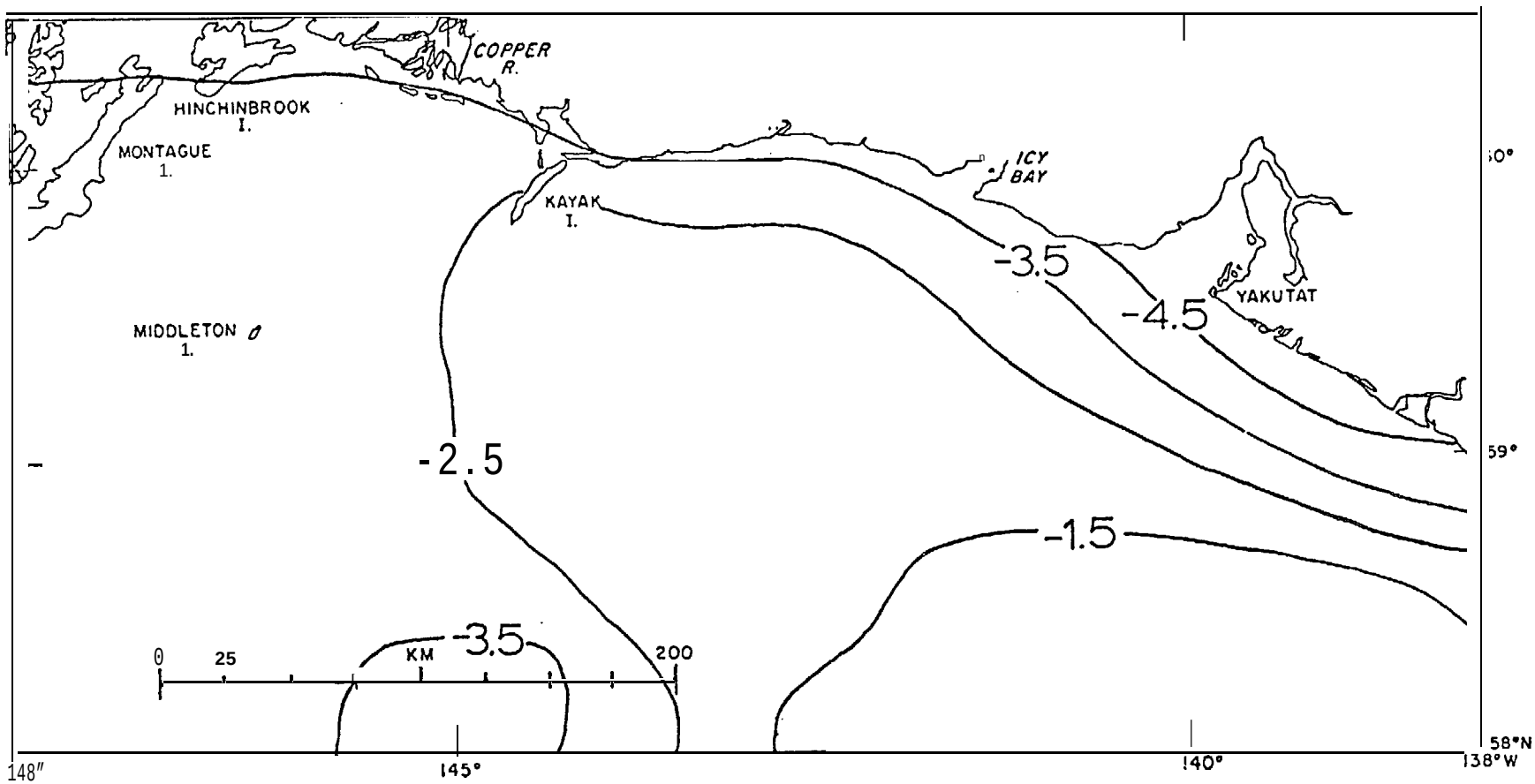

Figure 12. Air-sea temperature difference map used to estimate local winds for type 1.0.

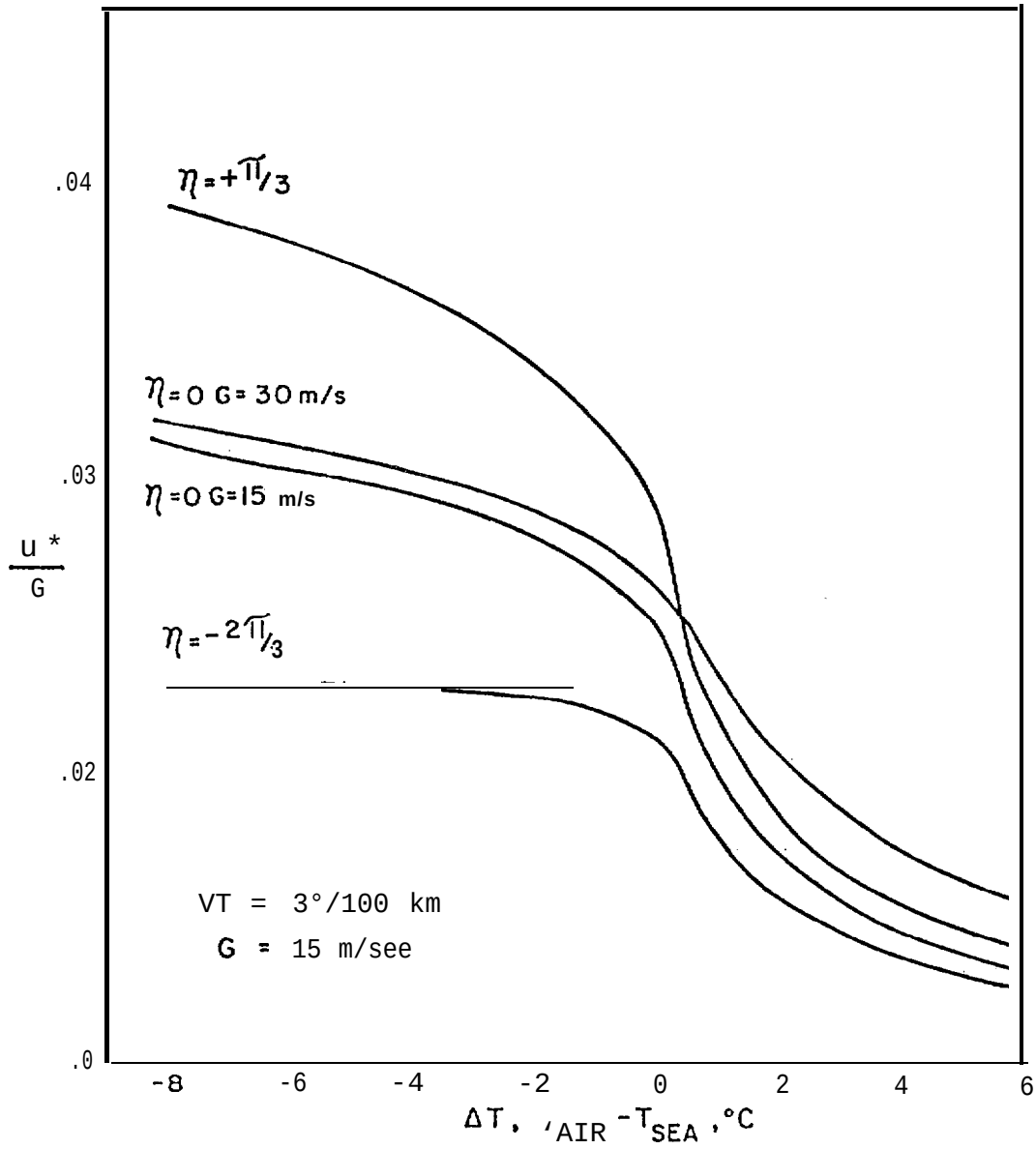

Figure 13. Geostrophic drag coefficient as a function of air-sea temperature difference for Cardone's model. The parameter η is the angle between the geostrophic and thermal wind; G is the gradient wind speed.

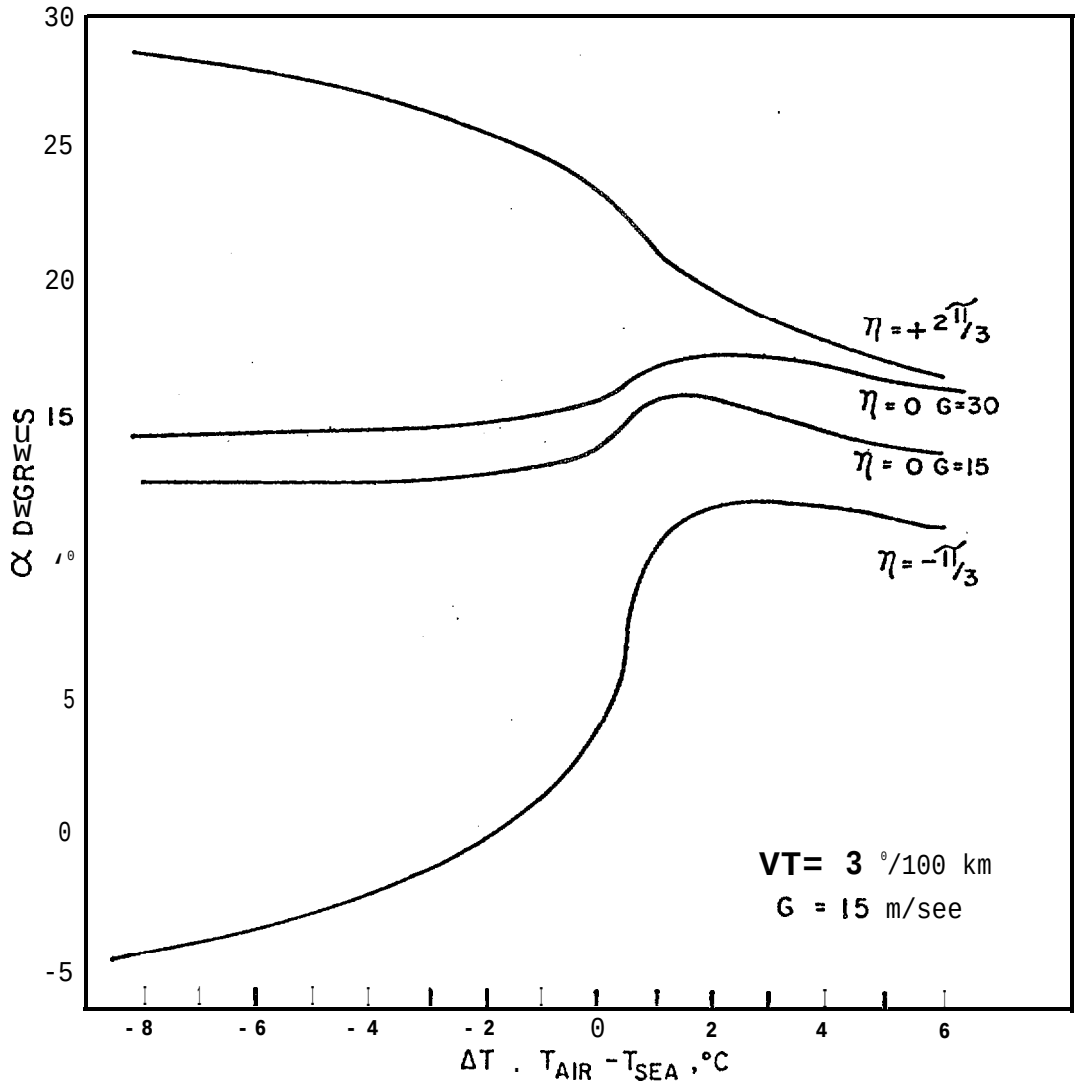

Figure 14. Similar to 13, but for inflow angle (angle of the surface wind to the left of the geostrophic direction).

By comparing the baroclinic, stability dependent 10 rewind field with a wind field based on a constant u*/G = 0.025 for pattern type 1.0, the effects of stability and baroclinicity are about 15%.

Within 50 - 100 km of the coast where Cardone's model is inappropriate, primary guidance was taken from actual measurements and descriptions of coastal processes reported in the draft NOAA Technical Report, "Coastal Meteorology in the Gulf of Alaska, Icy Bay to Yakutat Bay" (Reynolds, Hi ester, Macklin, 1978). That report dealt only with the Icy Bay to Yakutat coastline but the following principles of that area were applied to the remainder of the NEGOA coastline.

Planetary boundary layer air piles up against the sides of coastal mountains when the incident winds are obliquely onshore. A pressure gradient forms normal to the coastline which establishes a longshore geostrophic flow. This orographic forcing is part of the reason that low pressure systems stagnate in the Gulf of Alaska. The length scale of the seaward extent that this deviation from the incident geostrophic flow is discernible is poorly understood. The length scale probably depends on the angle between the initial geostrophic flow and the coast, and the speed of an impinging pressure system. There are indications that this length scale is on the order Of 100 km.

Near the surface and nearshore, the winds are not in geostrophic balance and blow at an angle to the coastline. Within 20 km of the coast, the winds can have an offshore katabatic component due to drainage of denser air from the mountain valleys and glaciers. This is an almost permanent feature in winter but occurs mainly at night in the summer. Winds nearshore also respond to the coastal discontinuity in frictional drag creating an offshore wind

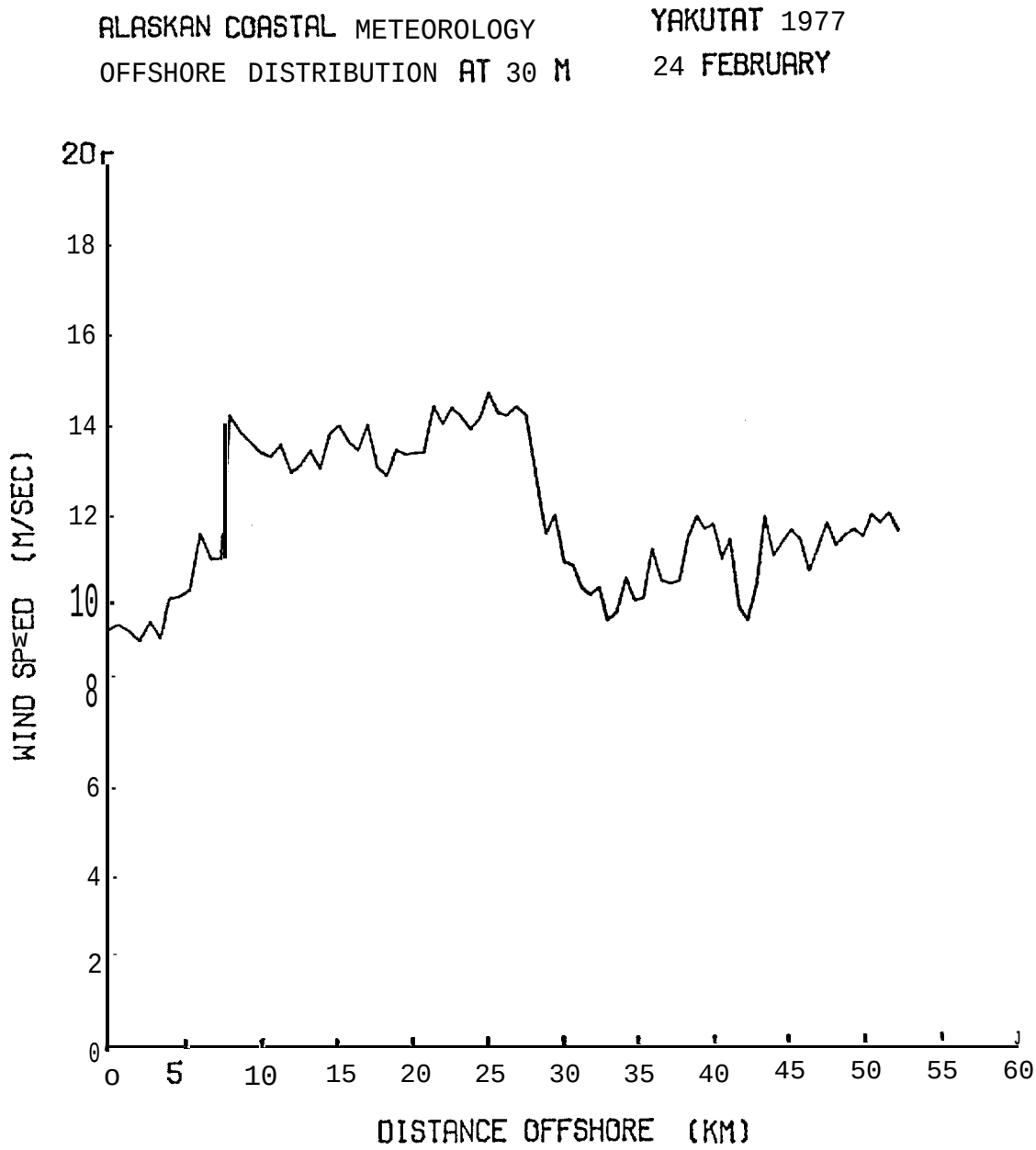

Figure 15a. Wind speed as a function of offshore distance.

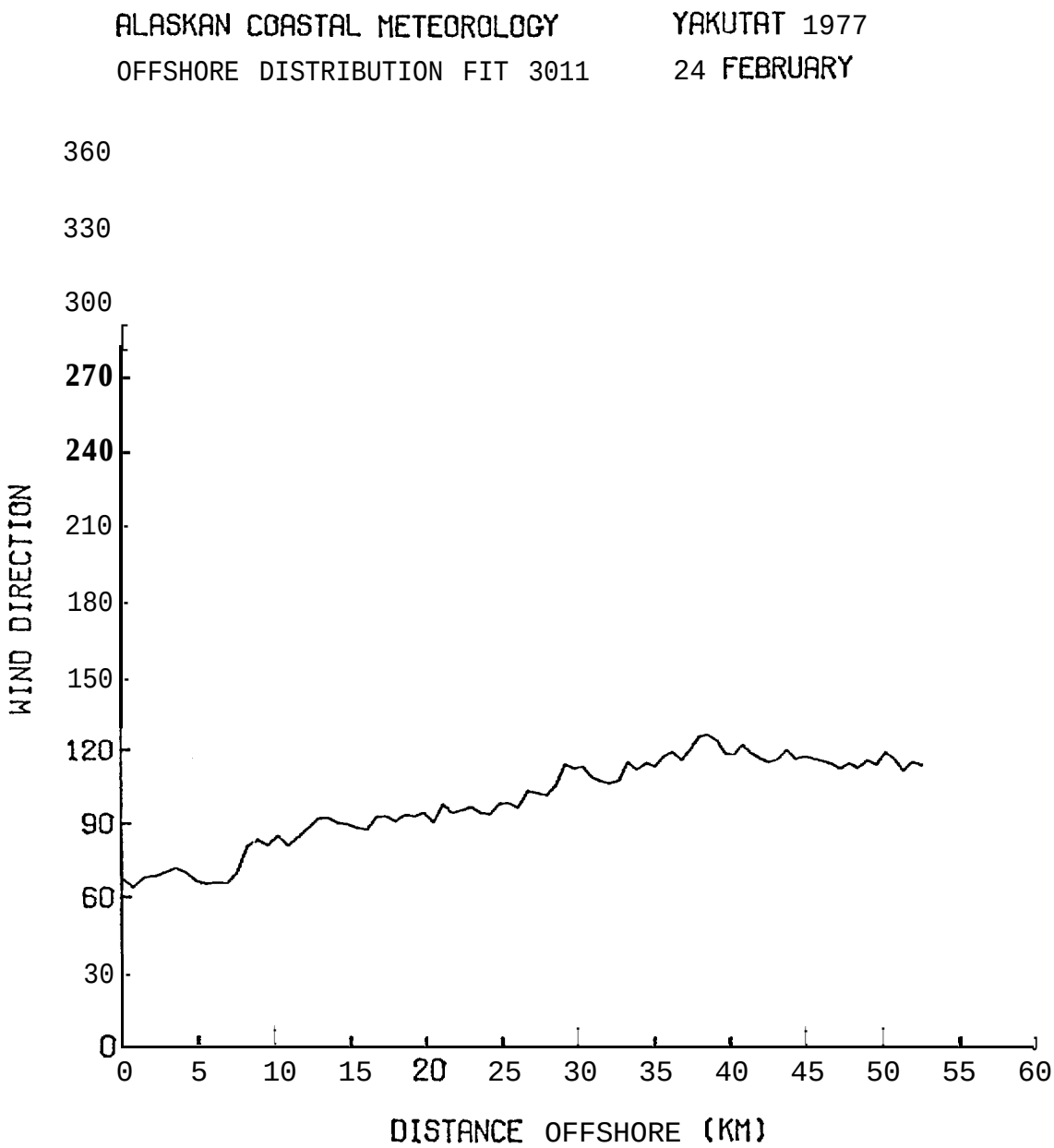

Figure 15b. Direction of the 30 meter wind as a function of offshore direction.

component when there are longshore easterlies in NEGOA and an onshore component for longshore westerlies.

Figure 15 shows the wind speed and direction measured from an aircraft in a line directly offshore of the Malaspina Glacier. Nearshore winds were blowing from the NNE, slightly offshore and out of Yakutat Bay, while 50 km offshore, the winds were from the SE. Where the offshore and the onshore winds merged, the flow accelerated and formed a coastal jet 10 to 30 km offshore and parallel to the shore. That was the best example measured, but we believe the jet is a frequently occurring feature. The sensitivity of the jet to variations in meteorological parameters remains unknown.

In winter the winds nearshore are persistently offshore but in summer the drainage winds are weak and easily overcome by an onshore push. There is a deceleration as the shore is approached. Data from EB-70, EB-43, and an anemometer at Pt. Riou (on the shore at the western tip of the Malaspina Glacier) were used to scale these decelerations.

After using the above principles to modify the coastal winds, the wind fields were smoothed. A nine point smoother was used on all grid boxes that were at least one box away from the shore. The filter smooths the effects of the interpolation and truncation error.

Finally, the divergence at each grid point was computed for every wind field. The contours of the divergence field (x 10^5) for type 1.0 are shown in figure 16. The values at the coastline cannot be taken too literally as the wind vectors only represent the over water wind. The figure provides confidence in the overall method. There is convergence (of sensible magnitude) at the center of the storm, divergence behind the cold front, and convergence just off the coast where onshore flow meets katabatic flow.

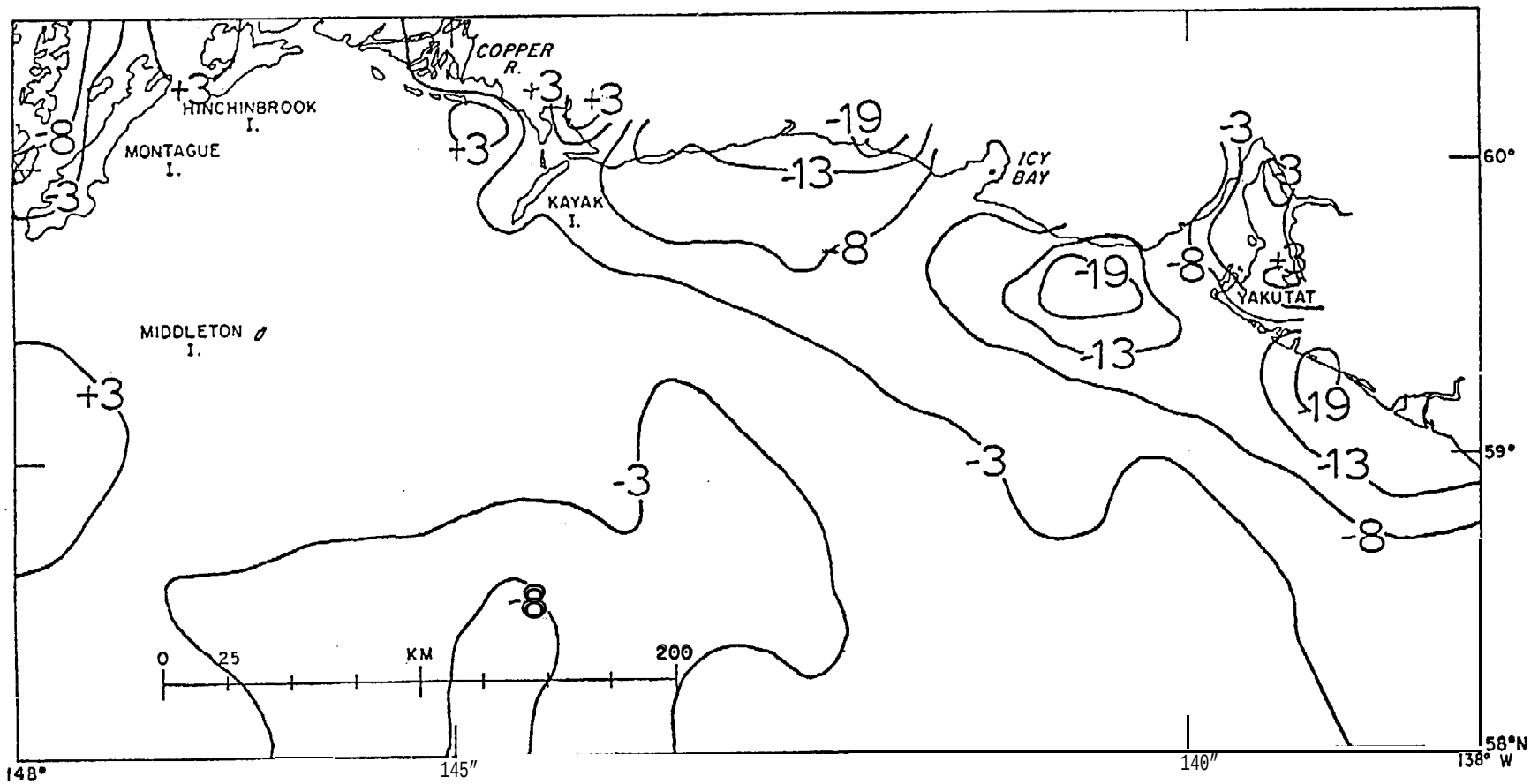

Figure 16. Divergence field calculated from the local wind field for type 1.0.

4.2 Description of Local Wind Fields

This section presents thirteen velocity fields for the synoptic subtypes described in section 2. Arrow plots are contained in Appendix C. A velocity vector applies only to the overwater portion of a box that spans the coastline. The length of each arrow is a measure of the relative wind speed, and each arrow points downwind.

Synoptic pattern 1 (figure 2) represents a low pressure system contained within the Gulf of Alaska by coastal mountains. This pattern was broken down into four subtypes corresponding to four positions of the storm center as it migrates through the Gulf. Figure C4 is the vector plot for type 1.3 with the storm center at 57°N 152°W, just east of Kodiak island. The topographical forcing of the boundary layer is not yet strong so the flow near shore, in the mid to western portions of our grid, is onshore. Near the shoreline and at the surface (not necessarily representative of the entire depth of the PBL) there is offshore katabatic flow. Fed by surrounding tributaries, the drainage flow is deeper in the estuaries such as Yakutat Bay and hence dominates the wind fields in those regions. Whenever flow encounters land it decelerates and turns toward lower pressure. For example, the winds that blow across Kayak Island are retarded and deflected to the south. The air accelerates around the southern tip of the island to rejoin undisturbed flow on the lee side. The winds are also generally slowed by the landforms at the entrances to the Copper River Delta and Prince William Sound, however some passes channel and accelerate the flow.

Figure C2 is the wind field for type 1.1 when the storm is centered

at about 50°N 148°W. The considerations are similar to those documented for type 1.3.

The archetype for this series, type 1.0 with the storm as shown in figure Al, is given in figure Cl. As the storm moves eastward into this position the orographic forcing of the PBL becomes strong, especially in the Yakutat to Kayak Island region. There the offshore flow (katabatically, frictionally and topographically forced) meets the onshore flow and the two form an alongshore jet. The winds blowing offshore in the western portion of the grid accelerate from their nearshore speeds up to their open ocean speeds, causing some divergence there.

Figure C3 shows the wind field for type 1.2. The storm is at it's eastern extreme; at about 58°N 141°W. The alongshore jet is mostly east of our grid region but is visible entering the region at the eastern border. The jet quickly dissipates in the difluent region in the northwest quadrant of the storm.

Type 2 represents an Aleutian low as shown in figure A5. The local wind field is shown in figure C5. There is also an alongshore jet for this type. Since the flow in the eastern part of the grid is roughly alongshore, there is no alongshore acceleration there. The jet forms between Icy Bay and Kayak Island where the geostrophic flow is more directly onshore. The confluence at the mouth of the Yakutat Bay and the deceleration windward of Kayak Island cause those areas to be convergence centers. There is relief behind Kayak Island where the winds turn northward to almost be in geostrophi c-frictional balance before encountering the drainage winds in the Copper River area. The winds are slowed by the land masses in the Cape Hinchinbrook region but are not blocked by them. Figure C6

represents an autumn case of type 2.1 with a remnant of high pressure to the east.

We have split the synoptic type 3 (figure A7) into two cases. Type 3.0 (figure C7) is the usual case where the anti cyclone over the Yukon dominates the NEGOA area. This is typically a time of clear skies. Radiational cooling of the land surfaces causes katabatic flow, especially off of the Bering, Malaspina, and Hubbard Glaciers. East of Yakutat, the winds accelerate offshore making it a region of divergence. From Yakutat Bay to Kayak Island there is convergence of katabatic and alongshore winds. West of the Bering Glacier is another region of divergence. The winds blowing from the Copper River delta hit Hinchinbrook and Montague Islands quite obliquely, so we show the air blowing roughly parallel to those shores and around the islands to the south rather than making the more energy consuming trip over the tops as in the previously described types. The eastern shores of these islands are therefore in a convergent region.

Type 3.1 (figure C8) allows for the reported cases of very strong (50 to 100 knots) winds near shore along the NEGOA coast. The surface pressure pattern is virtually indistinguishable from that of type 3.0. The air northeast of the coastal mountains is very cold throughout a very deep layer; i.e., the 1000-500 mb thickness is less northeast of the mountains than in the Gulf. When the reservoir of cold air gets deep enough, the cold air spills through the mountain passes like water over a dam. The low temperature is somewhat maintained (against adiabatic warming during descent) by flow over the radiationally cooled icefields. Large velocities build up as the air drains out of the prominent valleys. We have allowed strong winds to blow out of the Alsek River Valley, Yakutat Bay, Icy Bay, off the

Bering Glacier, and from the Copper River Valley.

The Icy Bay winds are strongest and actually blow off the Malaspina Glacier just east of Icy Bay. Guidance for this location came from a run of the regional meteorological model described by Overland et al. (1978). We assumed the core of strong winds would totally mix with the ambient air about 100 km downstream of the shore. Most cores turn to the right as they mix with the ambient flow. The Bering Glacier and Copper River winds meet and mutually interfere.

Synoptic pattern 4 (figure A8 and A9) is a summertime case when a large low pressure system over central Alaska dominates with the Pacific high retreating to the south. It is also observed if the Aleutian Low (type 2) drifts north. In the local wind fields (figure C9 and C10) we weaken the katabatic flow off the ice (the land surfaces may be warmer than the ocean), and the land-sea frictional differences encourage onshore flow. The winds also blow up estuaries, unlike previously described cases.

Synoptic pattern 5 (figure A10 and All) represent the predominate summer case of the Pacific anticyclone. The local wind fields, shown in figure Cll and Cl2 were treated similarly to type 4. There is some topographical forcing, however, as the isobars are slightly packed on the eastern side of the high. The central area of the high is divergent with the onshore flow at the coast being convergent.

Synoptic type 6 (figure A12) represents the low pressure center west of the Queen Charlotte Islands. Frequently this low stagnates and fills in place, but it also may move NNW into the Gulf of Alaska and become type 1.2. The local wind field (figure C13) is divergent over most of the NEGOA grid. Guidance in scaling the small horizontal variations for this pattern was

taken from aircraft measurements made under similar synoptic conditions, reported in the Reynolds et al. report.

4.3 Evaluation

July-August 1974 and February-March 1975 were visually typed from the hand drawn sea level pressure analyses from the National Meteorological Center every twelve hours through these periods (Table 6 and 7).

Figure 17 shows the direction of the local wind (meteorological) at Middleton Island for each weather type as inferred from figures Cl - C13. For comparison the anemometer record at Middleton Island during the sample periods was stratified by synoptic type. Vector mean winds were then computed within each type and plotted for the winter period on figure 17 and for the summer period in figure 18. A similar plot for winter at EB-33 is shown in figure 18. Middleton winds show good agreement with the subjective types. Figure 18 indicates that EB-33 contained more of an alongshore component to the winds than inferred subjectively.

TABLE 6. SUBJECTIVE TYPING--WINTER

DAY	TIME (GMT)	TYPE	DAY	TIME (GMT)	TYPE	DAY	TIME (GMT)	TYPE
FEBRUARY, 1975								
1	00	6.0	23	00	2.0	16	00	3.0
1	12	6.0	23	12	5.0	16	12	1.3
2	00	6.0	24	00	4.0	17	00	1.3
2	12	6.0	24	12	2.1	17	12	6.0
3	00	6.0	25	00	1.3	18	00	6.0
3	12	6.0	25	12	2.0	18	12	6.0
4	00	6.0	26	00	1.3	19	00	6.0
4	12	5.1	26	12	2.0	19	12	1.0
5	00	5.1	27	00	4.0	20	00	5.0
5	12	5.1	27	12	2.1	20	12	4.0
6	00	3.0	28	00	5.0	21	00	2.1
6	12	6.0	28	12	5.0	21	12	4.0
7	00	6.0	MARCH, 1975			22	00	4.1
7	12	1.2				22	12	1.2
8	00	2.0	1	00	6.0	23	00	1.1
8	12	2.0	1	12	6.0	23	12	1.1
9	00	4.1	2	00	5.1	24	00	1.1
9	12	6.0	2	12	3.0	24	12	4.0
10	00	6.0	3	00	6.0	25	00	4.1
10	12	6.0	3	12	5.0	25	12	4.1
11	00	6.0	4	00	2.1	26	00	1.3
11	12	1.0	4	12	2.0	26	12	1.3
12	00	1.0	5	00	1.3	27	00	2.0
12	12	1.0	5	12	1.0	27	12	2.0
13	00	1.1	6	00	1.0	28	00	2.0
13	12	1.1	6	12	1.2	28	12	3.0
14	00	1.1	7	00	6.0	29	00	2.0
14	12	2.0	7	12	6.0	29	12	4.1
15	00	4.0	8	00	5.1	30	00	5.1
15	12	4.0	8	12	1.2	30	12	5.0
16	00	5.0	9	00	1.0	31	00	1.3
16	12	2.0	9	12	2.0	31	12	5.0
17	00	1.3	10	00	3.0			
17	12	4.0	10	12	2.0			
18	00	2.0	11	00	2.0			
28	12	2.1	11	12	4.0			
19	00	2.0	12	00	5.0			
19	12	4.1	12	12	2.0			
20	00	4.0	13	00	3.0			
20	12	4.1	13	12	2.0			
21	00	2.0	14	00	1.3			
21	12	2.0	14	12	1.2			
22	00	2.0	15	00	1.3			
22	12	4.0	15	12	1.1			

TABLE 7. SUBJECTIVE TYPING--SUMMER

DAY	TIME (GMT)	TYPE	DAY	TIME (GMT)	TYPE	DAY	TIME (GMT)	TYPE
JULY, 1974								
1	00	1.3	23	00	1.3	13	00	5.1
1	12	1.3	23	12	2.1	13	12	5.1
2	00	4.1	24	00	1.1	14	00	5.1
2	12	2.1	24	12	4.0	14	12	5.?
3	00	4.1	25	00	4.0	15	00	5.1
3	12	4.0	25	12	1.1	15	12	5.1
4	00	5.0	26	00	5.0	16	00	5.1
4	12	5.1	26	12	5.1	16	12	5.0
5	00	5.1	27	00	5.1	17	00	5.1
5	12	1.1	27	12	5.1	17	12	5.1
6	00	1.1	28	00	5.0	18	00	1.0
6	12	5.1	28	12	5.0	18	12	4.1
7	00	5.1	29	00	4.0	19	00	5.1
7	12	5.0	29	12	5.0	19	12	5.1
8	00	5.1	30	00	5.1	20	00	4.1
8	12	5.0	30	12	5.1	20	12	1.1
9	00	5.1	31	00	5.1	21	00	4.1
9	12	5.1	31	12	4.0	21	12	4.0
0	00	5.1	AUGUST, 1974			22	00	4.0
0	12	1.1				22	12	4.0
1	00	1.1	1	00	3.0	23	00	1.1
1	12	1.3	1	12	2.0	23	12	4.1
2	00	1.1	2	00	1.3	24	00	4.1
2	12	1.1	2	12	1.3	24	12	5.0
3	00	2.1	3	00	1.1	25	00	1.3
3	12	2.0	3	12	1.1	25	12	1.3
4	00	4.0	4	00	1.1	26	00	1.0
4	12	5.1	4	12	6.0	26	12	4.0
5	00	5.1	5	00	5.0	27	00	2.1
5	12	5.1	5	12	4.0	27	12	2.0
6	00	4.0	6	00	2.1	28	00	2.1
6	12	5.1	6	12	2.1	28	12	2.1
7	00	4.1	7	00	2.1	29	00	2.1
7	12	5.1	7	12	1.3	29	12	2*1
8	00	5.0	8	00	1.1	30	00	2.1
8	12	4.0	8	12	4.0	30	12	2.1
9	00	4.0	9	00	5.0	31	00	5.1
9	12	2.1	9	12	5.0	31	12	4.0
0	00	2.1	10	00	5.0			
0	12	2.0	10	12	5.1			
1	00	2.0	11	00	5.1			
1	12	1.3	11	12	5.1			
2	00	1.3	12	00	5.1			
2	12	1.1	12	12	5.1			

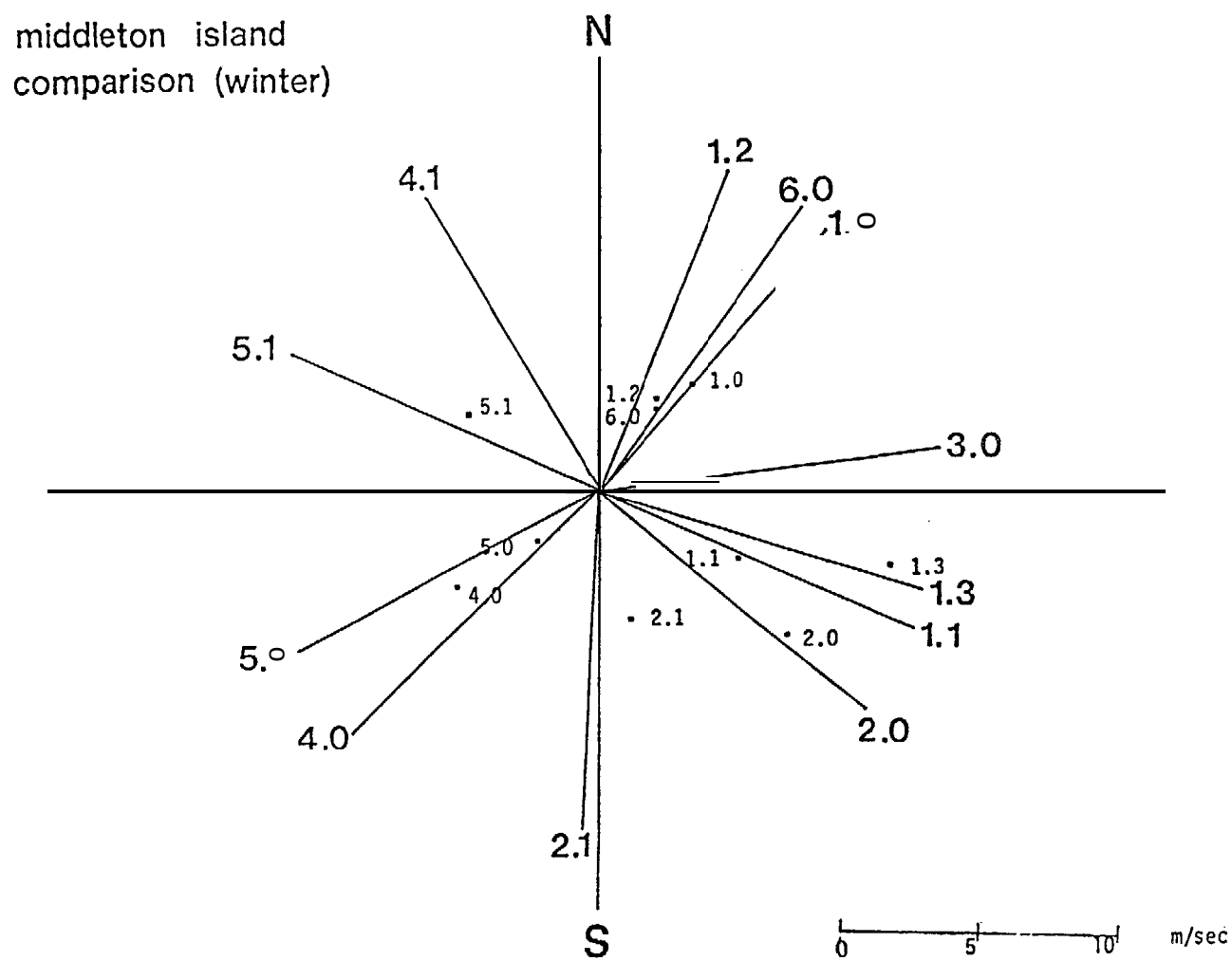

Figure 7. Direction of local wind types at Middleton Island. Dots represent the vector mean observed wind at Middleton stratified by subtypes for the February - March 1975 period.

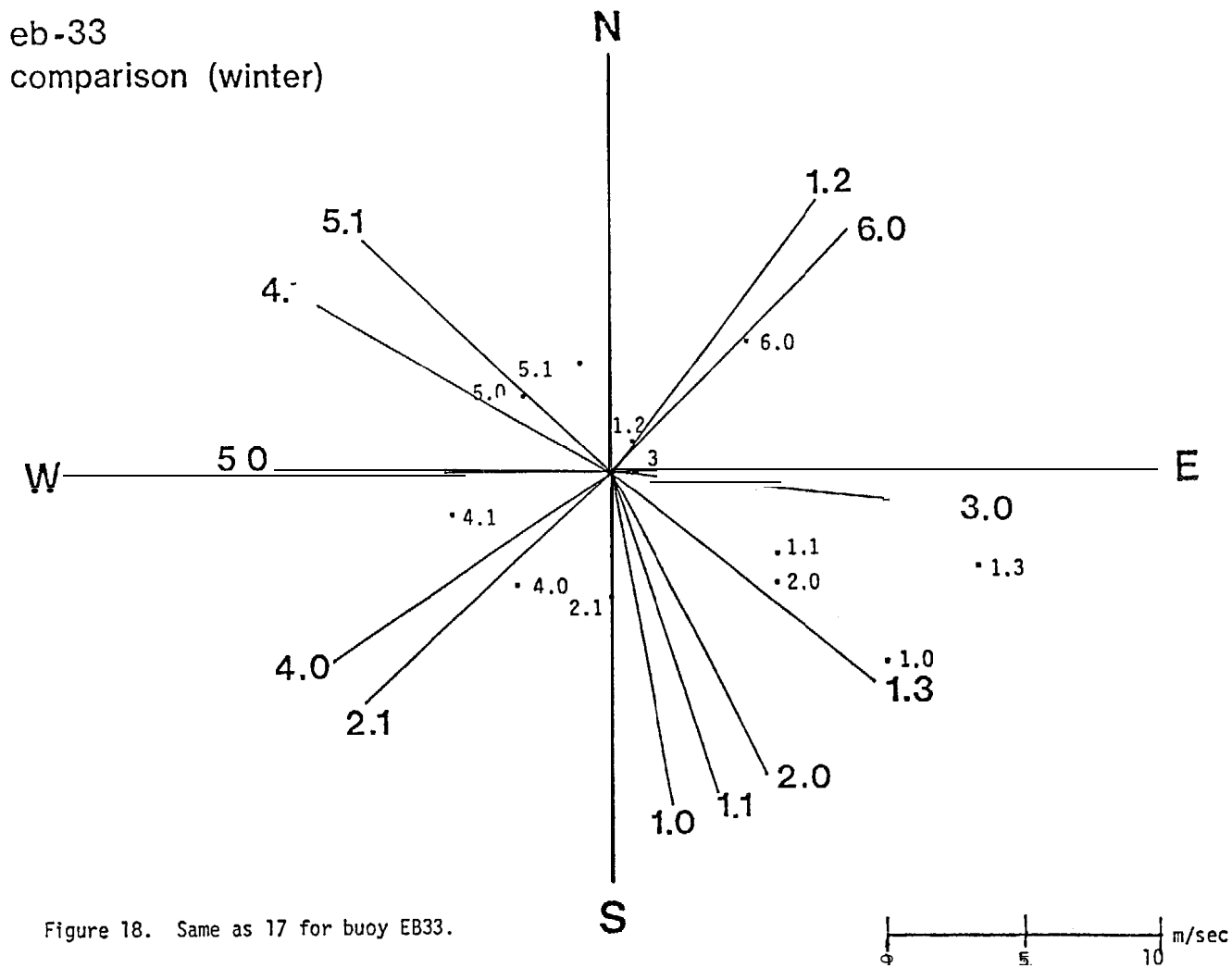

Figure 18. Same as 17 for buoy EB33.

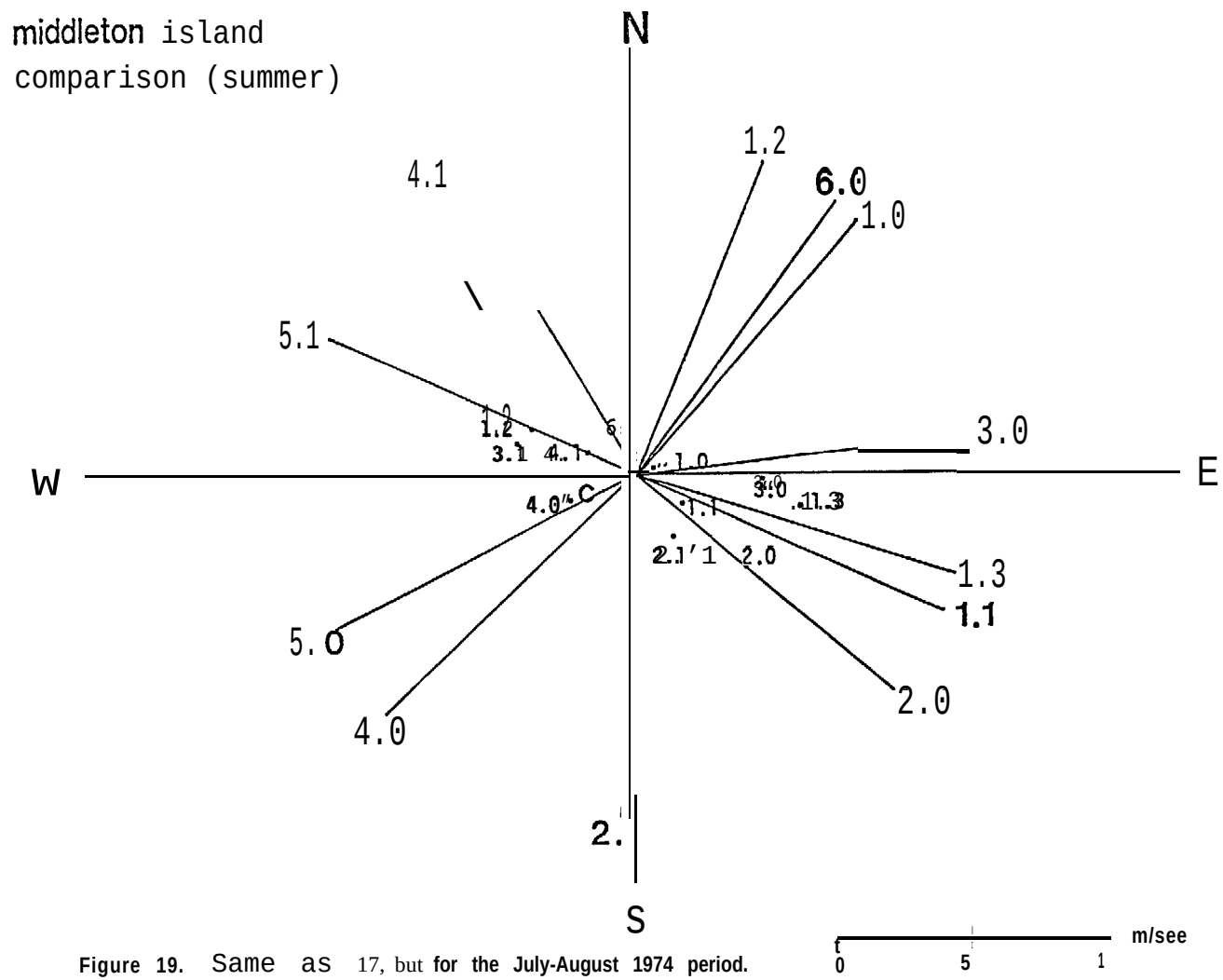

Figure 19. Same as 17, but for the July-August 1974 period.

REFERENCES

Barry, R.G., and A.H. Perry. Synoptic Climatology, Methods and Application. London: Methuen & Co., 1973, 553 pp.

Biasing, T.J. A comparison of map patterns correlation and principal component eigenvector methods for analyzing climate anomaly patterns, in Preprints Fourth Conf. Probability and Statistics in the Atmospheric Sciences, Amer. Meteor. Sot. 1975 p. 96-101.

Brewer, J.R.W.A. , Diaz H.F., Prechtel A.S. Searby, H.W. and J.L. Wise. Climatic Atlas of the Outer Continental Shelf waters and coastal Regions of Alaska: Vol. 1 Gulf of Alaska, National Climate Center, Environmental Data Service, NOAA, Ashville N.C. 1977, 439 pp.

Cardone, V.J. Specification of the wind distribution in the marine boundary layer for wave forecasting. Report GSL TR69-1 New York University School of Engineering and Science. 1969, 131 pp.

Cressman, G.P. An operational objective analysis system. Mon. Wea. Rev. 1959 87, 367-374.

Flattery, T.W. Spectral Models for global analysis and forecasting. in Proceedings sixth AWS Technical Exchange Conference, AWS Tech Rept. 242, Scott AFB, Ill., 1970, pp. 42-54.

Jenne, R.L. Data sets for meteorological research. NCAR Tech Note NCAR-TN/1A-111 1975, 194 pp.

Kendall, M.G. and A. Stewart. The Advanced Theory of Statistics Vol. 3. New York N.Y.: Hafner Press, 1975. 585 pp.

Lund, I.A. Map pattern classification by statistical methods. J. Appl. Meteor. 2 1963, p. 56-65.

Overland, J.E. Hitchman M.H. and Y.J. Han A Regional Surface Wind Model for Mountainous Coastal Areas PMEL/ERL/NOAA Tech Report (In Press) 1978

Putnins, P. The sequence of baric pressure patterns over Alaska. Studies on the meteorology of Alaska Ist Interim Report Washington. D.C. Environmental Data Service ESSA, 1966. 57 pp.

Reynolds, R.M. Hiester, T.R. and S.A. Macklin. Coastal Meteorology of the Gulf of Alaska Icy Bay to Yakutat Bay. PMEL/ERL/NOAA Tech Report IIn press) 1978.

Singh, S.V., Mooley D.A., and R.H. Kripalani Synoptic Climatology of the Daily 700mb Summer Monsoon Flow Patterns over India. Mon. Wea. Rev. 106 1978 510-525.

Sorkina A.I. Tipy atmosfernoi tsirkuliatsii Israel Program for Scientific Translations, Jerusalem 1963. pp. 247.

APPENDIX A

1. Subjective Subtype Patterns 1.0-6.0 (l-land Drawn)
2. Subjective Subtype Patterns 1.0-6.0 (Machine Drawn)
3. Percent of Occurrence and Transition Probabilities for Subtypes
4. Correlation Matrix Between Subjective Types

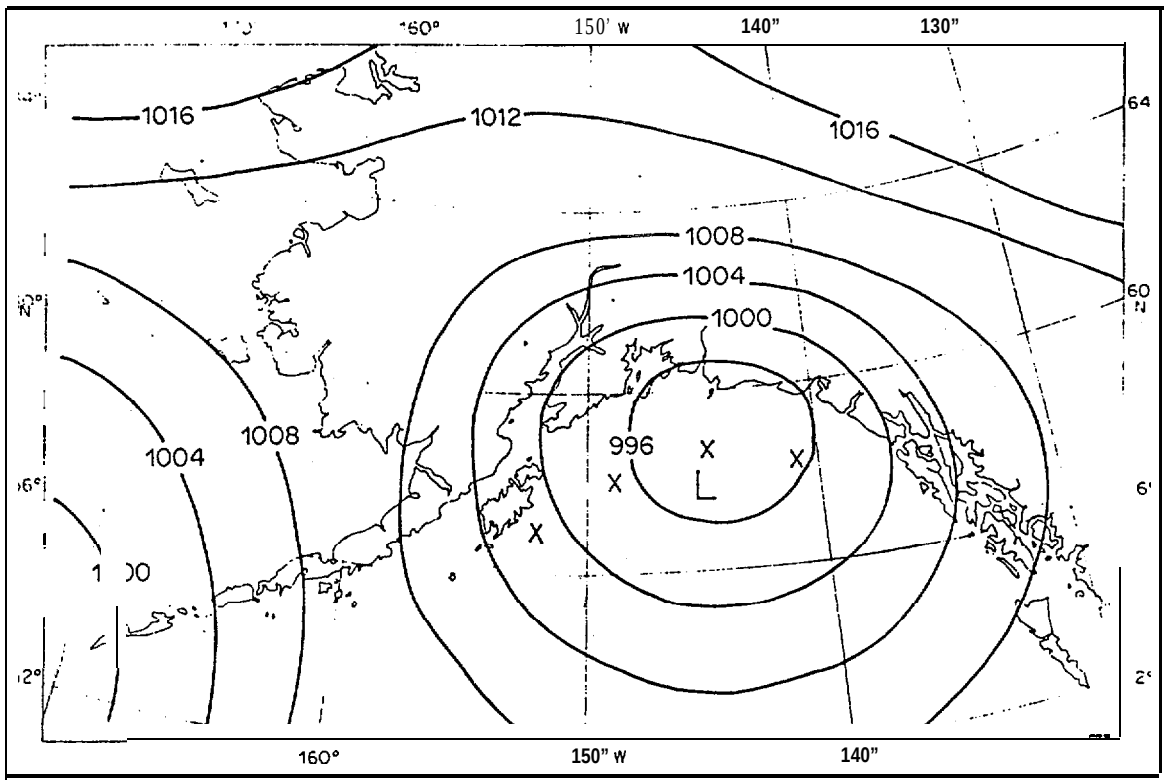
160°
150' W
140"
130"
1016
1012
1016
1008
1004
1000
996
L
1004
1008
160°
150" W
140"

1.0

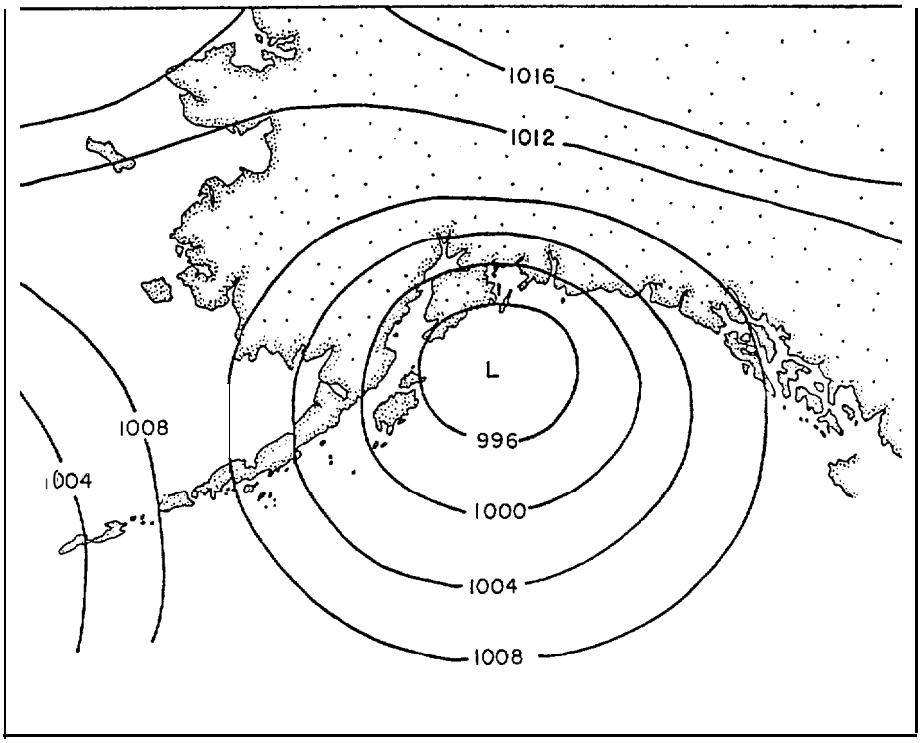
1016
1012
L
996
1008
1004
1000
1004
1008

1.1

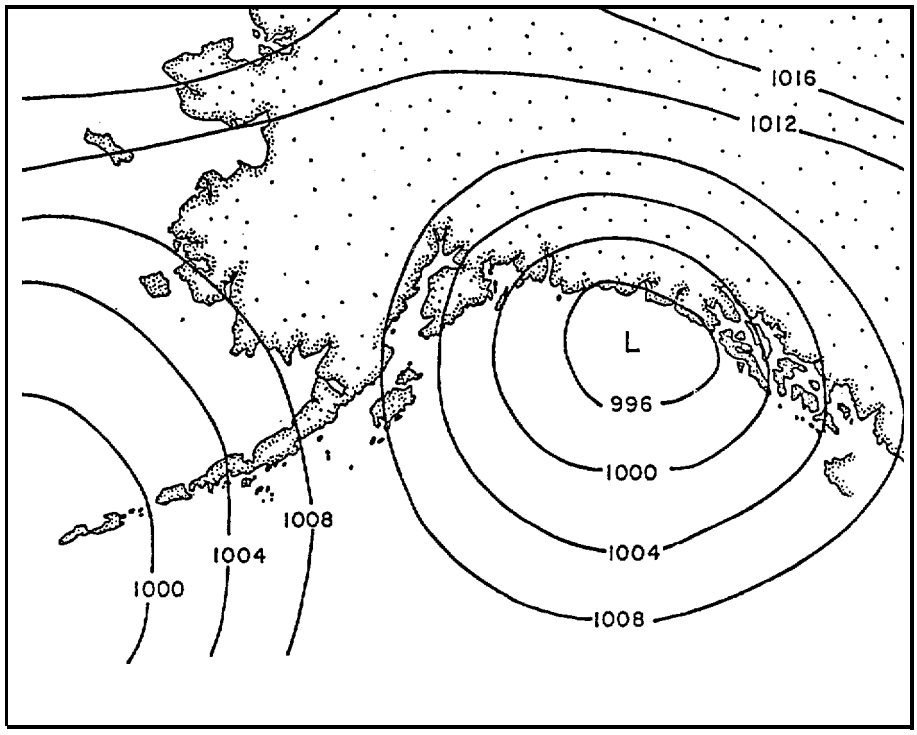
1016
1012
L
996
1000
1004
1008
1008
1004
1000

1.2

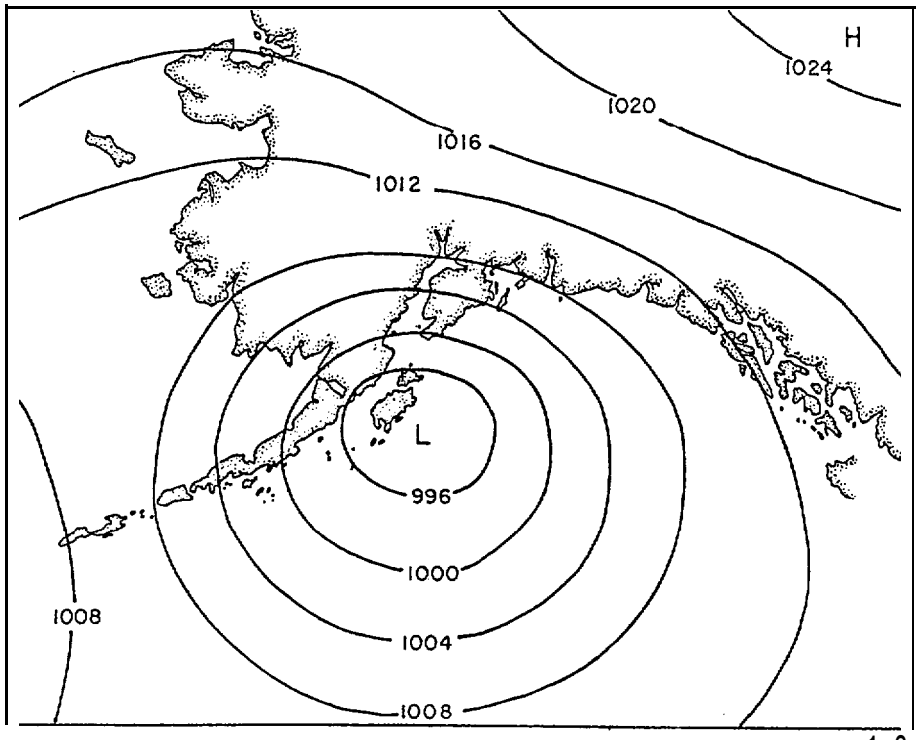
H
1024
1020
1016
1012
L
996
1000
1004
1008
1008

1.3

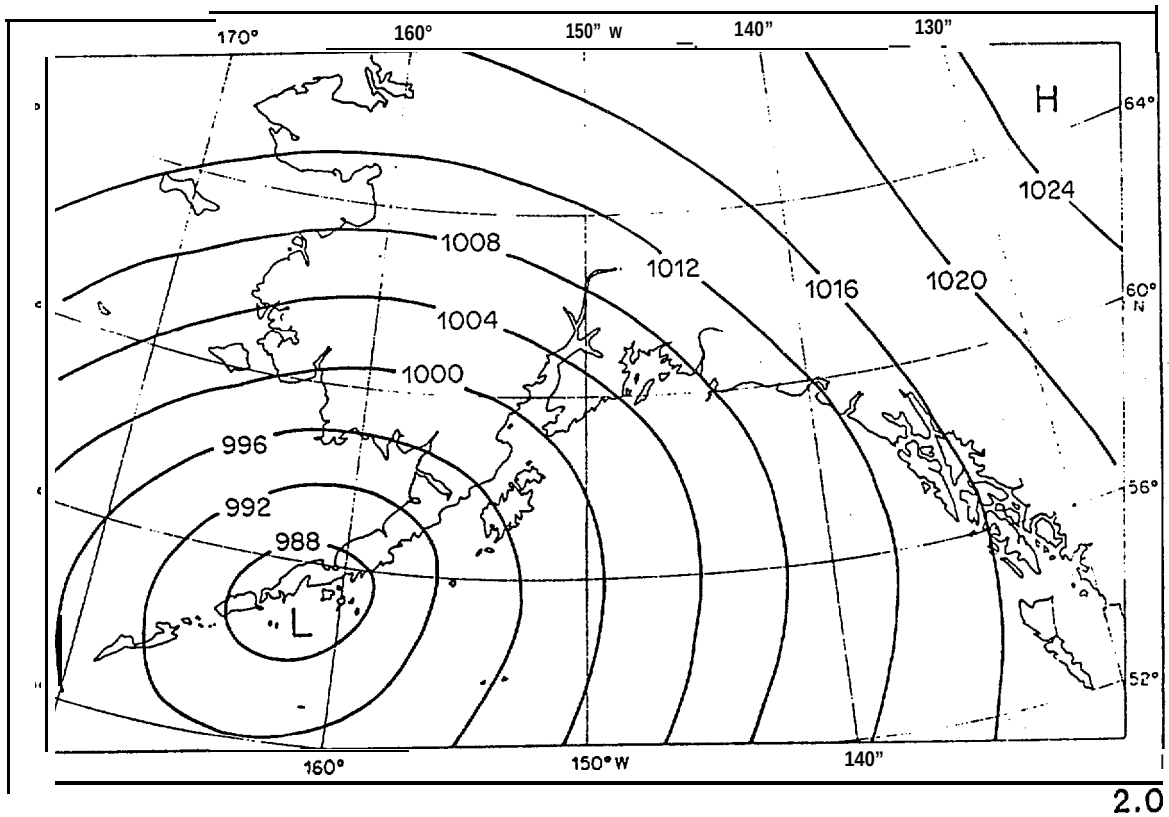
170°
160°
150° W
140°
130°
H
64°
1024
1008
1012
1016
1020
60° N
1004
1000
996
992
988
L
56°
52°
160°
150° W
140°

2.0

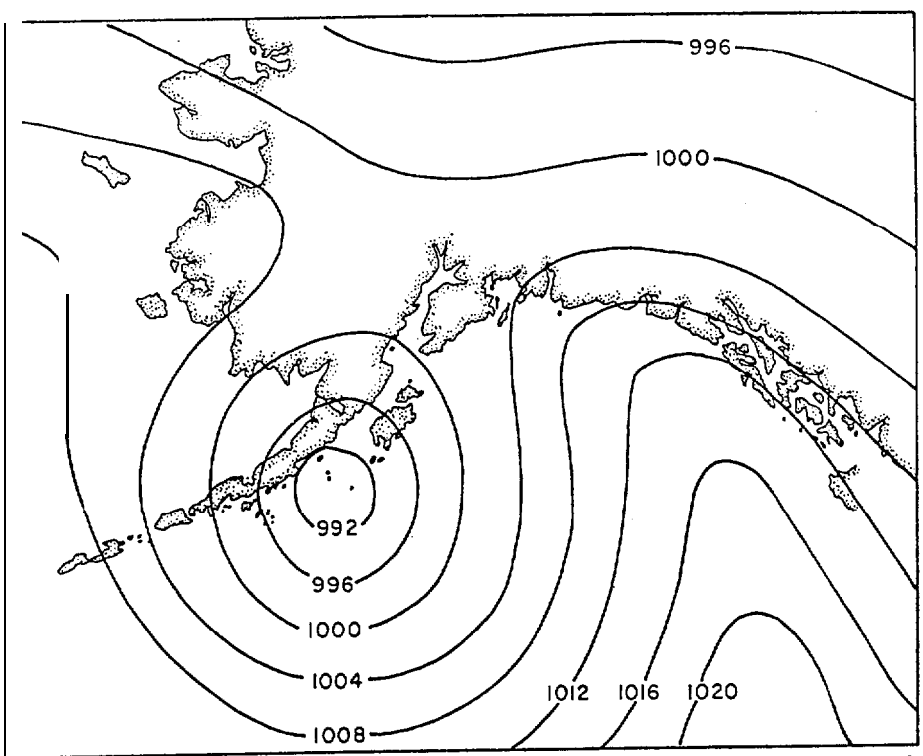
996
1000
992
996
1000
1004
1008
1012
1016
1020

2.1

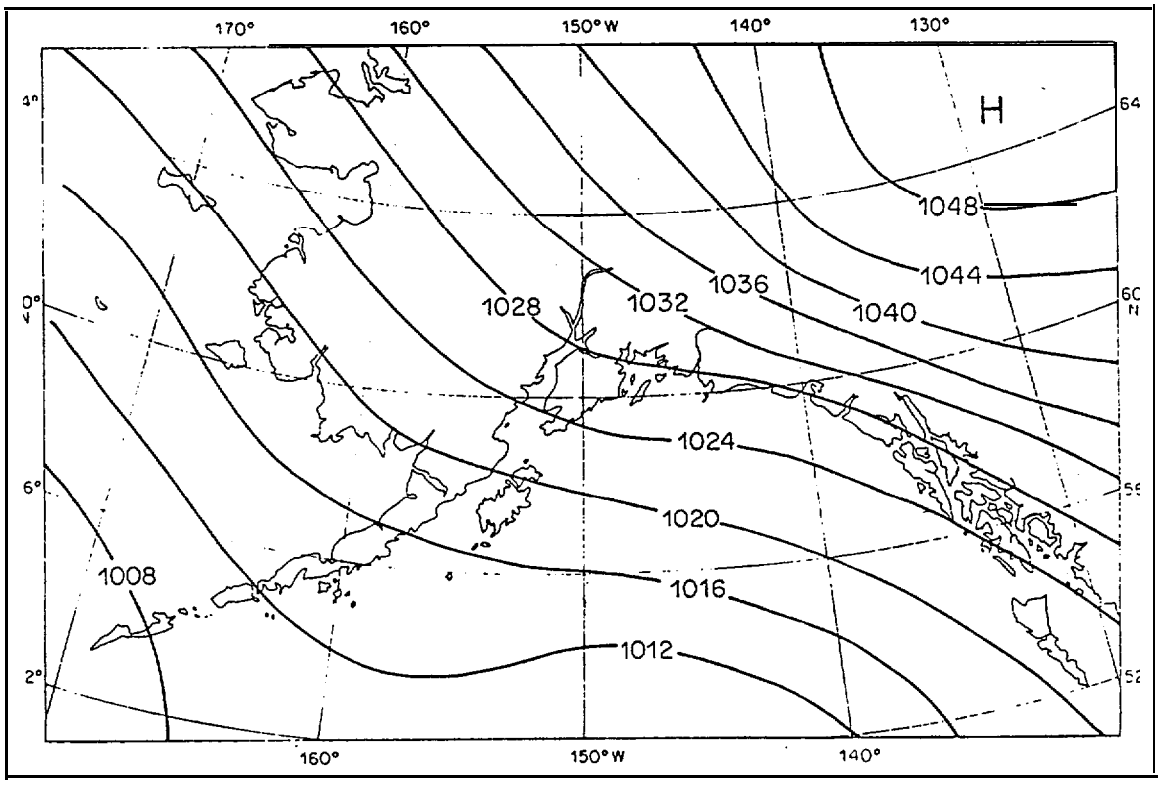
170°
160°
150° W
140°
130°
H
1048
1044
1040
1036
1032
1028
1024
1020
1016
1012
1008
64
60
56
52
160°
150° W
140°

300

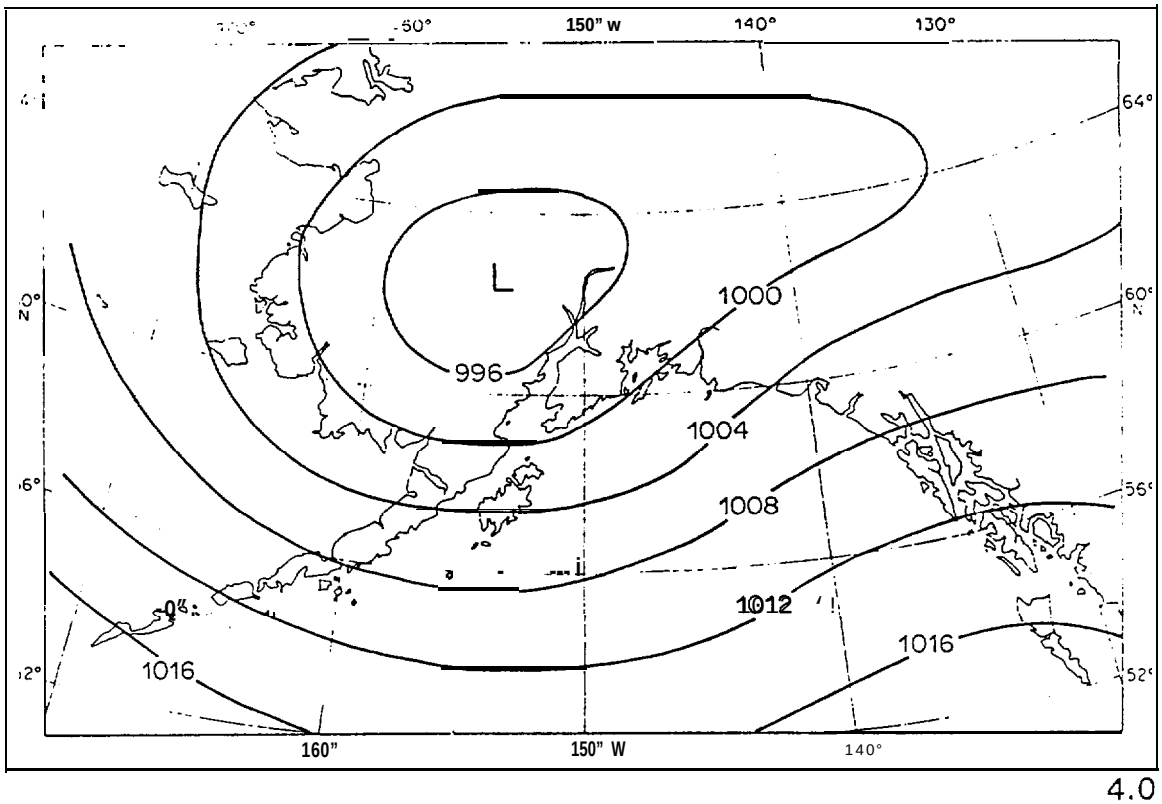
150" w
140°
130°
L
1000
996
1004
1008
1012
1016
1016
64°
60°
160"
150" W
140°

4.0

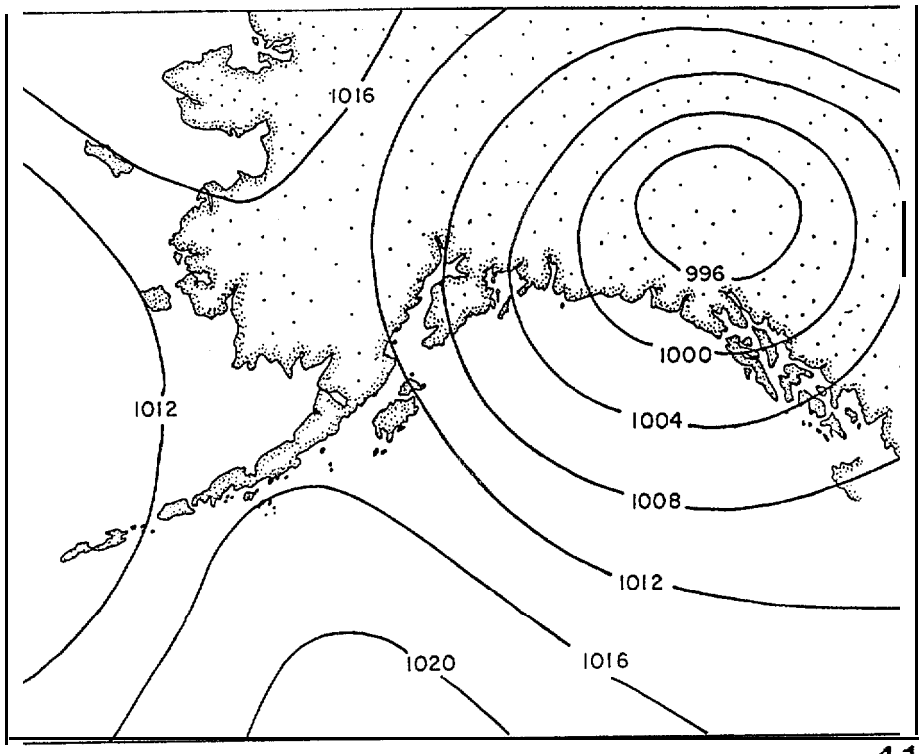
1016
996
1000
1004
1008
1012
1012
1020
1016

4.1

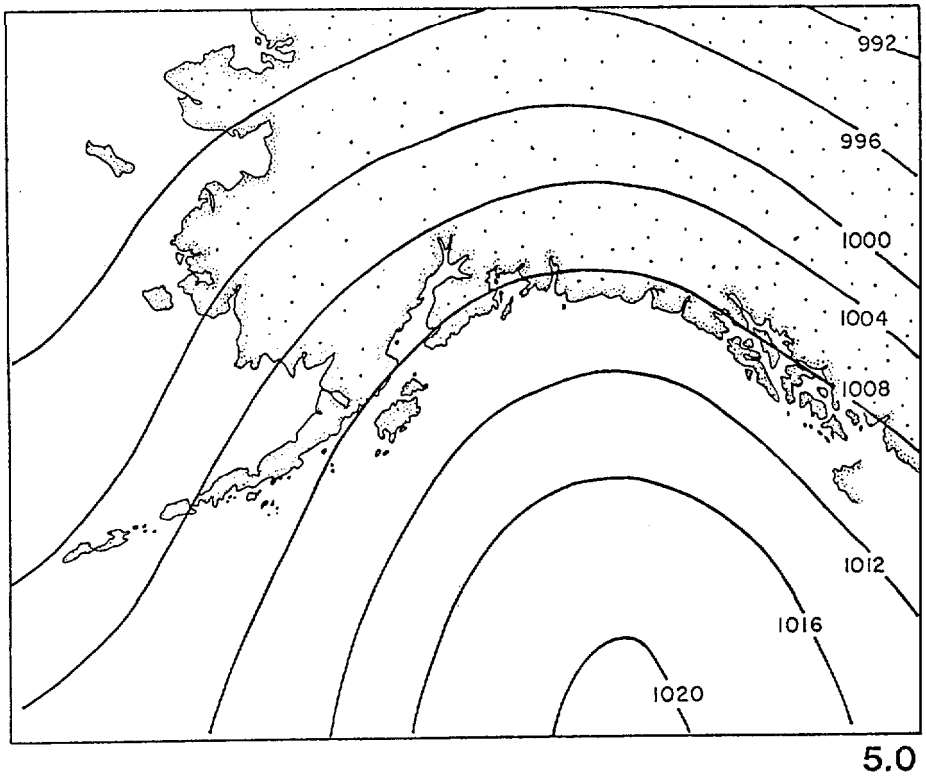
992
996
1000
1004
1008
1012
1016
1020

5.0

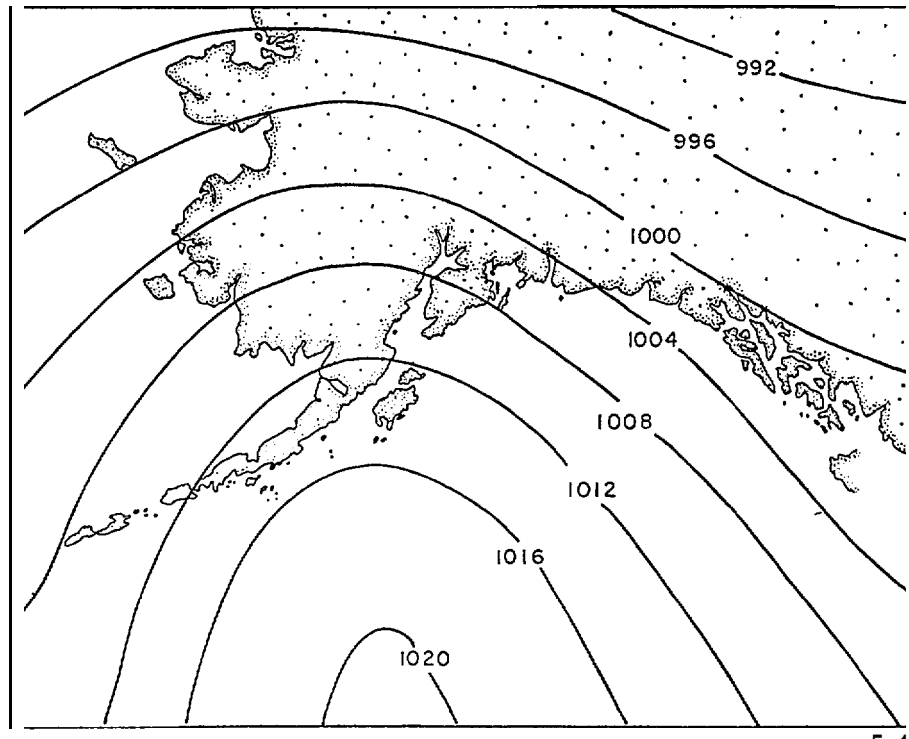
992
996
1000
1004
1008
1012
1016
1020

5.1

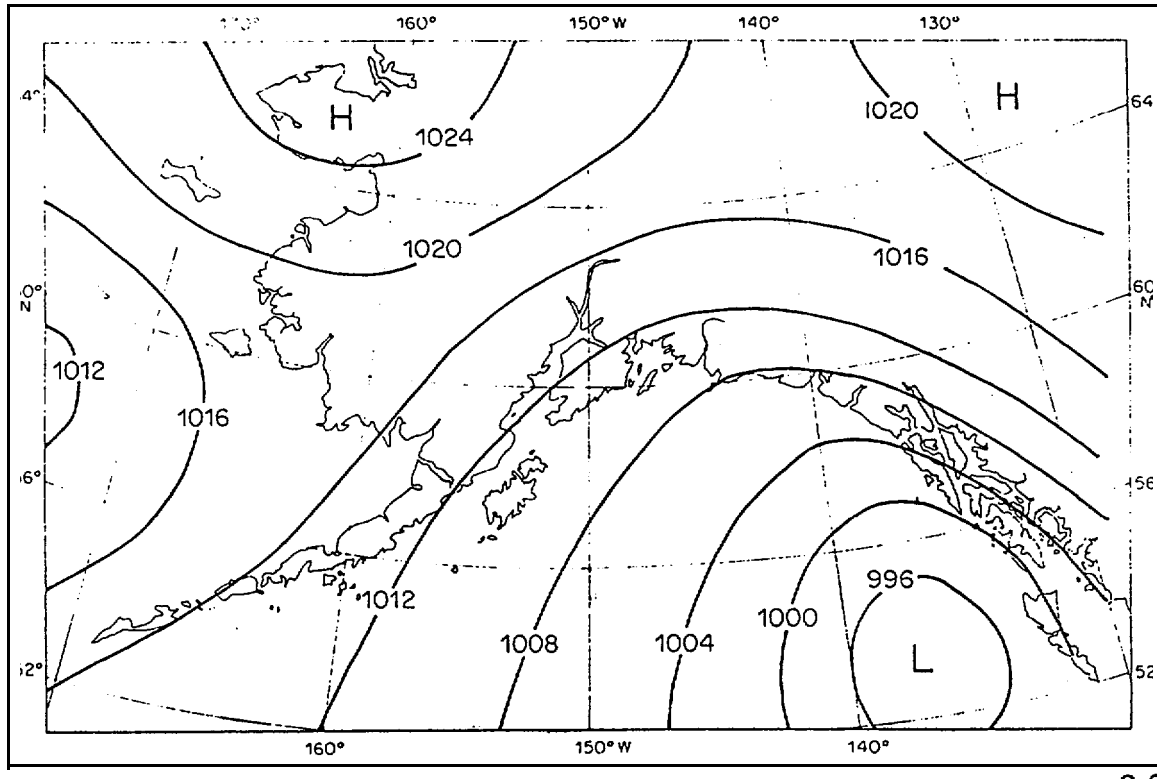
160°
150° W
140°
130°
H
1024
1020
H
1020
1016
1012
1016
1012
1008
1004
1000
996
L
160°
150° W
140°

6.0

CLIMAT≤ 10

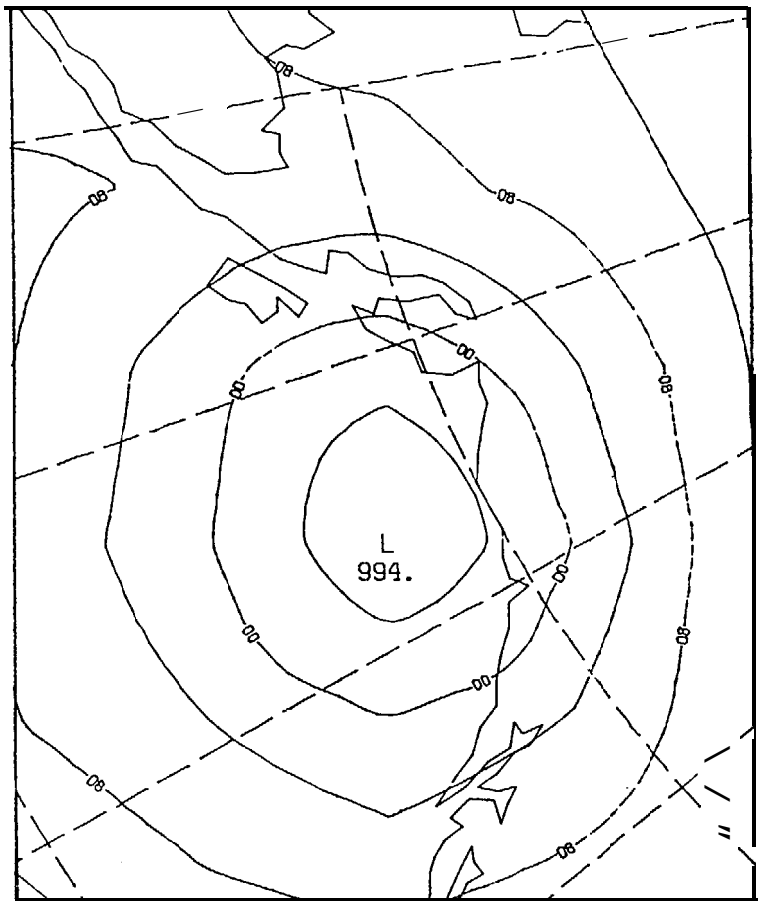

CLIMAT≤ 11

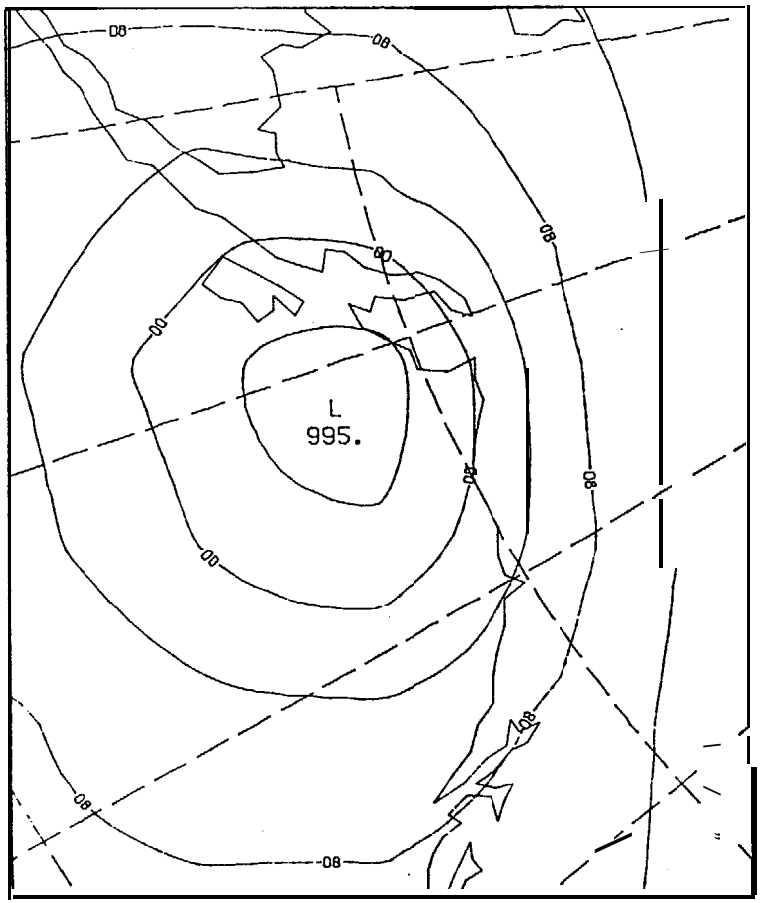

CLIMATE 12

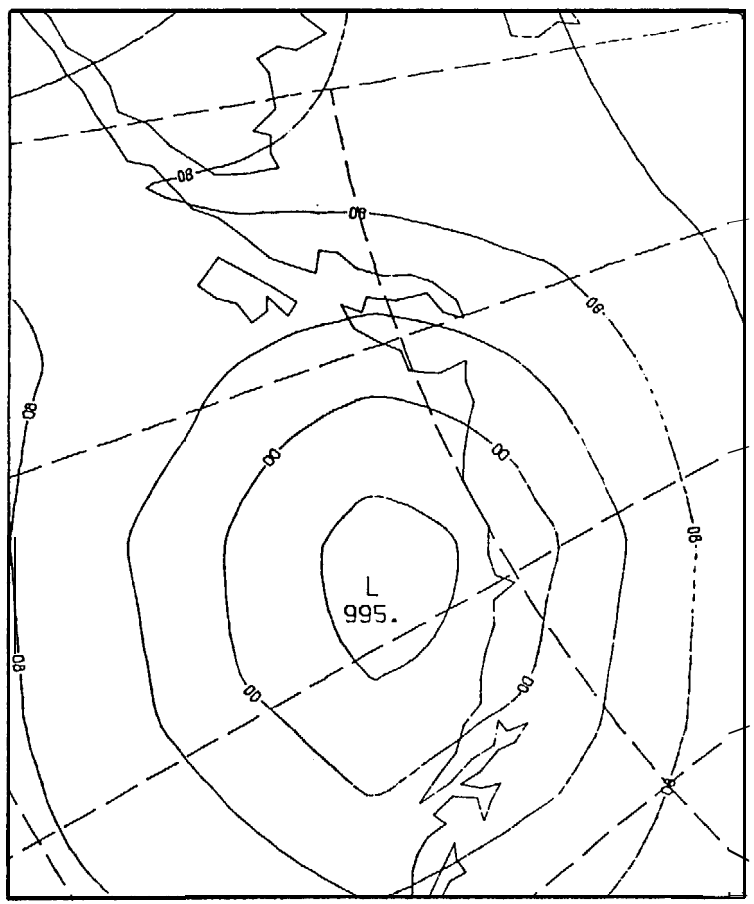

CLIMATE 13

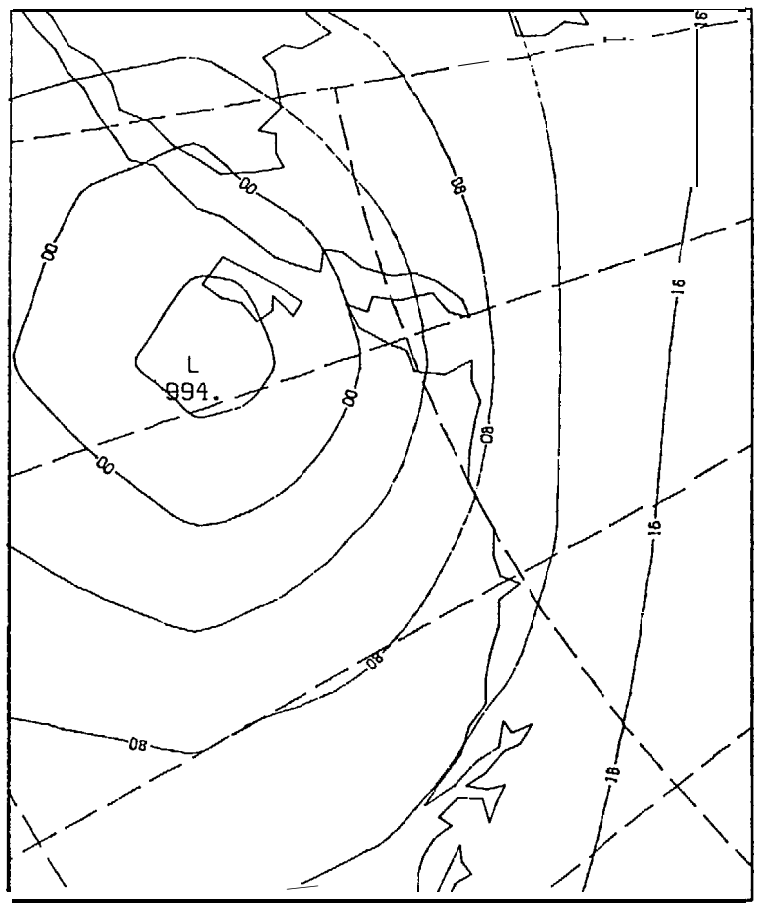

CLIMATE 20

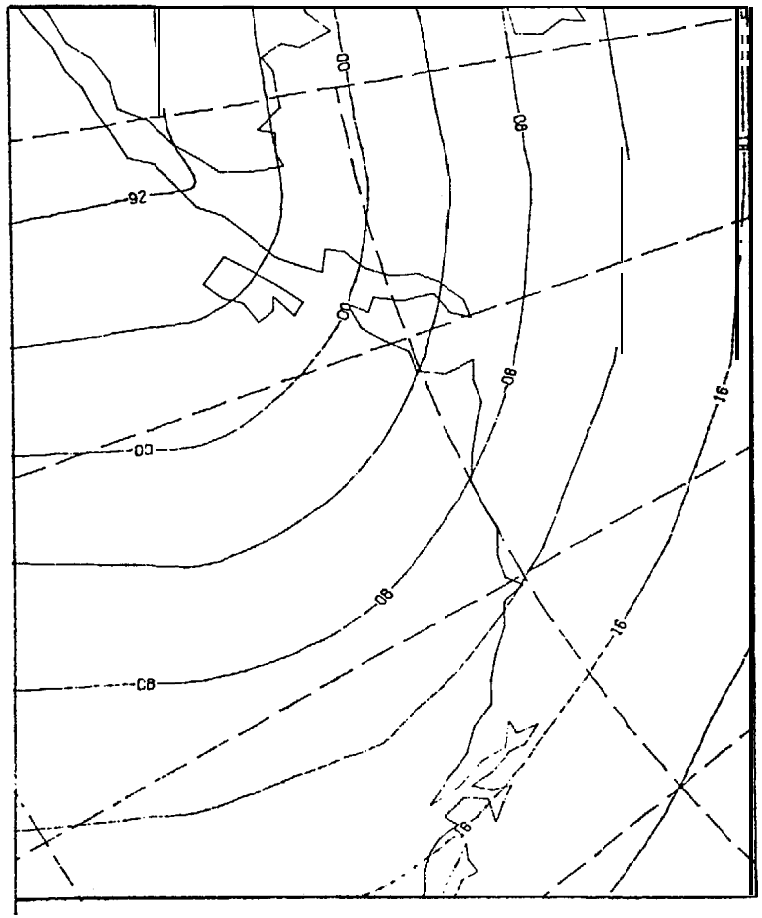

CLIMATE 21

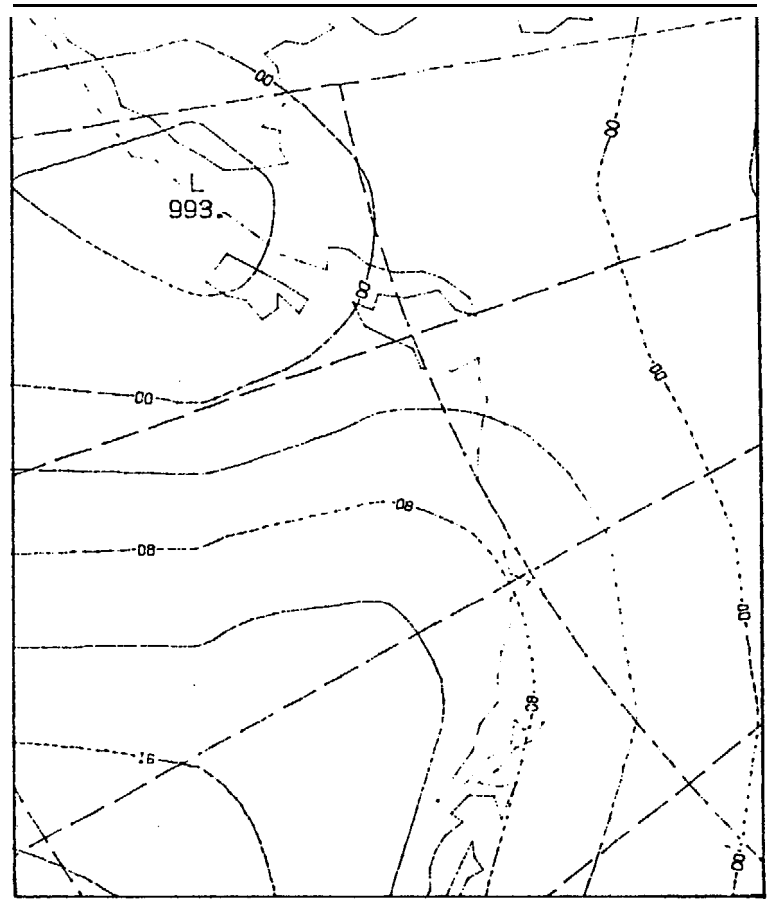

CLIMATE 30

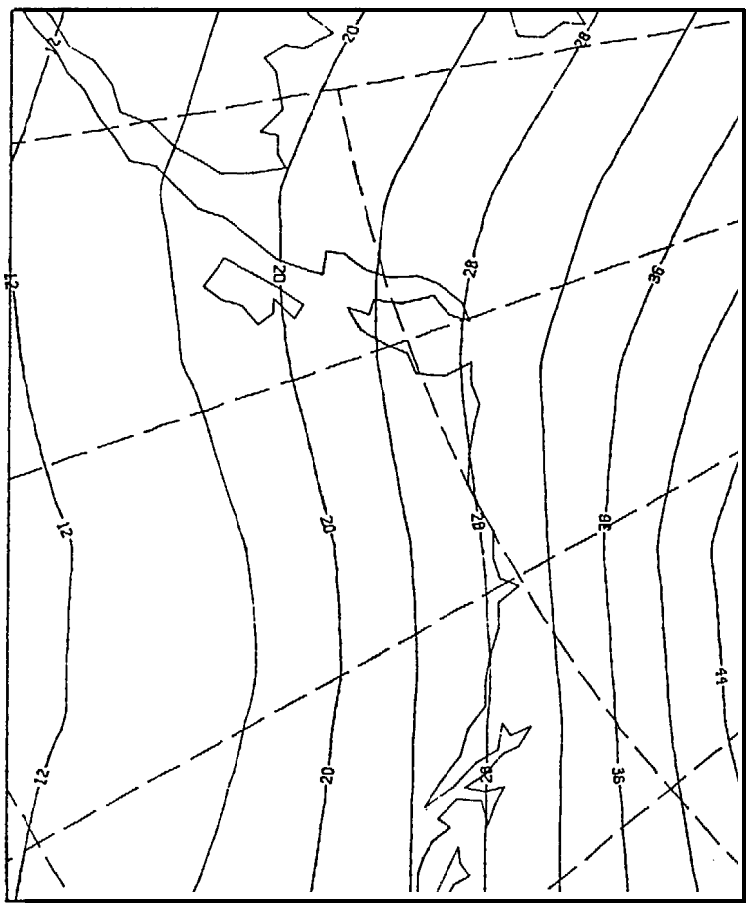

CLIMATE 40

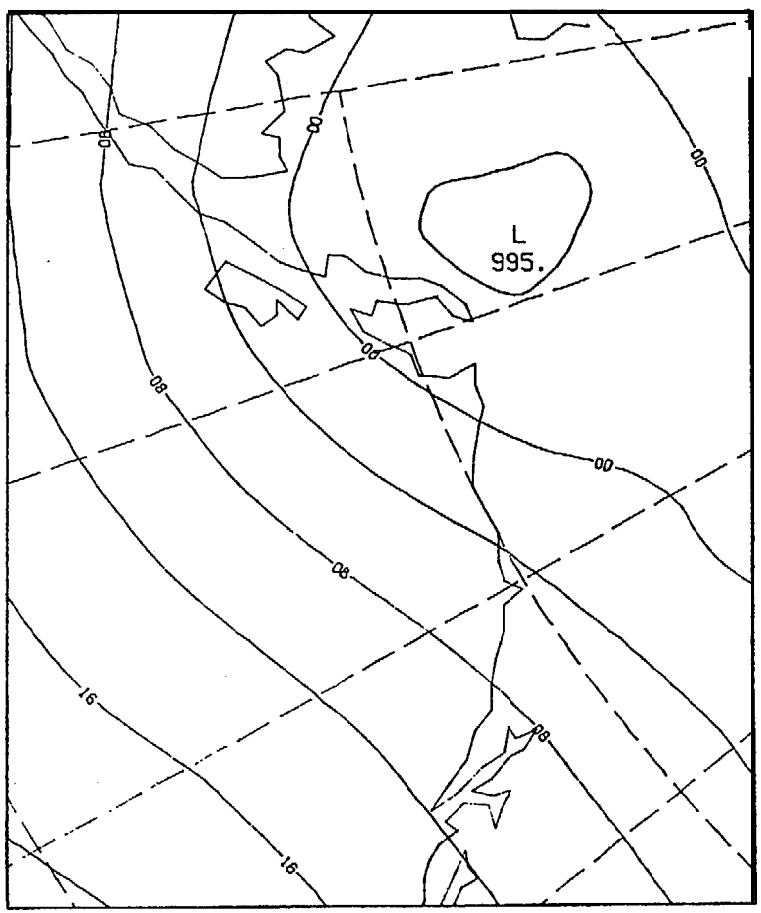

CLIMATE 41

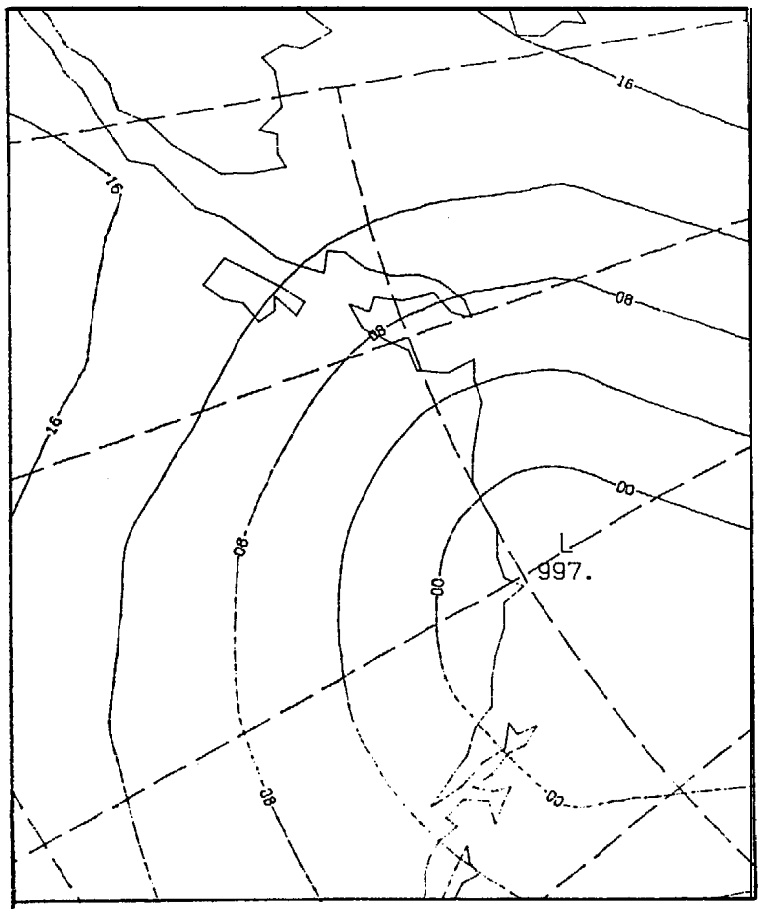

CLIMATE 5°

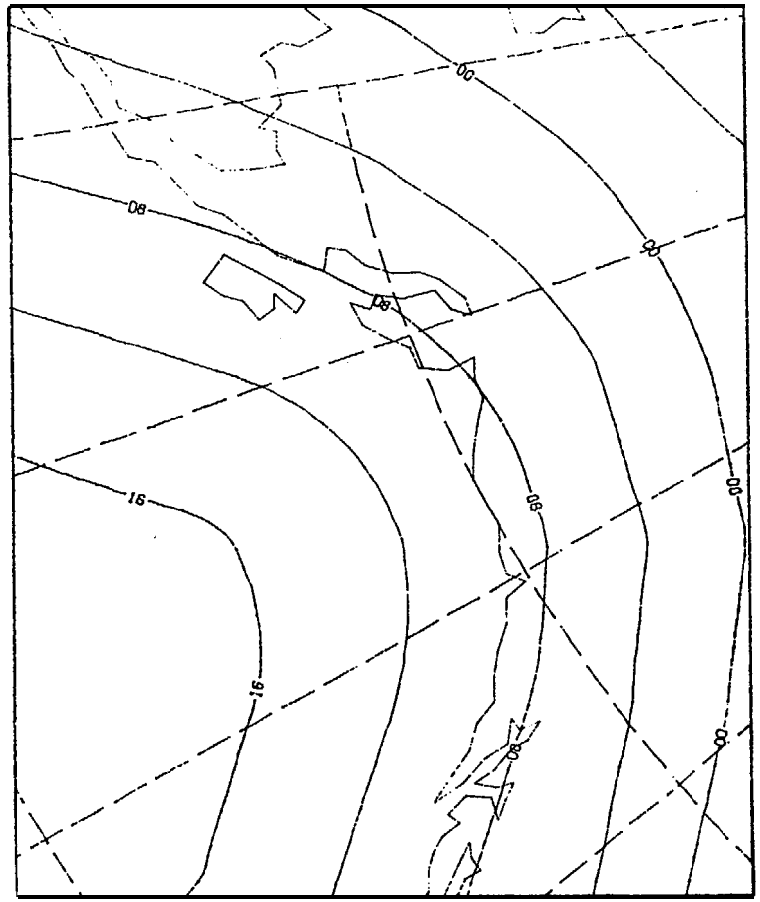

CLIMATE 51

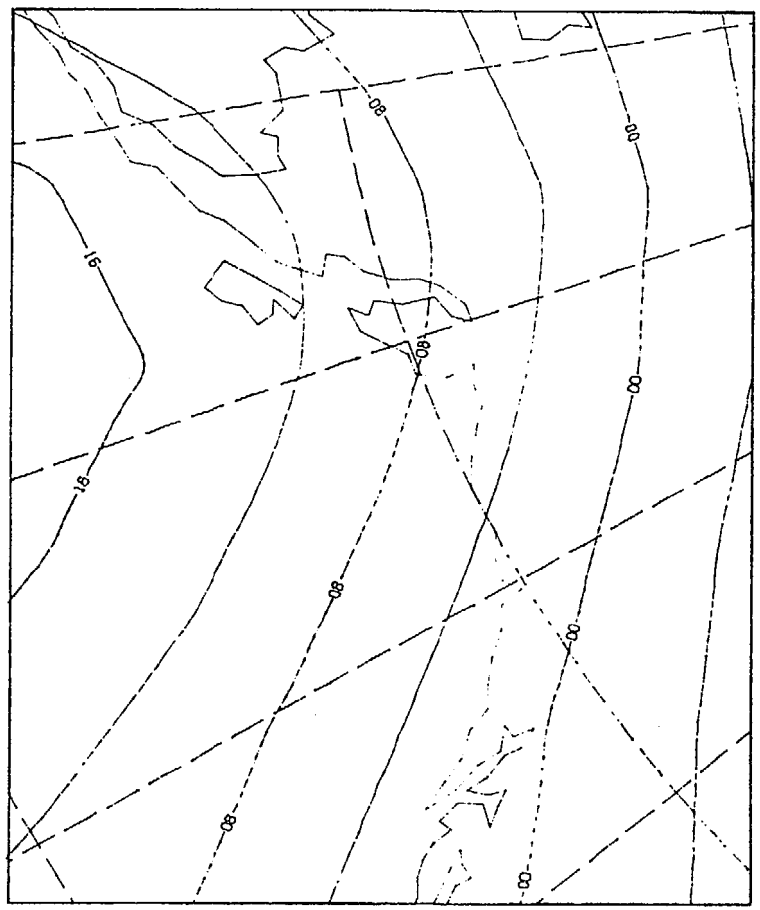

CLIMATE 60

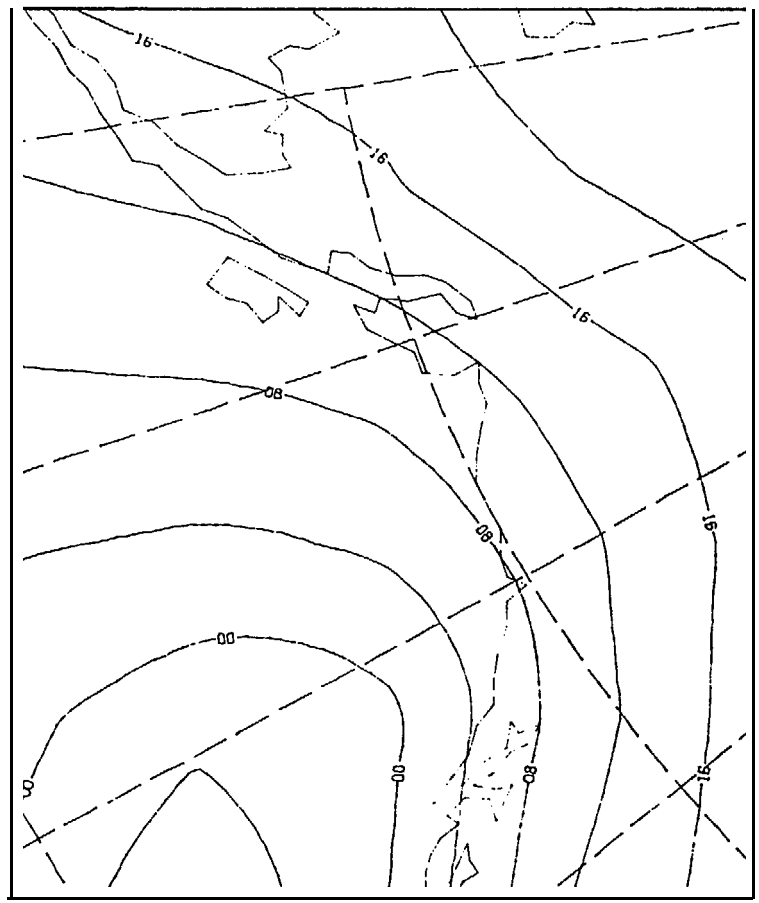

TRANSITIONS FROM INITIAL TYPE TO FOLLOWING TYPE

Based on 12 Hourly Analyses 1968-1974

	Initial Type	% of Occurrence of Initial Type	% of Initial Type Followed by Following Type											
			.0	1.1	1.2	1.3	2.0	2.1	3	4.0	4.1	5.0	5.1	6
	1.0	4	28	5	8	0	8	5	2	10	18	1	0	15
	1.1	4	14	23	2	10	7	1	3	9	7	1	1	22
	1.2	2	3	4	18	4	32	3	2	3	2	6	2	11
	1.3	6	5	18	1	31	15	4	8	5	1	a	<0	12
Y	2.0	25	1	1	<0	9	69	4	7	5	<0	3	<0	1
E	2.1	6	1	2	1	9	24	35	2	17	1	5	1	2
A	3	10	1	4	1	8	15	<0	7	<0	<0	1	0	13
R	4.0	10	3	2	<0	1	6	8	0	50	9	11	8	2
	4.1	8	4	1	5	1	4	3	0	5	55	5	9	8
	5.0	7	<0	0	0	0	19	16	1	7	<0	52	4	1
	5.1	4	0	0	<0	0	3	1	0	9	19	18	49	1
	6	14	5	4	5	1	3	<0	9	1	7	1	2	62
	1.0	6	39	5	12	0	8	4	1	4	8	0	0	19
	?.1	6	16	35	4	12	7	0	3	1	3	0	0	19
	1.2	3	0	0	21	5	36	0	1	3	0	3	3	18
W	1.3	8	5	20	2	38	14	0	0	2	1	0	0	8
I	2.0	25	1	1	0	10	70	2	9	5	0	1	0	1
N	2.1	1	0	0	12	18	40	12	0	18	0	0	0	0
T	3	19	<0	3	<0	6	10	0	1	0	0	1	0	9
E	4.0	3	14	0	3	0	12	8	0	24	13	13	8	5
R	4.1	4	10	0	10	0	4	4	2	2	45	2	4	17
	5.0	3	0	0	0	0	33	3	7	10	0	44	3	0
	5.1	1	0	0	0	0	8	0	0	0	25	33	34	0
	6	21	6	6	2	<0	2	0	9	<0	3	<0	<0	71
	1.0	3	11	11	6	0	9	6	D	11	32	0	0	14
	1.1	4	9	19	0	11	7	2	2	11	9	2	0	28
S	1.2	2	0	10	25	5	15	5	0	5	0	5	0	20
P	1.3	7	4	16	0	32	19	4	0	4	0	0	0	11
R	2.0	31	2	2	<0	7	71	3	7	5	<0	2	0	1
I	2.1	6	0	0	0	15	34	25	D	18	1	4	0	3
N	3	8	1	6	0	9	19	2	7	0	0	0	0	16
G	4.0	9	2	1	0	1	10	10	1	48	5	10	8	4
	4.1	8	6	1	5	0	3	3	D	4	53	9	6	10
	5.0	6	0	0	0	0	29	19	3	1	1	43	3	1
	5.1	3	0	0	0	0	6	0	0	3	25	31	35	0
	6	13	5	5	4	2	4	0	B	1	8	1	2	60

TRANSITIONS FROM INITIAL TYPE TO FOLLOWING TYPE (Cont.)

Based on 12 Hourly Analyses 1968-1974

	Initial Type	% of Occurrence of Initial Type	% of Initial Type Followed by Following Type											
			.0	1.1	1.2	.3	.0	.1	3	.0	.1	.0	.1	5
	1.0	2	24	0	4	0	8	8	0	16	32	4	0	4
	1.1	1	14	7	0	7	0	0	0	37	14	0	7	14
	1.2	1	8	0	16	0	15	15	15	8	8	15	0	0
S	1.3	4	6	8	0	27	13	13	4	10	2	0	2	15
U	2.0	18	0	0	0	8	65	9	7	2	0	7	50	1
M	2.1	13	1	1	0	6	13	47	3	17	1	7	2	2
M	3	3	5	5	7	10	20	0	29	0	2	7	0	15
E	4.0	15	1	2	0	1	3	7	0	57	6	12	10	1
R	4.1	11	2	1	2	0	1	1	0	11	60	3	15	4
	5.0	16	0	0	0	0	12	18	50	4	0	61	5	0
	5.1	10	0	0	1	0	1	2	0	9	13	15	57	2
	6	6	7	1	4	1	6	1	4	0	16	1	6	53
	1.0	3	27	3	5	0	8	3	5	15	19	0	0	15
	1.1	5	16	20	2	7	7	2	4	11	9	0	0	22
	1.2	3	6	6	14	3	43	0	13	0	3	6	3	3
	1.3	7	6	24	0	25	14	2	6	5	1	0	0	17
F	2.0	25	0	2	50	12	67	4	7	6	50	2	0	0
A	2.1	5	0	5	2	11	39	23	2	16	0	0	0	2
L	3	8	1	2	0	13	18	0	43	2	1	1	0	19
L	4.0	11	3	3	0	1	5	8	1	49	14	9	5	2
	4.1	11	1	1	7	2	7	4	0	1	57	4	7	9
	5.0	4	2	0	0	0	23	15	0	26	0	32	2	0
	5.1	3	0	0	0	0	0	3	0	14	31	11	29	3
	6	15	3	2	10	1	2	1	0	2	7	1	2	60

Type	1.0	1.1	1.2	1.3	2.0	2.1	3.0	4.0	.4.1	5.0	5.1	6.0
1.0	1.00	,81	.89	.46	.18	-.32	.28	-.08	.22	-.50	-.26	.40
1.1	.81	1.00	.57	.84	.50	-.10	.58	-.12	-.27	-.62	-.66	.38
1.2	.89	.57	1.00	.25	.10	-.52	.30	-.31	.31	-.45	-.14	.48
1.3	.46	.84	.25	1.00	.82	.17	.81	-.23	-.68	-.55	-.92	.24
2.0	.18	.50	.10	.82	1.00	.38	.76	-.10	-.78	-.15	-.84	-.13
2.1	-.32	-.10	-.52	.17	.38	1.00	-.23	.58	-.22	.57	-.05	-.80
3.0	.28	,58	.30	.81	.76	-.23	1.00	-.62	-.76	-.66	-.93	.47
4.0	-.08	-,12	-.31	-.23	-.10	.58	-.62	1.00	.22	.73	,44	-.78
4.1	.22	-.27	.31	-.68	-.78	-.22	-.76	.22	1.00	.24	.82	-.01
5.0	-.50	-.62	-.45	-.55	-.15	.57	-.66	.73	.24	1.00	.62	-.88
5.1	-.26	-.66	-.14	-.92	-.84	-.05	-.93	.44	.82	.62	1.00	-.32
6.0	.40	.38	.48	.24	-.13	-.80	.47	-.78	-.01	-.88	-.32	1.00

APPENDIX B

1. Objective Patterns A-I (correlation cutoff= 0.8)
2. Objective Patterns AA-HH (correlation cutoff = 0.7)

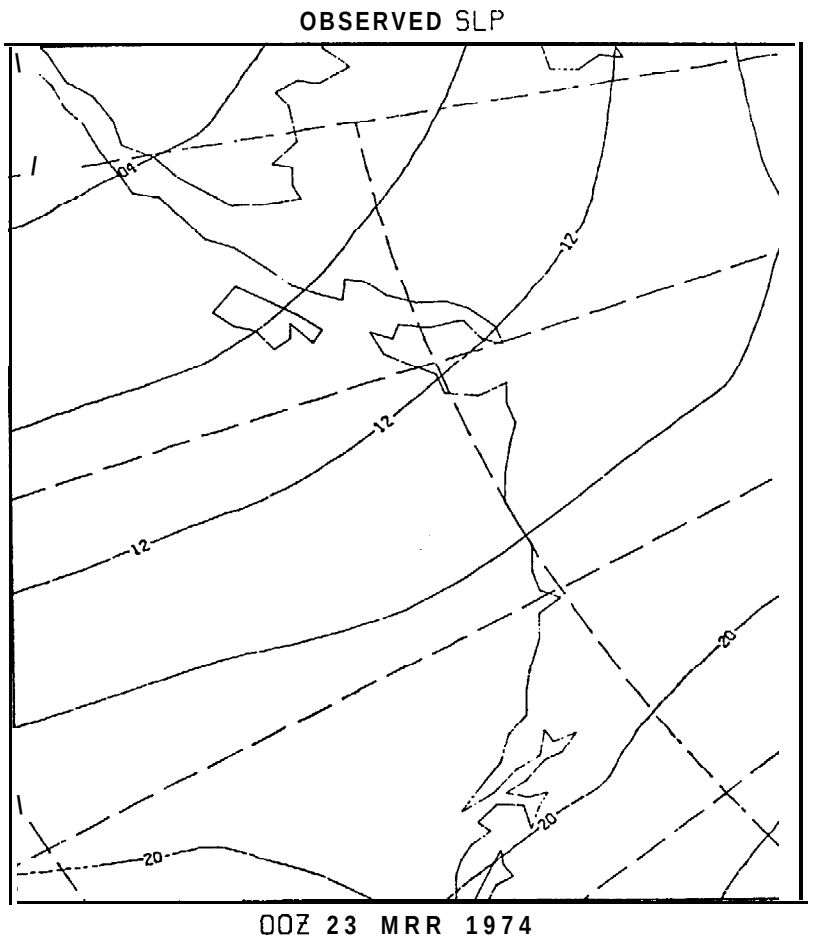
OBSERVED SLP
12
12
12
20
20
20
00Z 23 MRR 1974

Type A

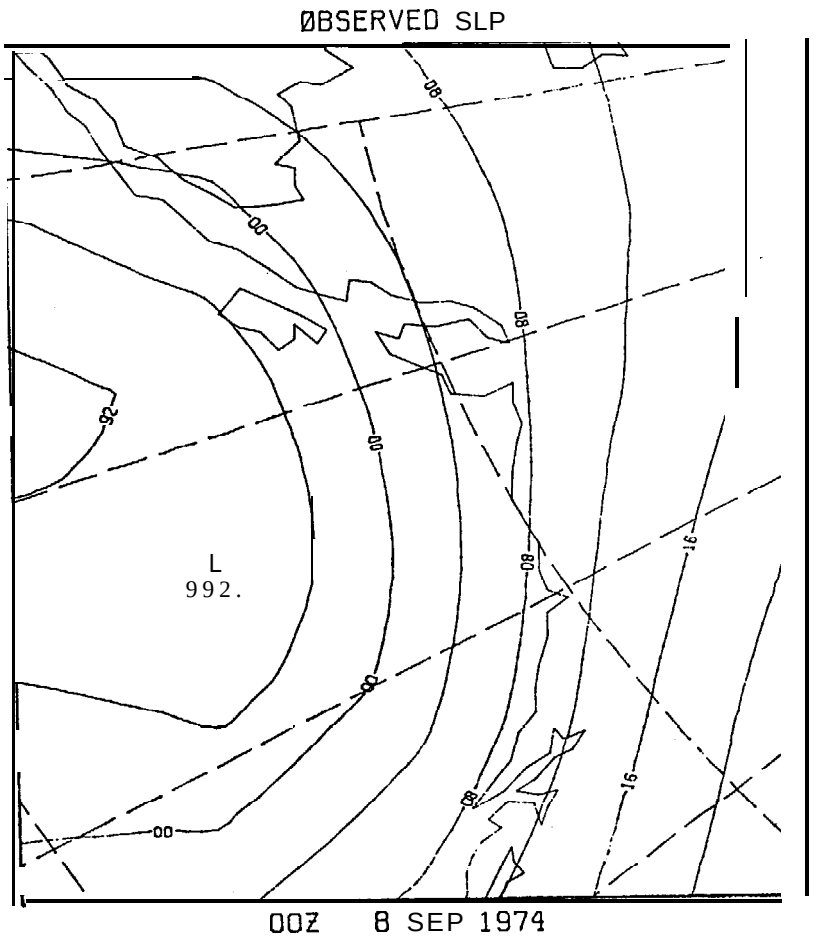
ØBSERVED SLP
L
992.
00Z 8 SEP 1974

Type B

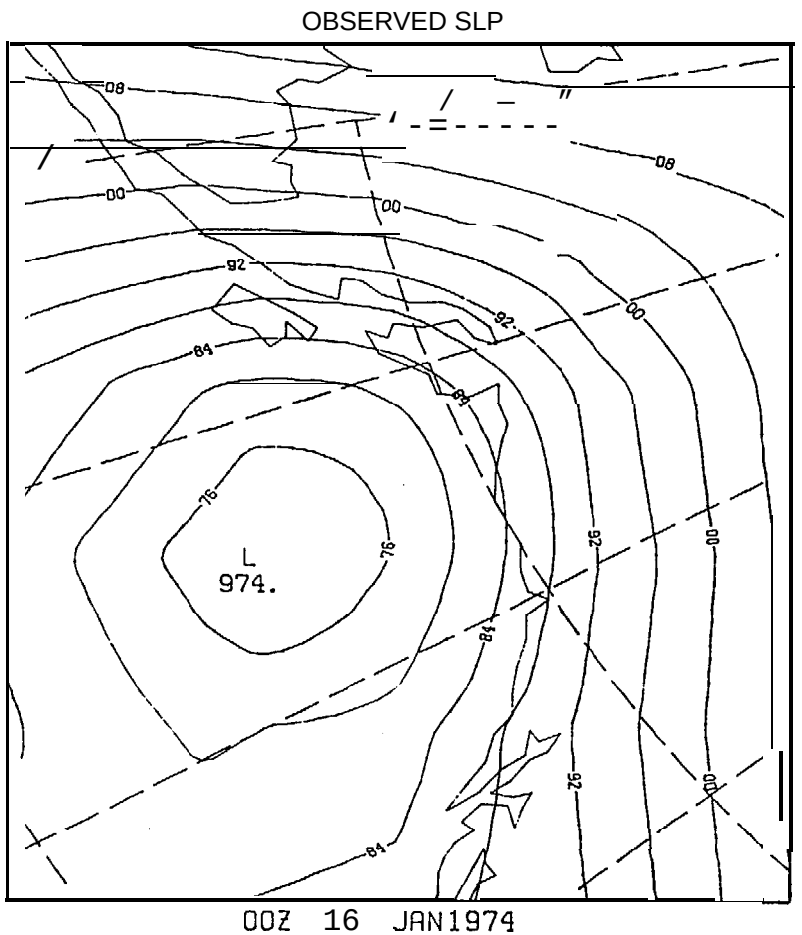
OBSERVED SLP
L
974.
00Z 16 JAN1974

Type C

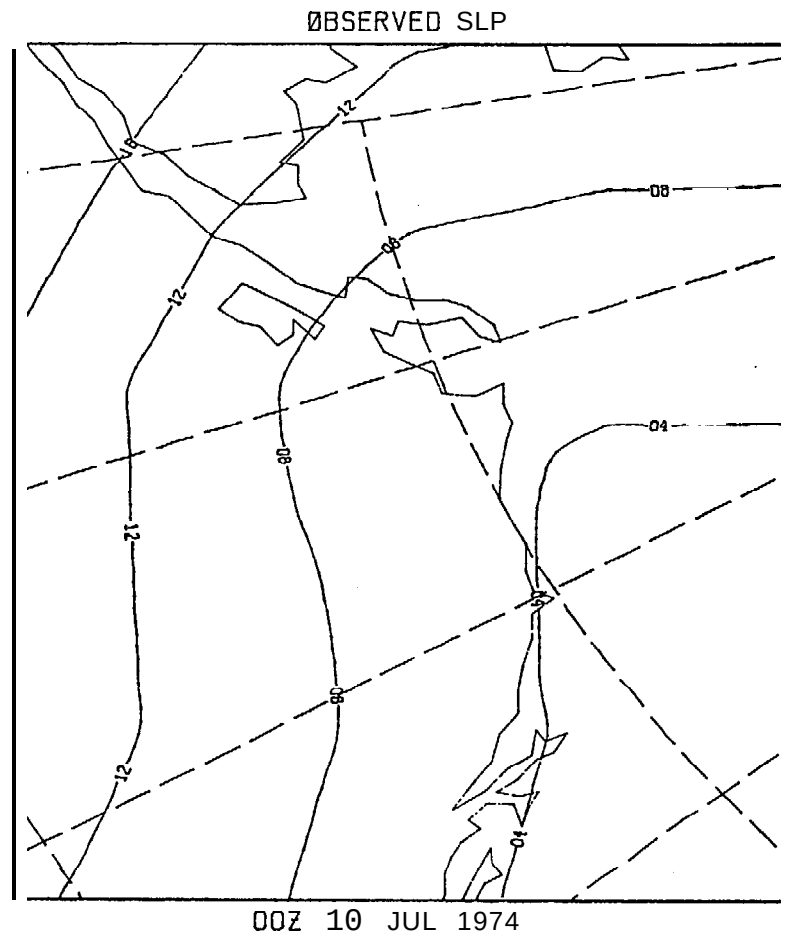
ØBSERVED SLP
00Z 10 JUL 1974

Type D

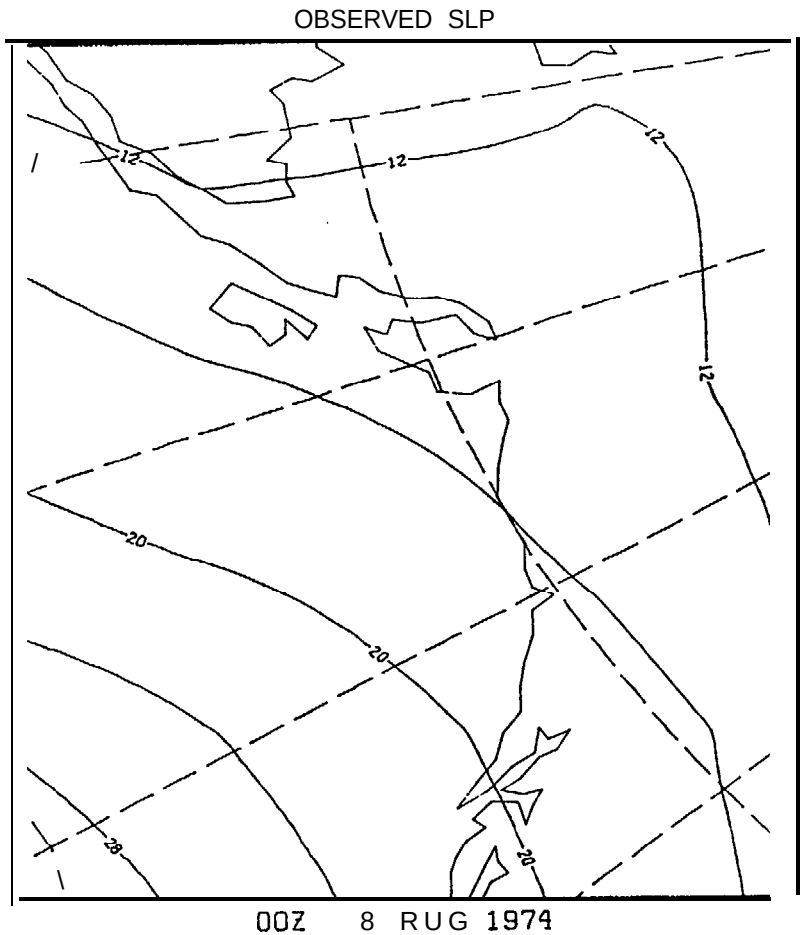
OBSERVED SLP
12
12
12
12
20
20
20
20
00Z 8 RUG 1974

Type E

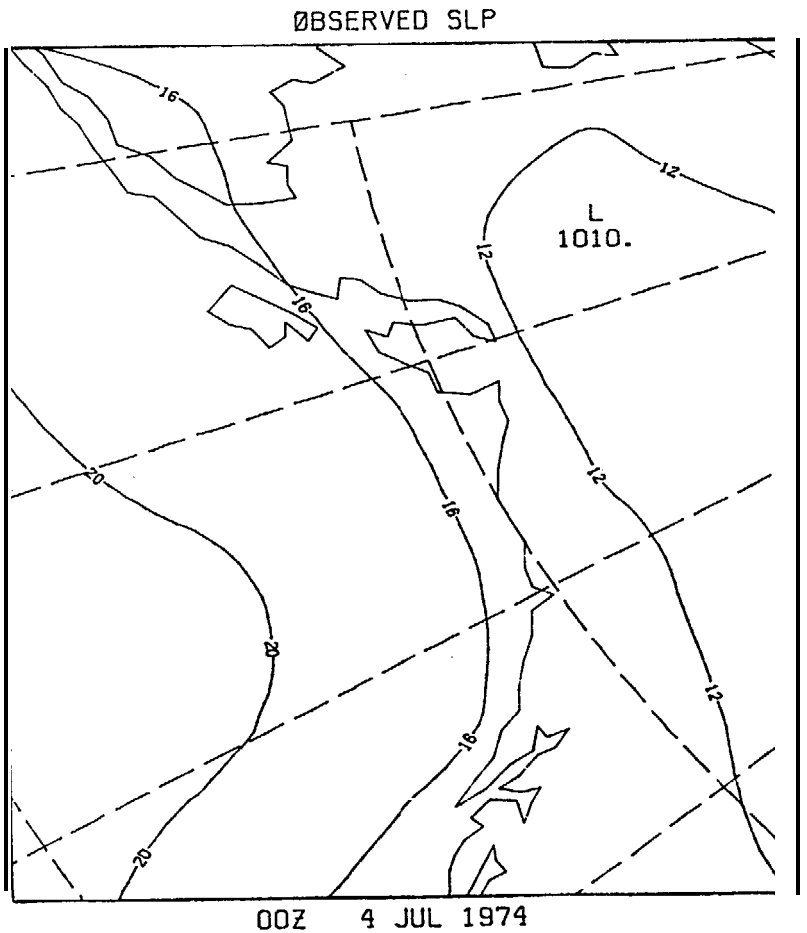
ØBSERVED SLP
16
12
L
1010.
12
16
20
16
12
20
16
12
20
00Z 4 JUL 1974

Type F

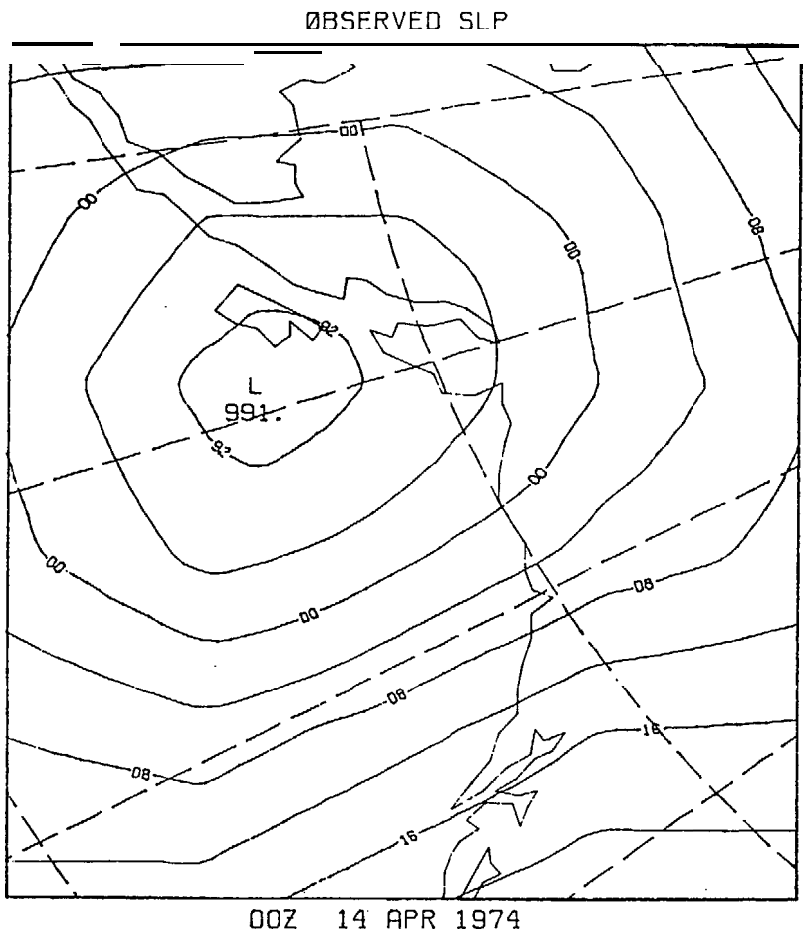
ØBSERVED SLP
L
991.
00Z 14 APR 1974

Type. G

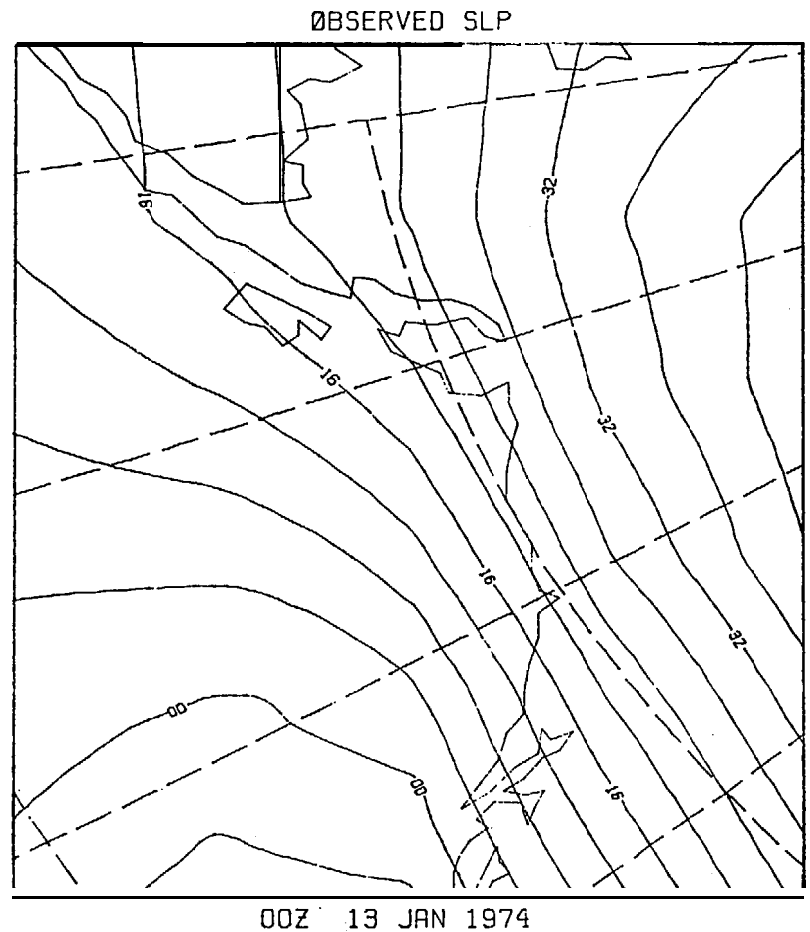
ØBSERVED SLP
00Z 13 JAN 1974

Type H

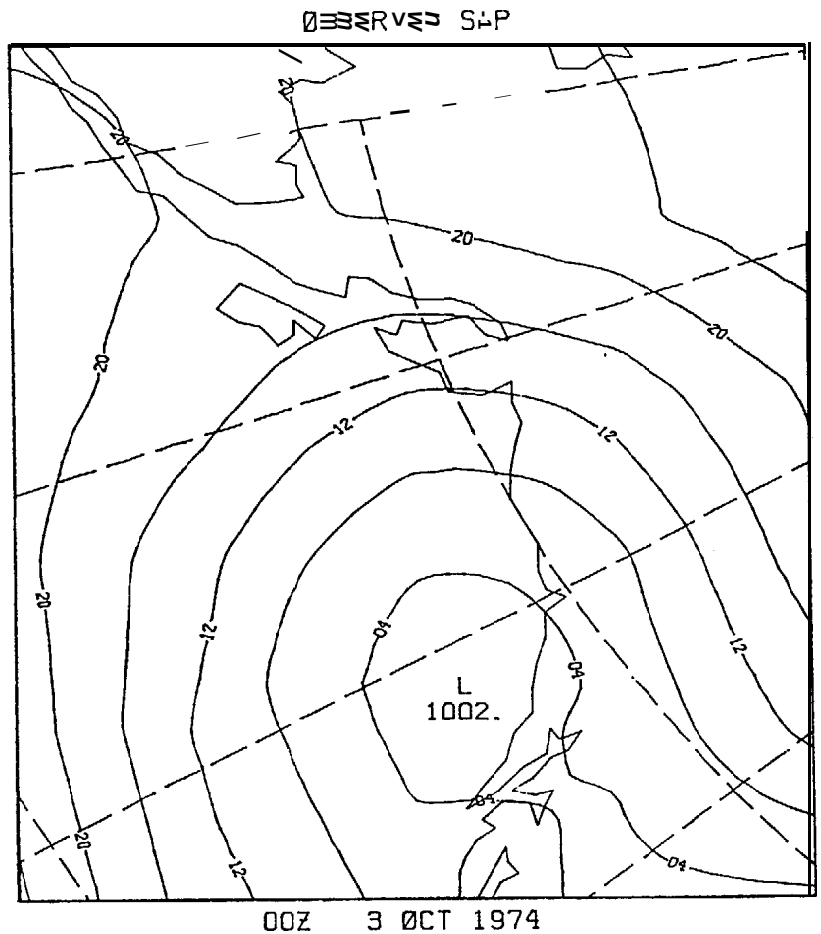

Type I

Cutoff = 0.7

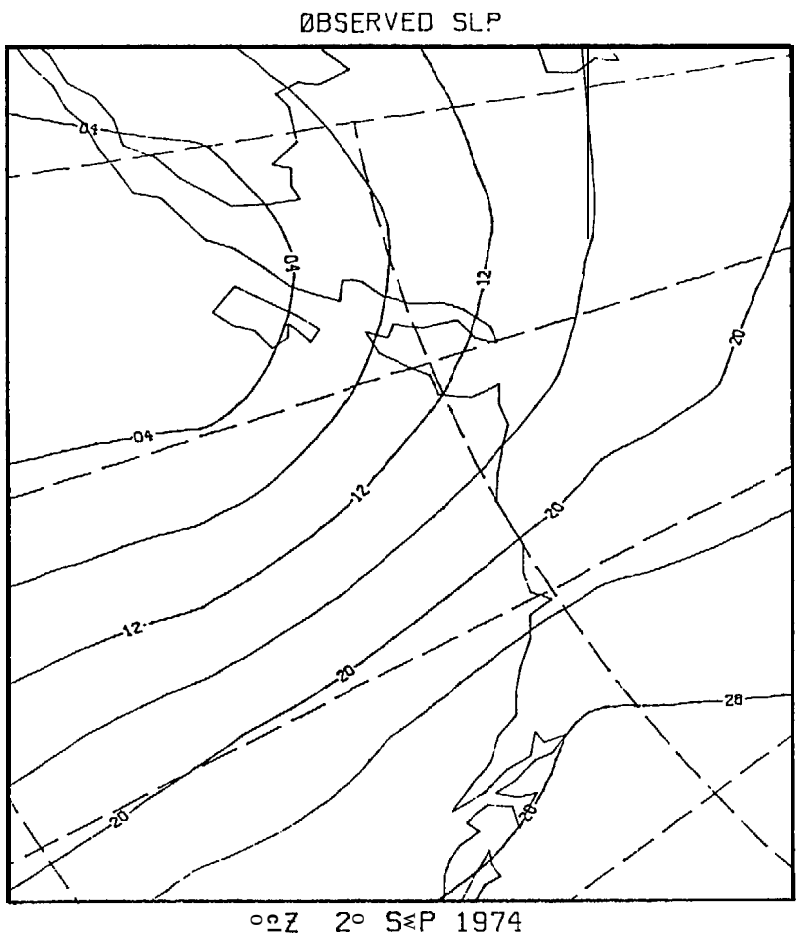

Type AA

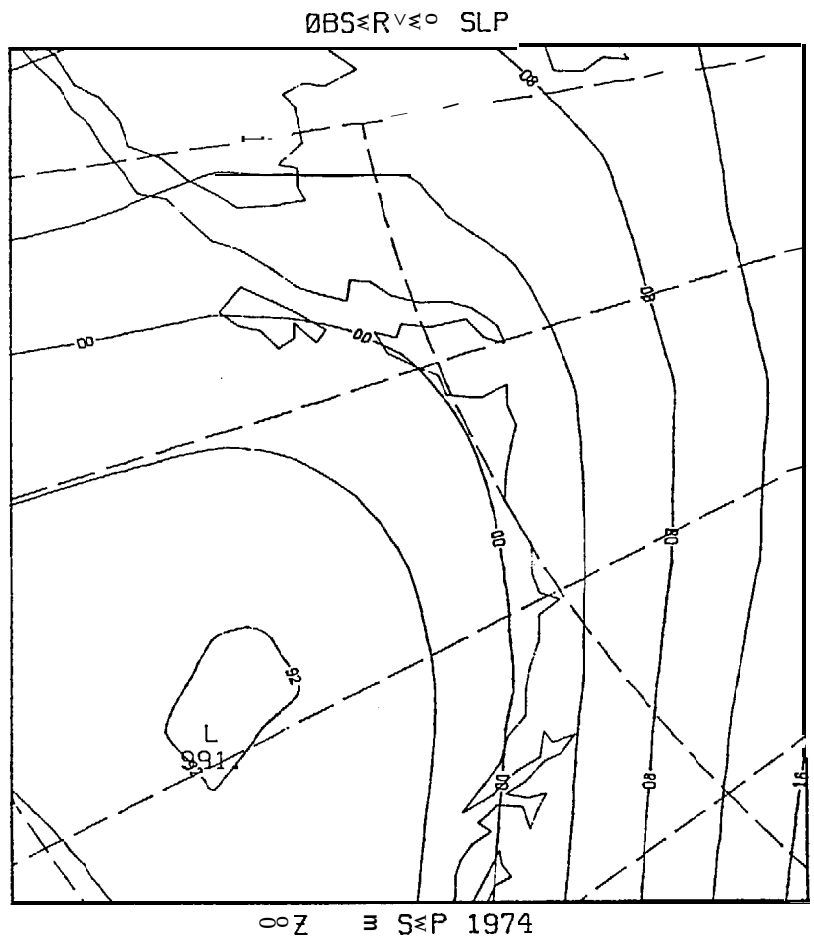
ØBSERVED SLP
00
00
00

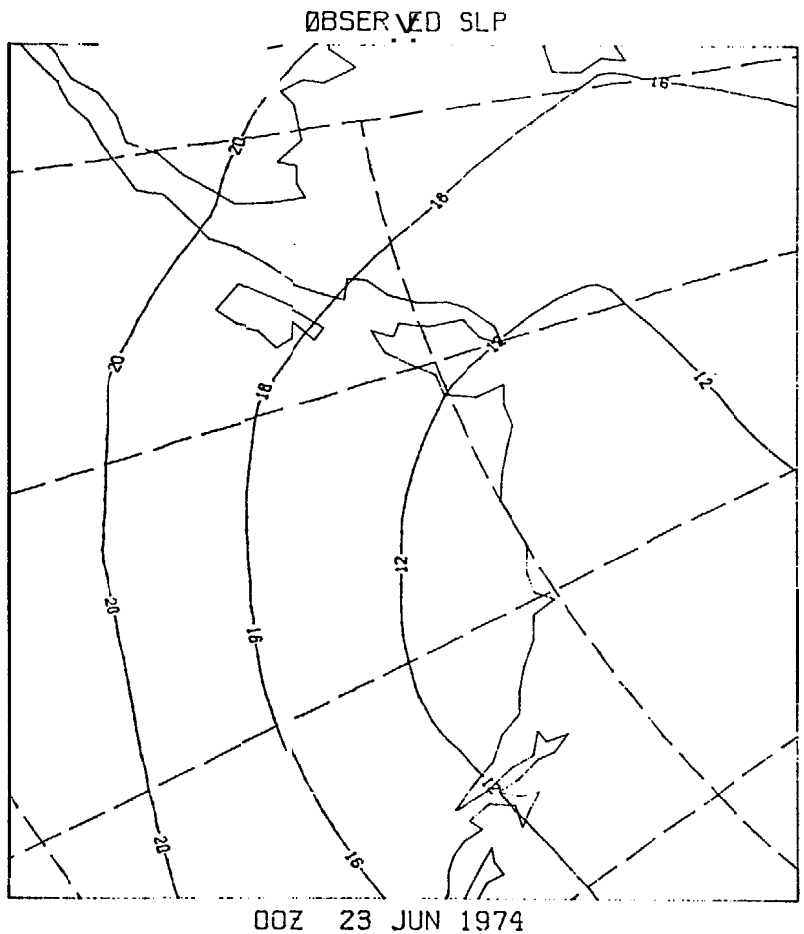

Type CC

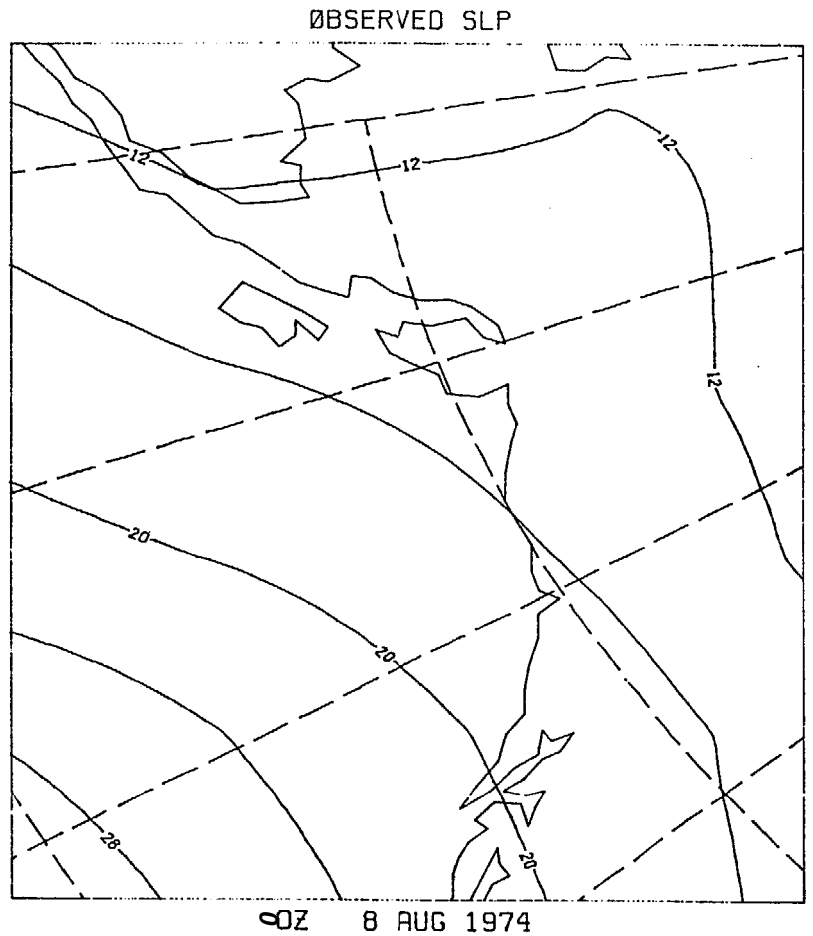

Type DD

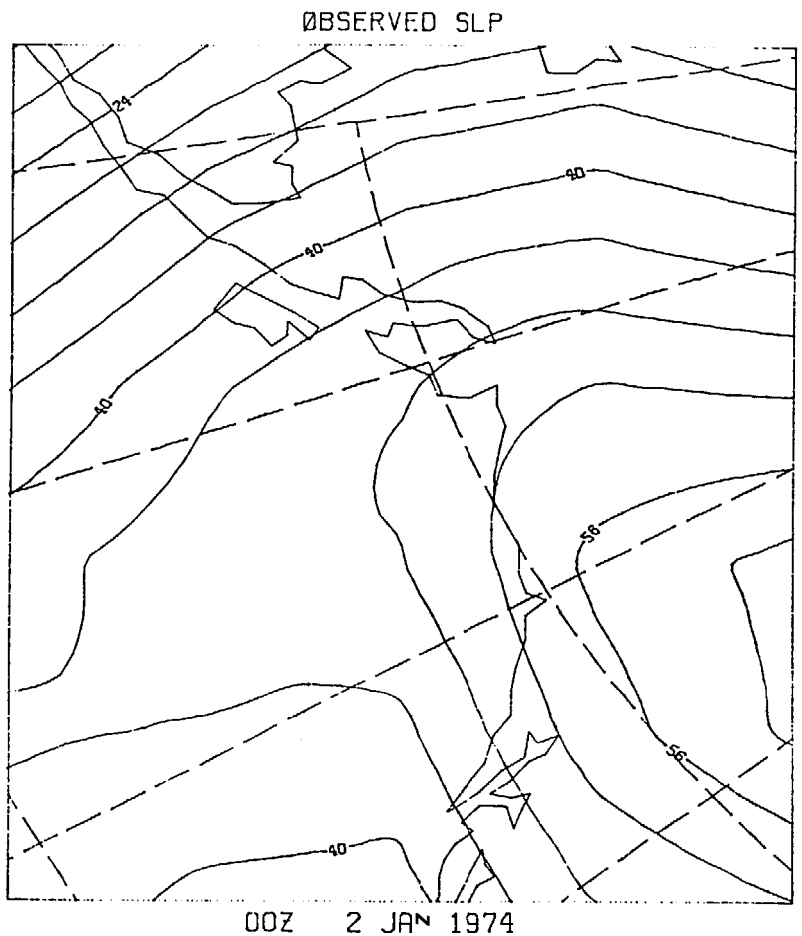

Type EE

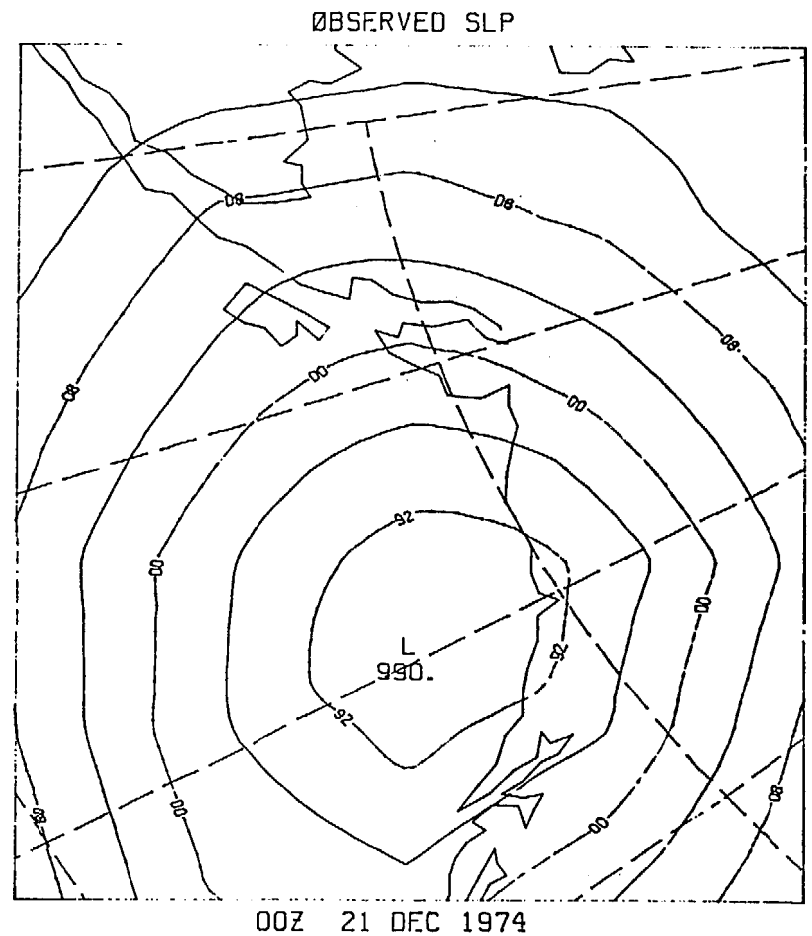

Type FF

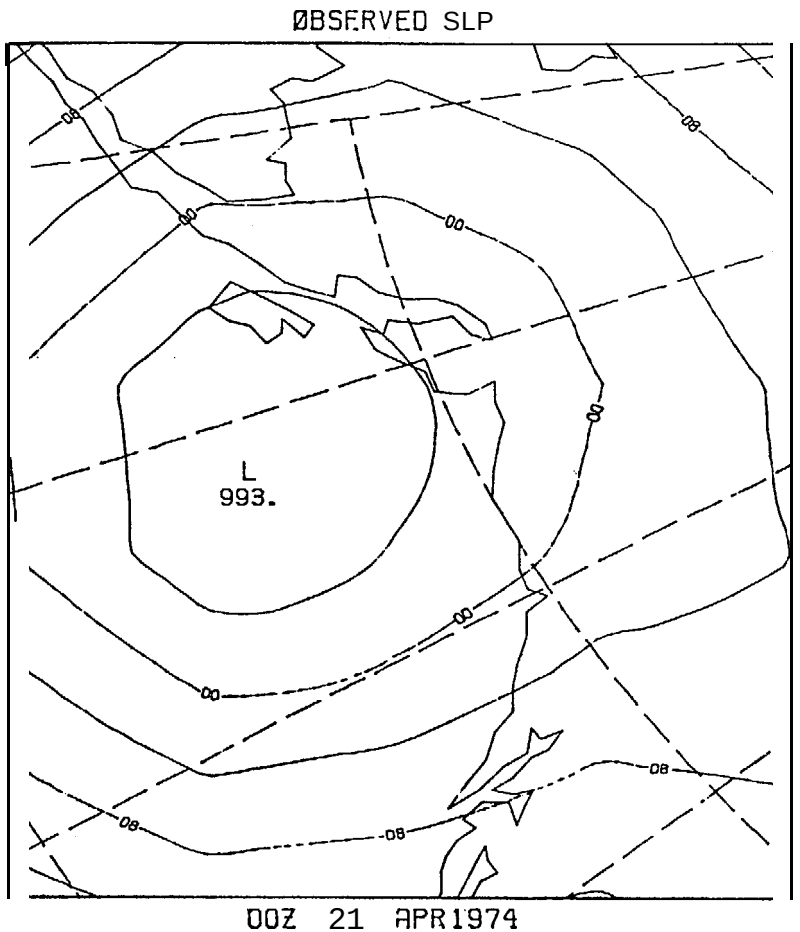

Type GG

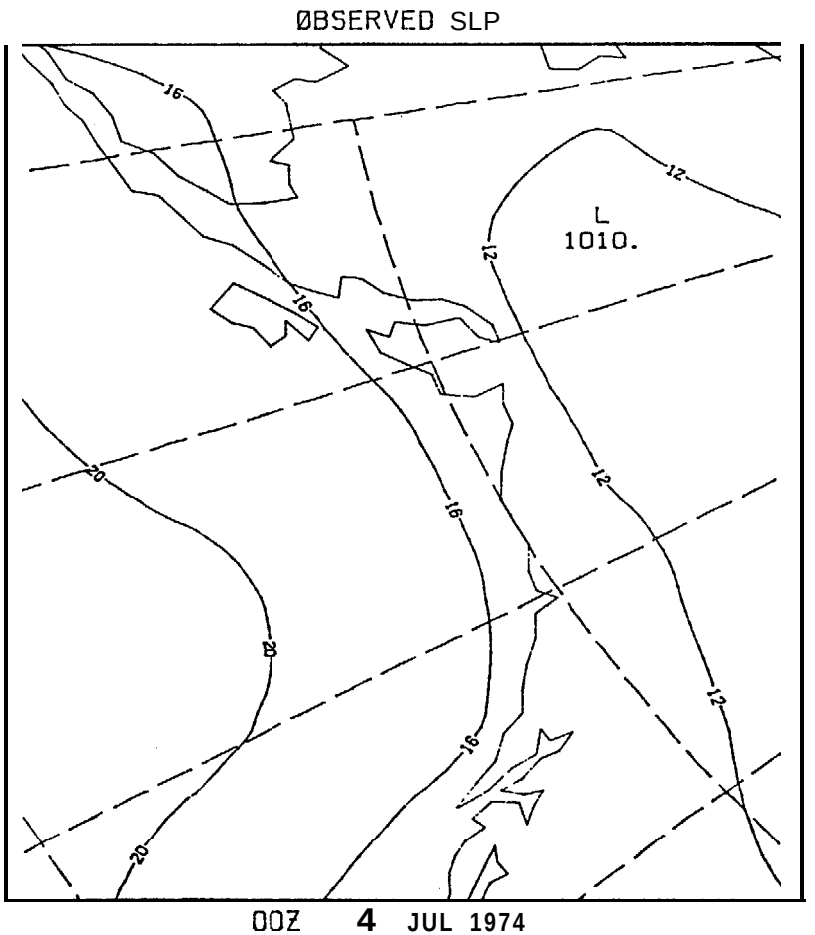

Type HH

APPENDIX C

1. Local Wind Patterns for Subtypes 1.0-6.0.

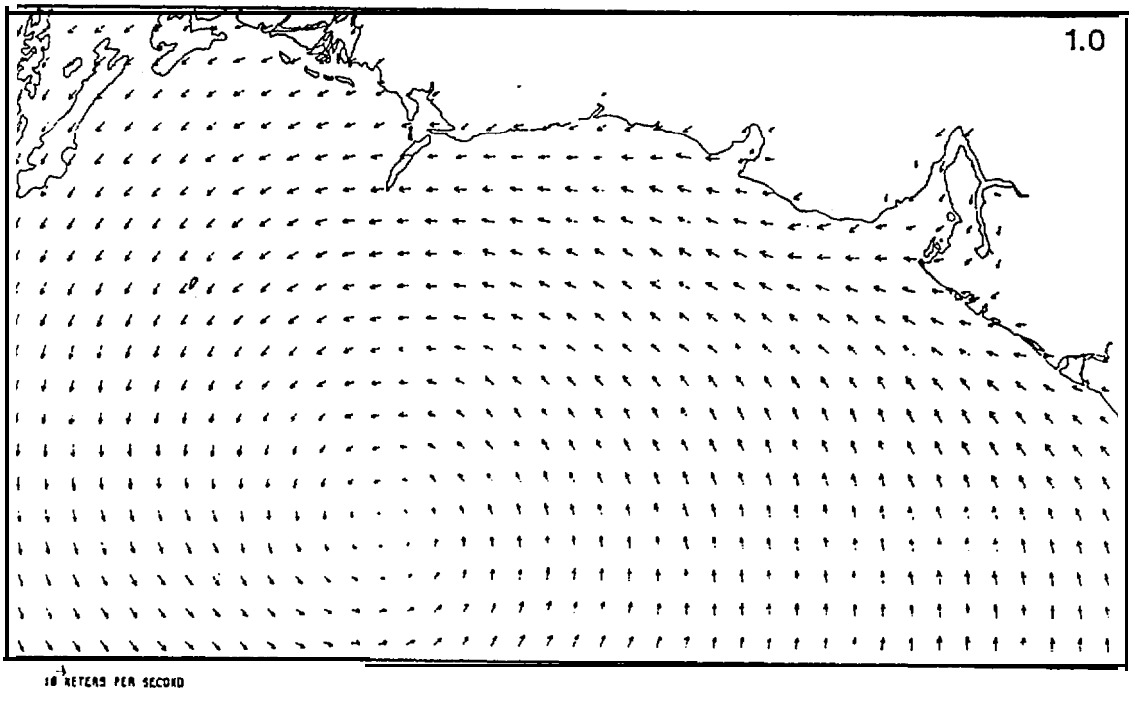

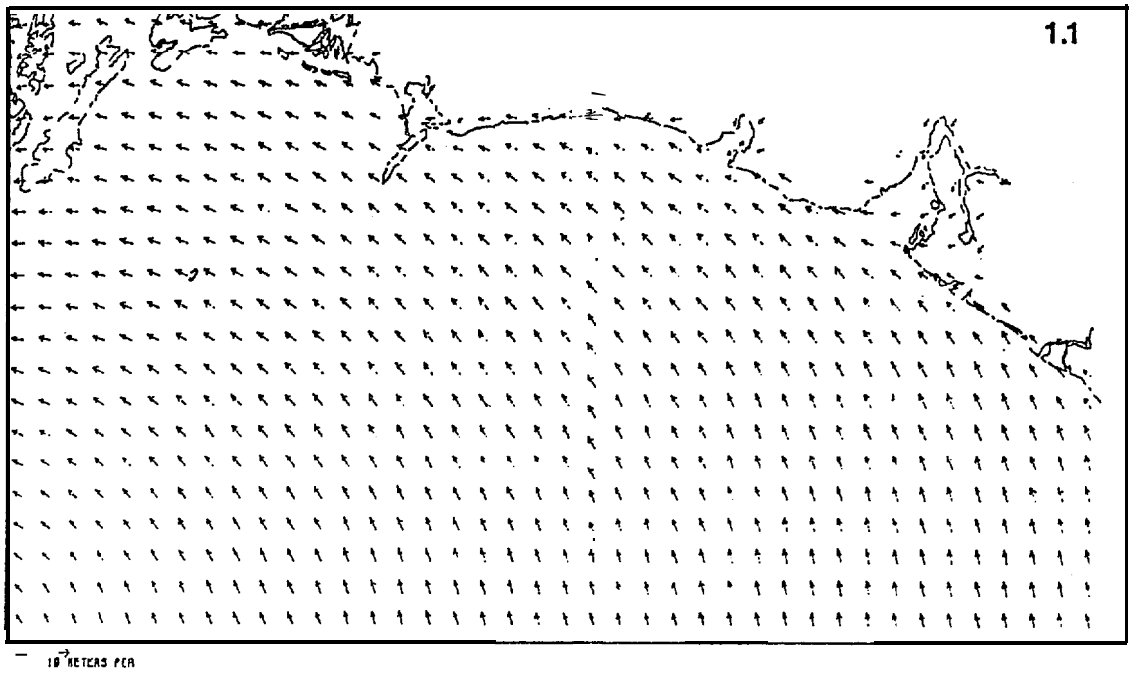
1.1
10 METERS PER

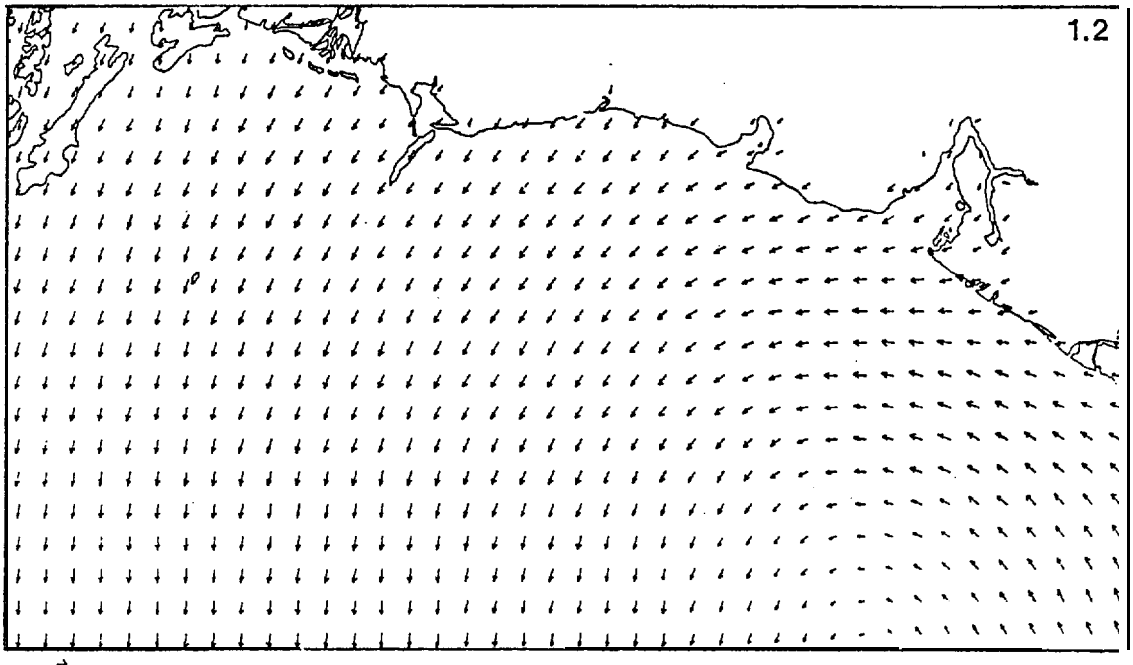
1.2
READ METERS PER SECOND

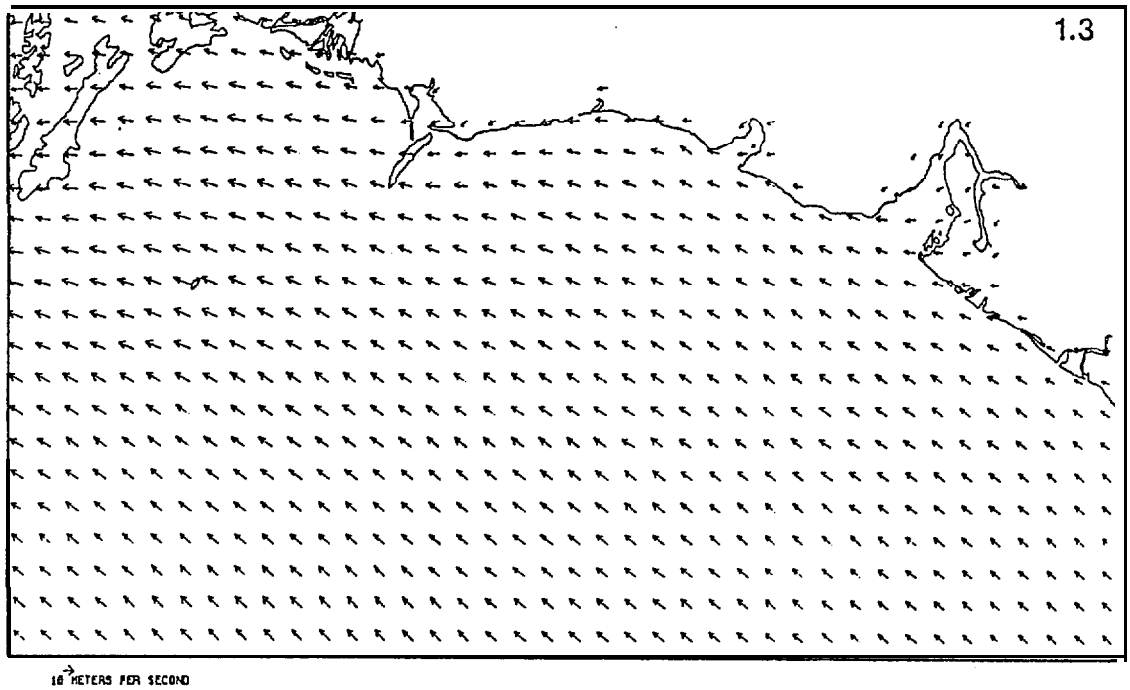

10 METERS PER SECOND

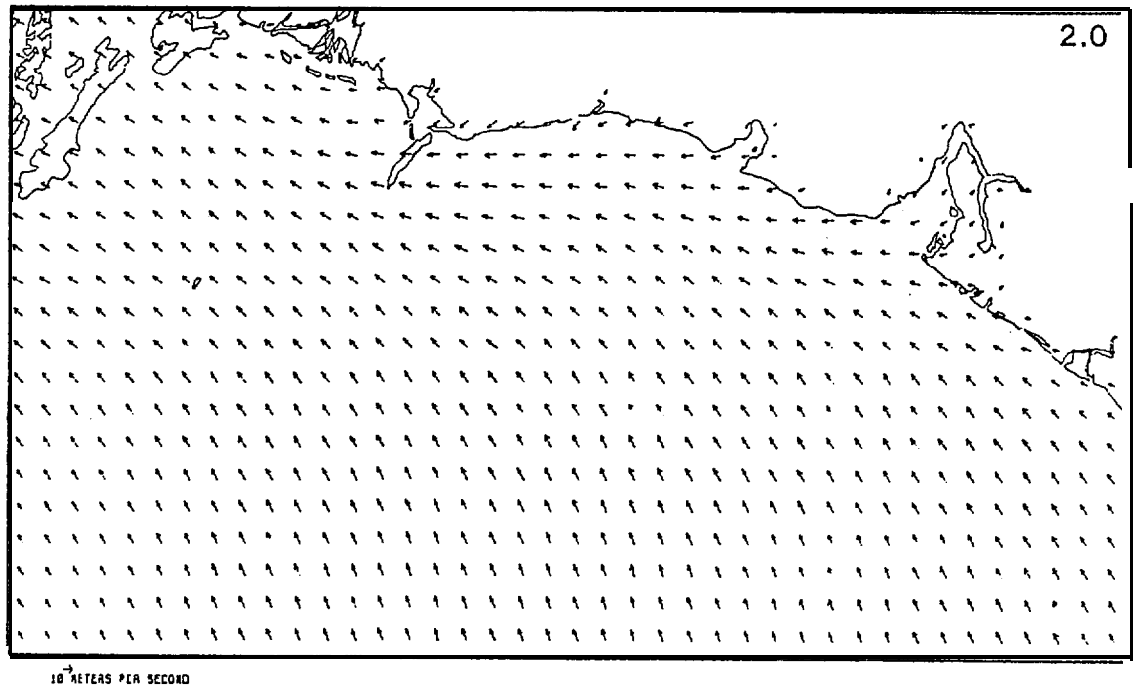

10 METERS PER SECOND

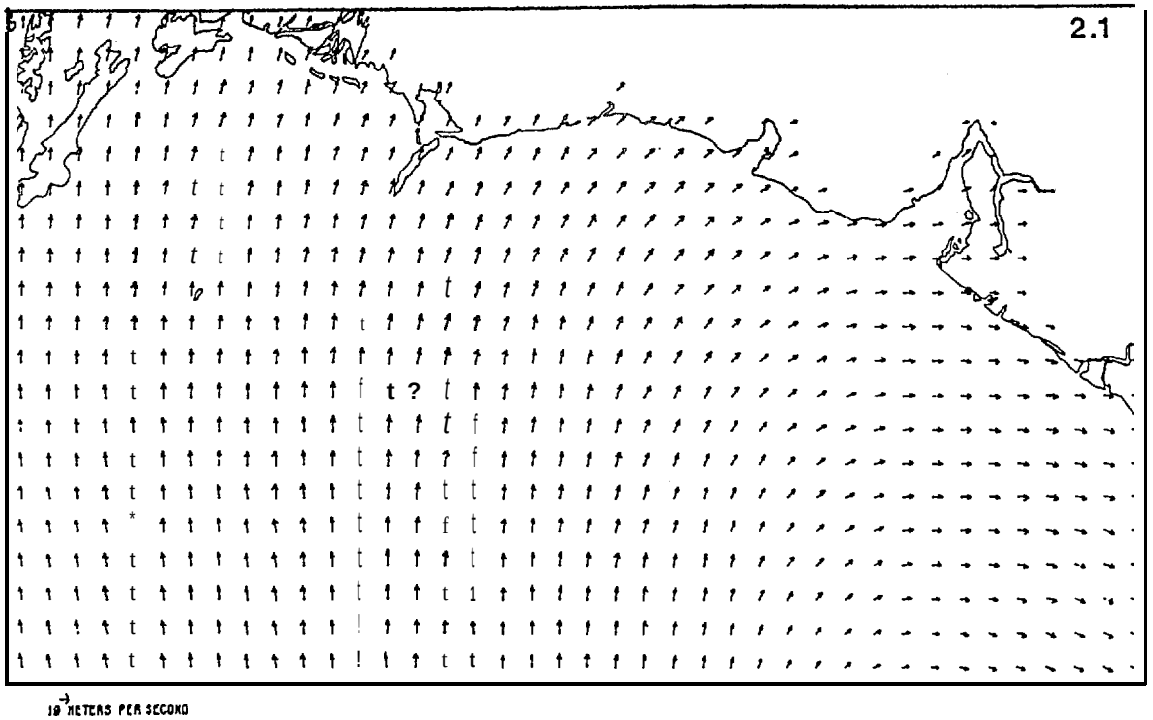
2.1
10 METERS PER SECOND

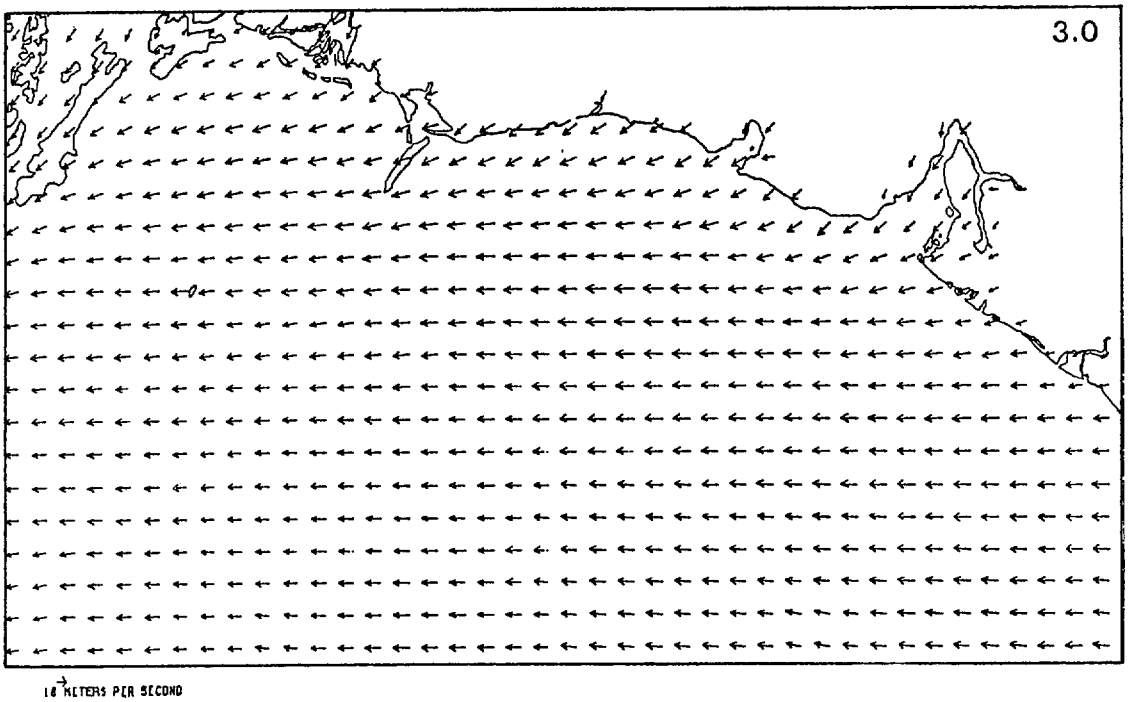
3.0
10 METERS PER SECOND

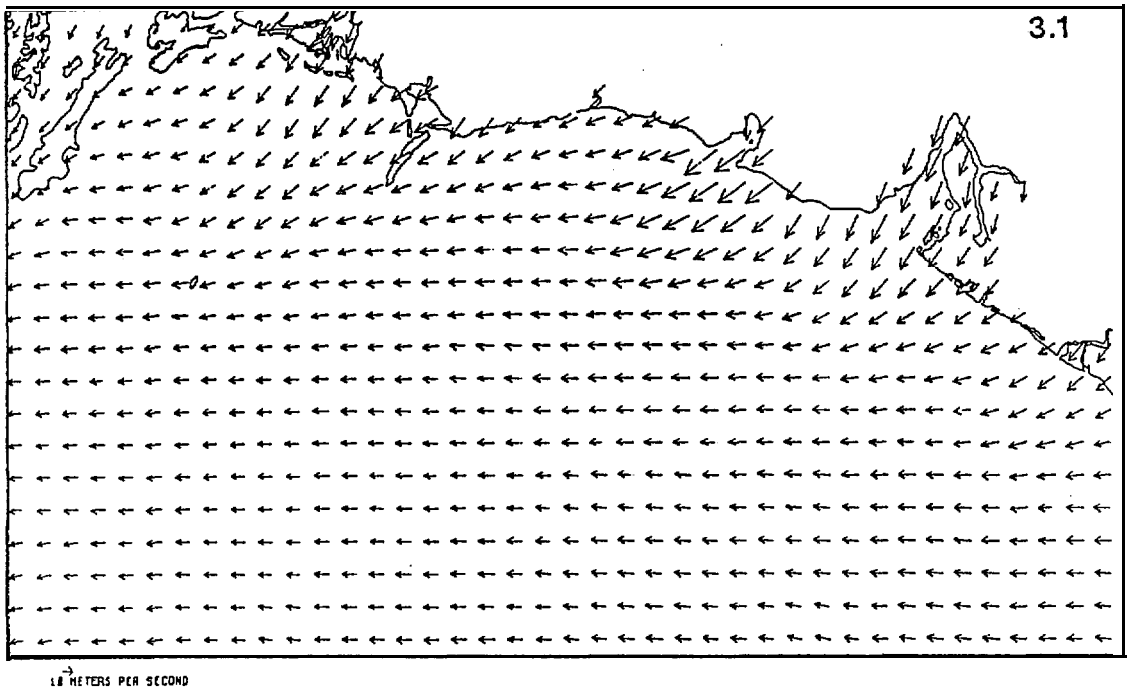
3.1
1.0 METERS PER SECOND

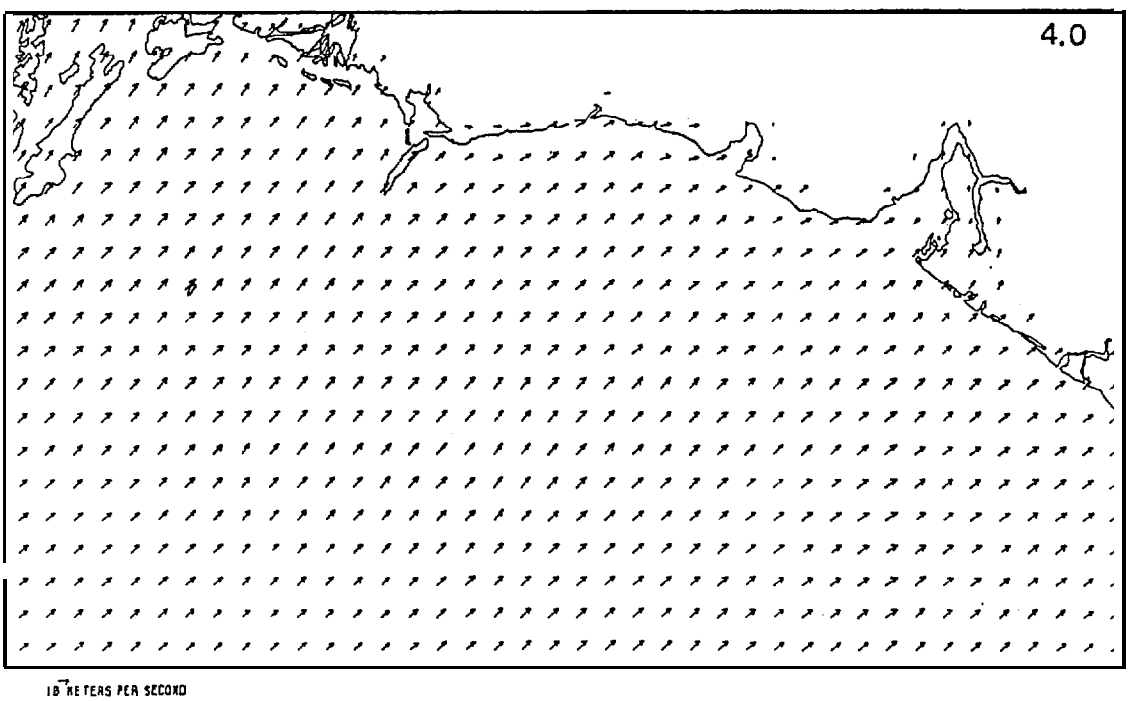
4.0
1.0 METERS PER SECOND

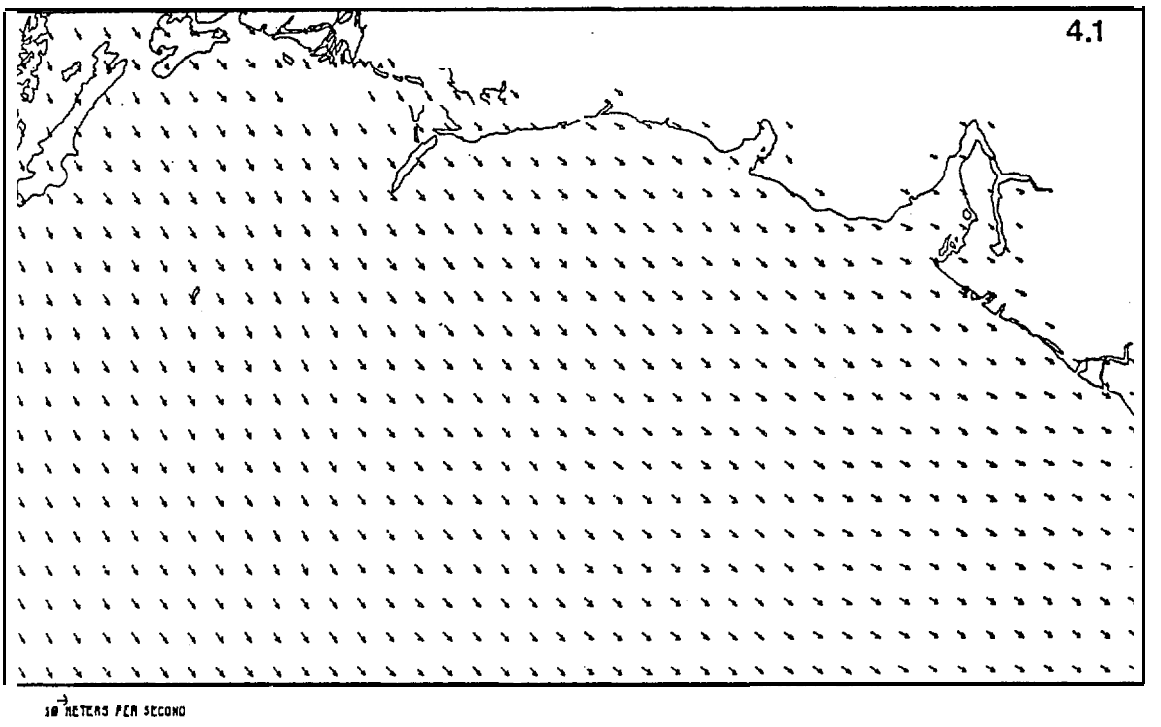
4.1
10 METERS PER SECOND

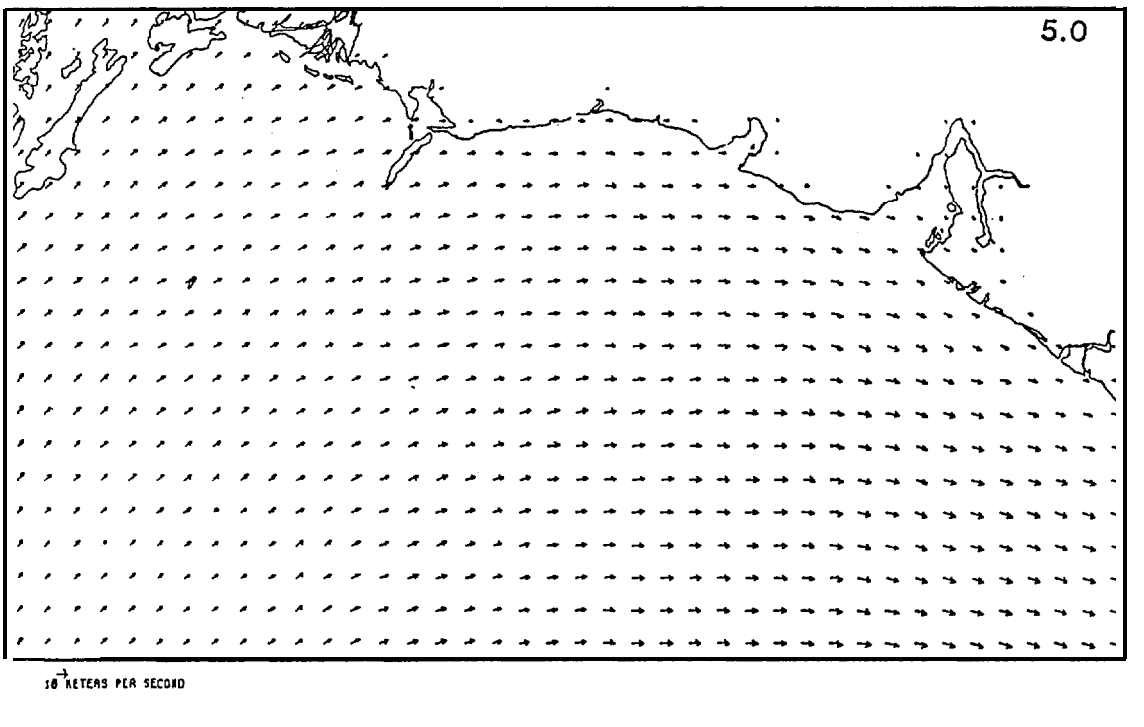
5.0
10 METERS PER SECOND

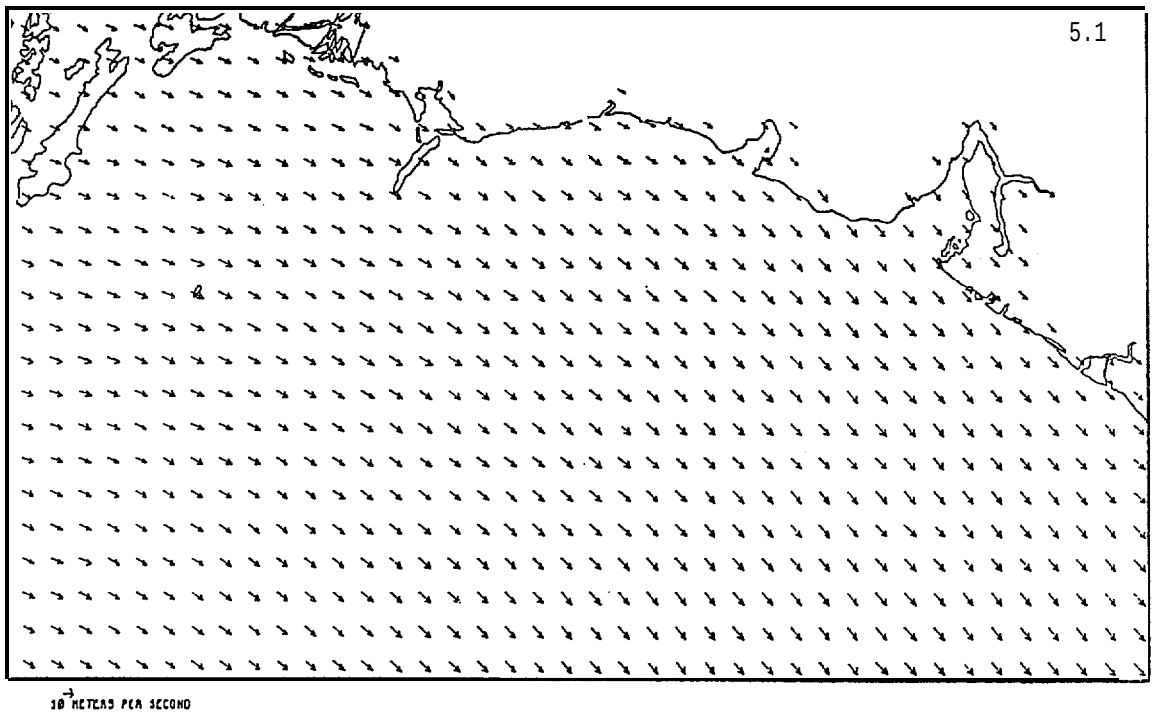
5.1
10 METERS PER SECOND

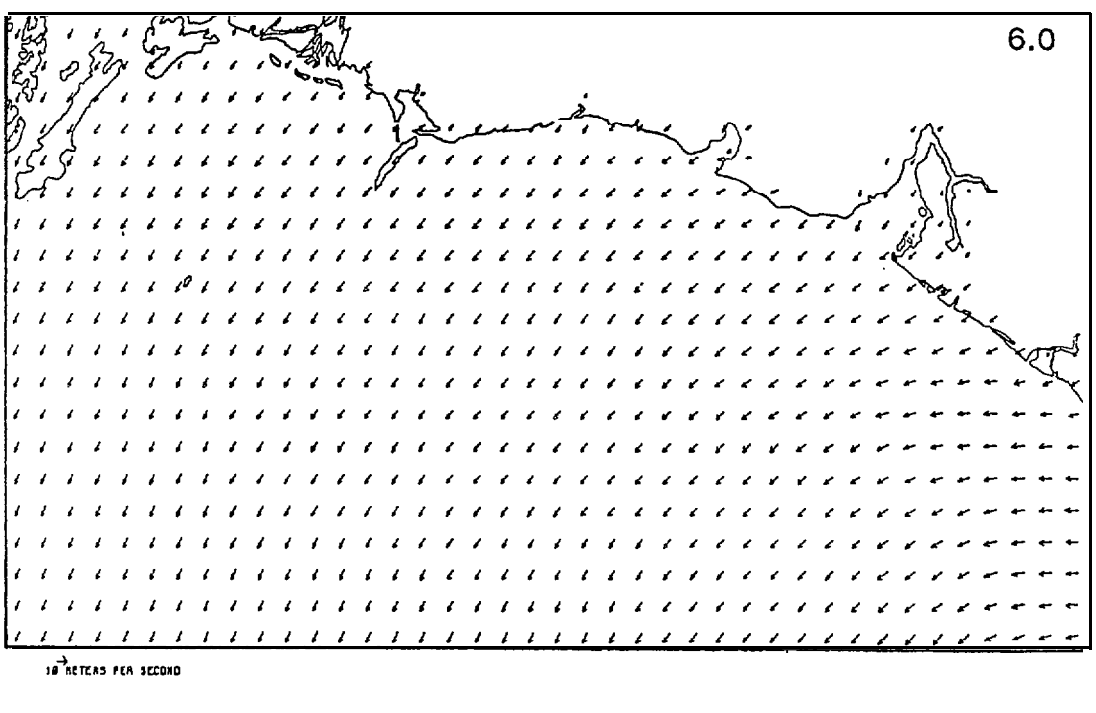
6.0
10 METERS PER SECOND